

THE DETERMINATION OF OPTIMAL COMBINATIONS OF VARIABLES
FOR NOMINAL DEPLOYMENT AND INFLATION OF NASA'S MARS
PATHFINDER AIRBAG SUBSYSTEM

by

ELIZABETH ANN STAUB

Bachelor of Science in Mechanical Engineering
Massachusetts Institute of Technology, 1994

Submitted to the Department of Mechanical Engineering in
Partial Fulfillment of the Requirements for the Degree of

MASTER OF SCIENCE

IN MECHANICAL ENGINEERING

at the

MASSACHUSETTS INSTITUTE OF TECHNOLOGY
February 1995

© 1994 Elizabeth Ann Staub. All rights reserved.

The author hereby grants to MIT permission to reproduce and to distribute
publicly paper and electronic copies of this thesis document in whole or in part.

Signature of Author _____
Massachusetts Institute of Technology Department of Mechanical Engineering
December 10, 1994

Certified by _____
Igor Paul, Adjunct Professor of Mechanical Engineering
Massachusetts Institute of Technology Department of Mechanical Engineering
Thesis Supervisor

Certified by _____
Donald Bickler, Group Supervisor of Technology and Advanced Systems
NASA Jet Propulsion Laboratory, Mechanical Systems Development Section
Thesis Supervisor

Accepted by _____
Ain A. Sonin, Chairman, Committee on Graduate Studies
Massachusetts Institute of Technology Department of Mechanical Engineering

MASSACHUSETTS INSTITUTE
OF TECHNOLOGY

APR 06 1995

Eng.

THE DETERMINATION OF OPTIMAL COMBINATIONS OF VARIABLES FOR NOMINAL DEPLOYMENT AND INFLATION OF NASA'S MARS PATHFINDER AIRBAG SUBSYSTEM

by

Elizabeth Ann Staub

Submitted to the Department of Mechanical Engineering on
December 2, 1994 in partial fulfillment of the requirements for the Degree of

MASTER OF SCIENCE IN MECHANICAL ENGINEERING.

A series of experiments was performed using a quarter scale Mars Pathfinder Airbag Subsystem to achieve several goals. The Airbag Subsystem consists of four twenty cubic meter airbag chambers, each of which is packaged separately on one of the four petals of the tetrahedron-shaped lander. First, numerous folding methods were explored after taking cues from parachute rigging and the packaging of automotive airbags. Then the knowledge gained was incorporated into a coherent set of 'good' folding schemes, where 'good' schemes were defined as those that allowed for smooth deployment (no violent motions) and inflation without major damage to the airbag. After experimenting with different methods of recording the information being gathered with each folding scheme and its subsequent inflation, I performed inflations with many iterations of promising folding scheme candidates and varying inflation pressures, flow orifice sizes, diffusers, and deflectors in hopes of finding an optimal combination of variables. Finally, I recorded the folding and inflation of four different folding schemes, as well as the inflation of each of the schemes with four varying gas inlet conditions to ensure that the schemes that were good candidates were good for a variety of inlet conditions, not just one.

Thesis Supervisor: Dr. Igor Paul, Adjunct Professor of Mechanical Engineering,
Massachusetts Institute of Technology Department of Mechanical Engineering

Thesis Supervisor: Donald Bickler, Group Supervisor of Technology and Advanced
Systems, NASA Jet Propulsion Laboratory, Mechanical Systems Development Section

Acknowledgment

I would like to thank Professor Igor Paul of the MIT Department of Mechanical Engineering for his supervision of my Master's thesis. Advising on this project from afar, and doing so under somewhat arduous time constraints, was much appreciated. Working with Professor Paul over the years on everything from 2.671 Project Laboratory to organizing ASME events to associate advising for Engineering Ethics, the Law, and Professional Responsibility has provided me with more knowledge of the field of mechanical engineering than any one course in my curriculum. I would also like to thank Don Bickler for his supervision over my work at the Jet Propulsion Laboratory. His enthusiasm for mechanical design and his distaste for approaching problems in a typical, methodical manner helped me keep an open mind at all times.

Also deserving of thanks are Tom Rivellini and Tom Hill, both of the Jet Propulsion Laboratory. Tom Rivellini's advice always proved to be a useful and fundamental part of my experiments, and his tips for how to get business taken care of at the Laboratory in a quick and efficient manner were invaluable. I am grateful for the use of Tom Hill's tools, machine shop, and testing room, and for his general advice. They were welcome and necessary parts of my endeavors. I would also like to thank Skip Wilson, of ILC Dover, Incorporated, for his input on the fourth folding scheme and his feedback on the first three.

The combined efforts of Dr. William Whitney, MIT - JPL Liaison, Linda Rodgers, JPL Cooperative Education Coordinator, and Maria Acevedo, of the JPL Cooperative Education Office, made life as a student employee of the Laboratory much more interesting and educational. I would also like to thank William Ramsey, Director of the MIT Engineering Internship Program, for his help over the past four years with everything pertaining to my

involvement in the Engineering Internship Program. Leslie Regan of the MIT Mechanical Engineering Graduate Office deserves praise for helping me ferret out answers to difficult questions and solve all the tactical problems that presented themselves while doing a thesis away from MIT's campus.

I am indebted to the MIT Space Grant Program for the NASA Space Grant Fellowship that funded my year of graduate study at MIT, and to JPL for its help with MIT tuition during my graduate term spent here at the Laboratory. Without this financial help, my studies would not have been possible.

Finally, I would like to thank my parents, Lester and Della Jean Staub, and my brother, Erik Staub, for their ongoing support and encouragement. Good times spent my last year in Boston with Kim Kohlhepp, Maia Singer, Daphne Shih, Colin Chapman, Q Bilimoria, and Kristen Bohlke made my life as a graduate student not only tolerable, but memorable. As a group, they helped me master the fine art of working hard and playing harder. The comic relief they provided kept me smiling, and the pop psychology sessions with some of them will probably save me thousands in psychiatric bills later on in life.

My officemates here at the Laboratory, Andy Rose and Geoff Harvey, and the rest of the lunch gang, Eric Slimko and Andy Stone, always found ways to keep me from working on my thesis by creating pleasant diversions. During my relatively short time here in California, I learned a lot about life in the real world (outside of an academic environment). My biking buddies Kevin Burke, Laura Sakamoto, and Sugi Sorensen, among others, welcomed me into their Southern Californian lifestyles and mind-sets, and made me a bit better of a biker, in spite of myself. They opened my eyes to many new worlds, only one of which was cycling, and more importantly, they inspired me to pursue my passions.

Persistence...

“Nothing in the world can take the place of persistence. Talent will not; nothing is more common than unsuccessful men with talent. Genius will not; unrewarded genius is almost a proverb. Education will not; the world is full of educated derelicts. Persistence and determination alone are omnipotent.”

Calvin Coolidge

Table of Contents

Chapter One: Introduction	9
Mission Overview	9
Mars Landing	11
Pathfinder versus Viking	11
Priority of Airbag Development	15
Background Information	15
Parachute Rigging	15
Automotive Airbags	18
Guide to this Thesis	25
Chapter Two: Apparatus	26
General Test Hardware	26
Mars Pathfinder Airbag	29
Mars Pathfinder Lander Petal	31
Flow Diffusion and Redirection	33
Diffusers	33
Deflectors	34
Data Recording Media	35
Chapter Three: Procedure	36
Operating Procedure	37
Preparation	37
Before Each Fold	37
After Each Fold	39
Inflation	40
Folding Schemes	40
Folding Scheme One	40
Folding Scheme Two	57
Folding Scheme Three	70
Folding Scheme Four	87
Trials	92
Trials One through Six	92
Trials Seven through Ten	92
Trials Eleven through Fourteen	93
Chapter Four: Results	94
Folding Schemes	94
Folding Scheme One	94
Folding Scheme Two	100
Folding Scheme Three	104
Folding Scheme Four	104
Comparisons Between the Folding Schemes	108

Diffusers and Deflectors	109
Diffusers	109
Deflectors	109
Chapter Five: Discussion	111
General Scope of this Project	111
JPL's Involvement in the Pathfinder Efforts	111
The Scope of this Thesis	112
Results	113
Folding Schemes	113
Diffusers and Deflectors	113
Chapter Six: Conclusion	116
Summary of Work Done	116
Recommendations for Future Work	117
References	118
Appendix A: Video Tape Program Guide	120

List of Figures

Figure 1. Mars Landing	10
Figure 2. Mars Pathfinder, Side View	12
Figure 3. Mars Pathfinder, Exploded View	13
Figure 4. The Lander, Closed Configuration	14
Figure 5. The Lander, Open Configuration	14
Figure 6. Typical Drag-Area Versus Time for Various Parachute Types	16
Figure 7. Slotted Parachutes	16
Figure 8. Solid Textile Parachutes	17
Figure 9. Cross Section of Automotive Airbag Gas Generator for Modeling Purposes	19
Figure 10. Cross Section of Thiokol Gas Generator for Modeling Purposes	19
Figure 11. Mars Pathfinder Mathematical Model for Gas Generator	21
Figure 12. Mars Pathfinder Gas Generator Thermal Models	22
Figure 13. Mass Flow Rate out of the Propellant Chamber Versus Time, Pathfinder	23
Figure 14. Mass Flow Rate out of the Coolant Chamber Versus Time, Pathfinder	24
Figure 15. Mass Flow Rate out of the Combustion and Discharge Chambers, Automotive	24
Figure 16. Base Structure and Shield, Top View	26
Figure 17. Base Structure and Shield, Side View	27
Figure 18. Base Structure and Shield, Front View	27
Figure 19. Test Hardware, View from Front	20
Figure 20. Test Hardware, View from Rear	20
Figure 21. Quarter Scale Mars Pathfinder Airbag, Fully Inflated	30
Figure 22. Mars Pathfinder Airbag Internal and External Hardware	30
Figure 23. Six Lobe Airbag Design, Top View	31
Figure 24. Quarter Scale Lander Petal, Top and Side Views	32
Figure 25. Diffusers, Low Porosity and High Porosity	34
Figure 26. Deflectors, Tri-chute and Redirection Sock	34
Figure 27. Fold Form for Step A of Scheme Two	38
Figure 28. Fold Forms for Folding Scheme One	42
Figure 29. Pictures of the Steps of Folding Scheme One	53
Figure 30. Fold Forms for Folding Scheme Two	58
Figure 31. Pictures of the Steps of Folding Scheme Two	66
Figure 32. Fold Forms for Folding Scheme Three	71
Figure 33. Pictures of the Steps of Folding Scheme Three	82
Figure 34. Pictures of the Steps of Folding Scheme Four	88
Figure 35. Inflation of Folding Scheme One	95
Figure 36. Inflation of Folding Scheme Two	102
Figure 37. Inflation of Folding Scheme Three	105

Chapter One: Introduction

In this thesis done at the Jet Propulsion Laboratory, a series of experiments was performed using a quarter scale Mars Pathfinder Airbag Subsystem to achieve several goals. The Airbag Subsystem consists of four twenty cubic meter airbag chambers, each of which is packaged separately on one of the four petals of the tetrahedron-shaped lander. First, numerous folding methods were explored after taking cues from parachute rigging and the packaging of automotive airbags. Then the knowledge gained was incorporated into a coherent set of ‘good’ folding schemes, where ‘good’ schemes were defined as those that allowed for smooth deployment (no violent motions) and inflation without major damage to the airbag. After experimenting with different methods of recording the information being gathered with each folding scheme and it’s subsequent inflation, I performed inflations with many iterations of promising folding scheme candidates and varying inflation pressures, flow orifice sizes, diffusers, and deflectors in hopes of finding an optimal combination of variables. Finally, I recorded the folding and inflation of four different folding schemes, as well as the inflation of each of the schemes with four varying gas inlet conditions to ensure that the schemes that were good candidates were good for a variety of inlet conditions, not just one.

MISSION OVERVIEW

NASA’s Mars Pathfinder, launching in December, 1996 and landing July 4, 1997, demonstrates a low cost delivery system to the surface of Mars. Spacecraft that land on a distant body usually carry a large amount of fuel for braking at the planet, but Pathfinder

requires fuel only to navigate to Mars. It then aerobrakes into the Martian atmosphere, which is similar to Earth's in structure, but is less than one-hundredth the pressure, and deploys a parachute about six miles above the surface. Within three hundred feet of the surface, it fires solid rockets for final braking prior to deployment of the airbags. As shown below in Figure 1, the airbags will then cushion the touchdown.

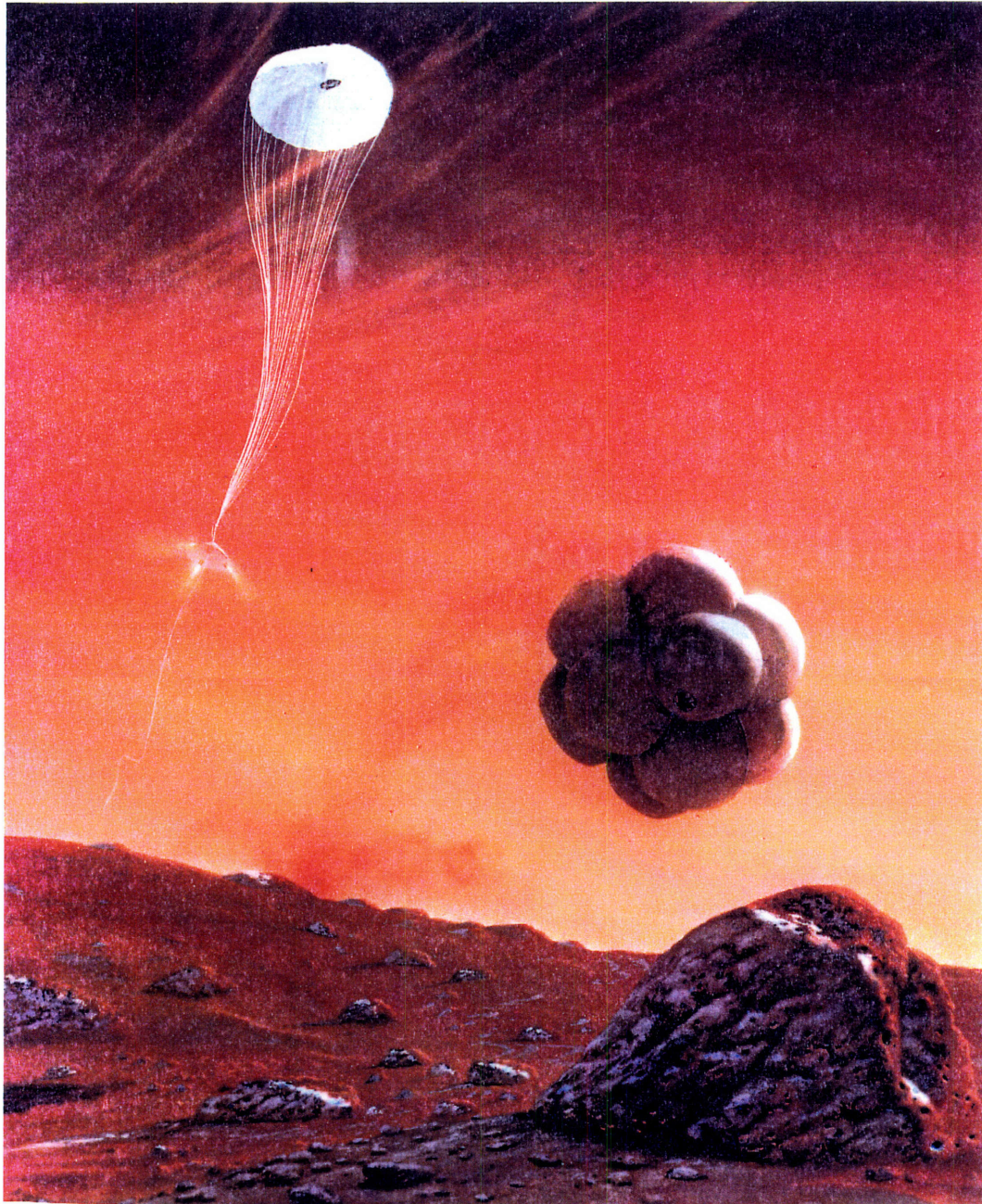


Figure 1. Mars Landing.

MARS LANDING

After landing, petals open to upright the tetrahedron-shaped lander. The acquisition and return of engineering data on entry, descent, and landing -- the major objective of Pathfinder -- will be completed within hours of landing on Mars. The lander will transmit panoramic images of the Martian surface on the first day, and a rover will be deployed to perform mobility tests, image its surroundings (including the lander), and place an alpha proton x-ray spectrometer against a rock to make elemental composition measurements. While the primary mission durations are one week and one month for the rover and the lander, respectively, both are expected to operate longer.

Though Mars Pathfinder is touted as a cost-effective project implementation, it accomplishes an exciting set of scientific investigations with a stereo, multicolor lander imager; atmospheric instrumentation, used as a weather station after landing; the alpha proton x-ray spectrometer; and the rover, including its aft and forward cameras.

PATHFINDER VERSUS VIKING

A demonstrated set of capabilities for future Mars landers will be obtained by combining the experience base acquired by Viking with that of Pathfinder. In 1976 two Viking landers were carried into orbit by orbiters. After aerobraking with an aeroshell and parachute combination, final deceleration was performed with rocket deceleration against Mars' gravity, with active three-axis attitude control, using a liquid propellant system. Both horizontal and vertical velocities were near zero at touchdown, and the landers touched down on legs. The main telemetry path to Earth was via a relay link through the orbiters, but the Viking landers also had a direct link backup. Access to the

Martian soil was achieved through an arm, and the landers were both powered by radioisotope thermal generators.

For comparison, Pathfinder's flight system, which is shown below in Figure 2, is self-contained and will cruise to Mars on its own. It will directly enter the Martian atmosphere without orbiting Mars, aerobrake with a Viking derivative aeroshell and parachute, but will land roughly at up to sixty feet per second horizontal and sixty feet per

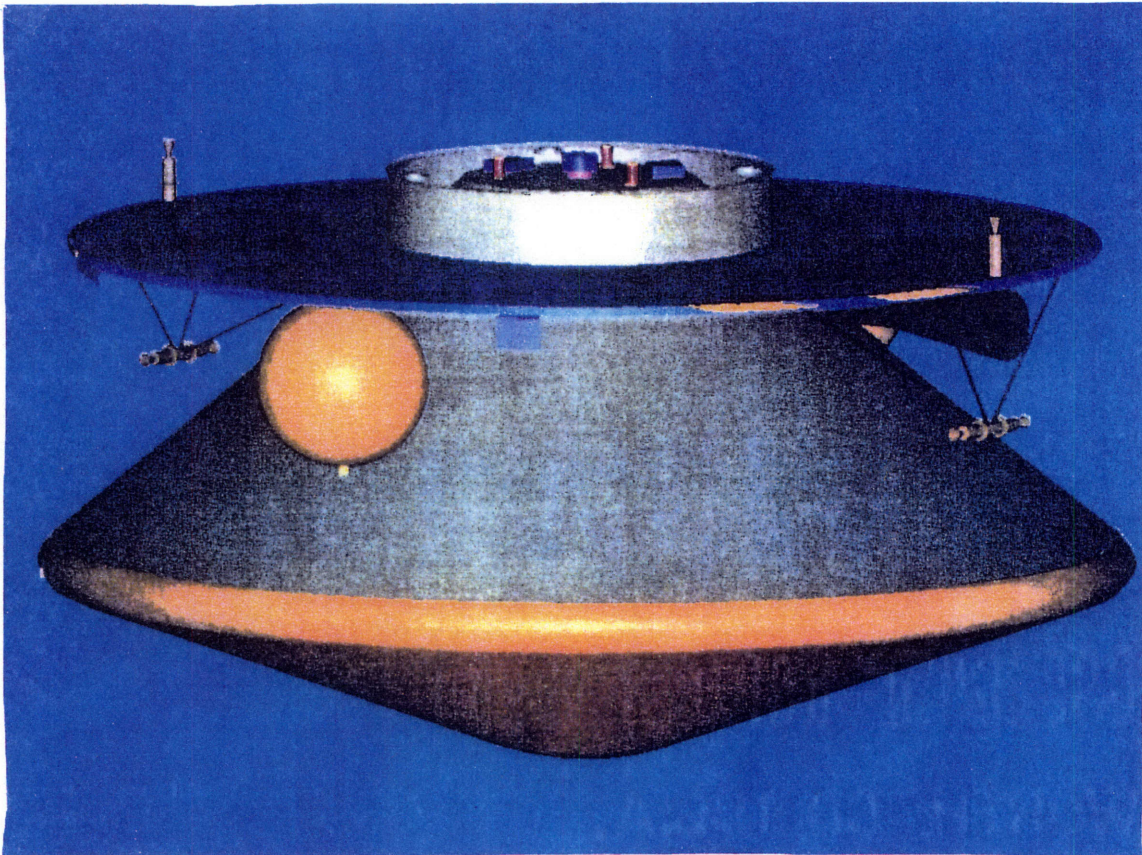


Figure 2. Mars Pathfinder, Side View.

second vertical velocities. Landing will be limited to less than fifty g using an airbag system designed to accommodate rocks up to a foot and a half in diameter. The lander,

which is shown as part of the following exploded view below and in Figure 4 on the following page, tumbles and rolls across the surface and rights itself by opening petals radially outward from the base of the lander, much like an opening flower.

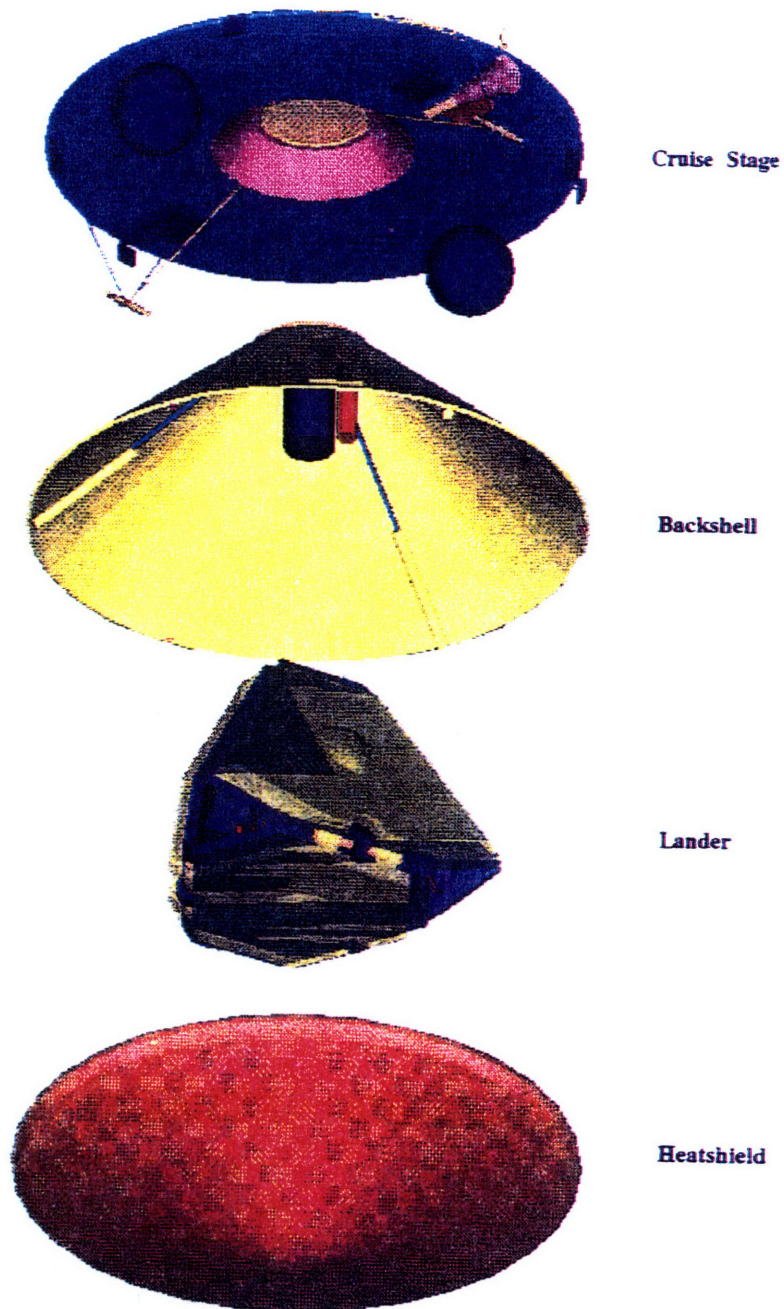
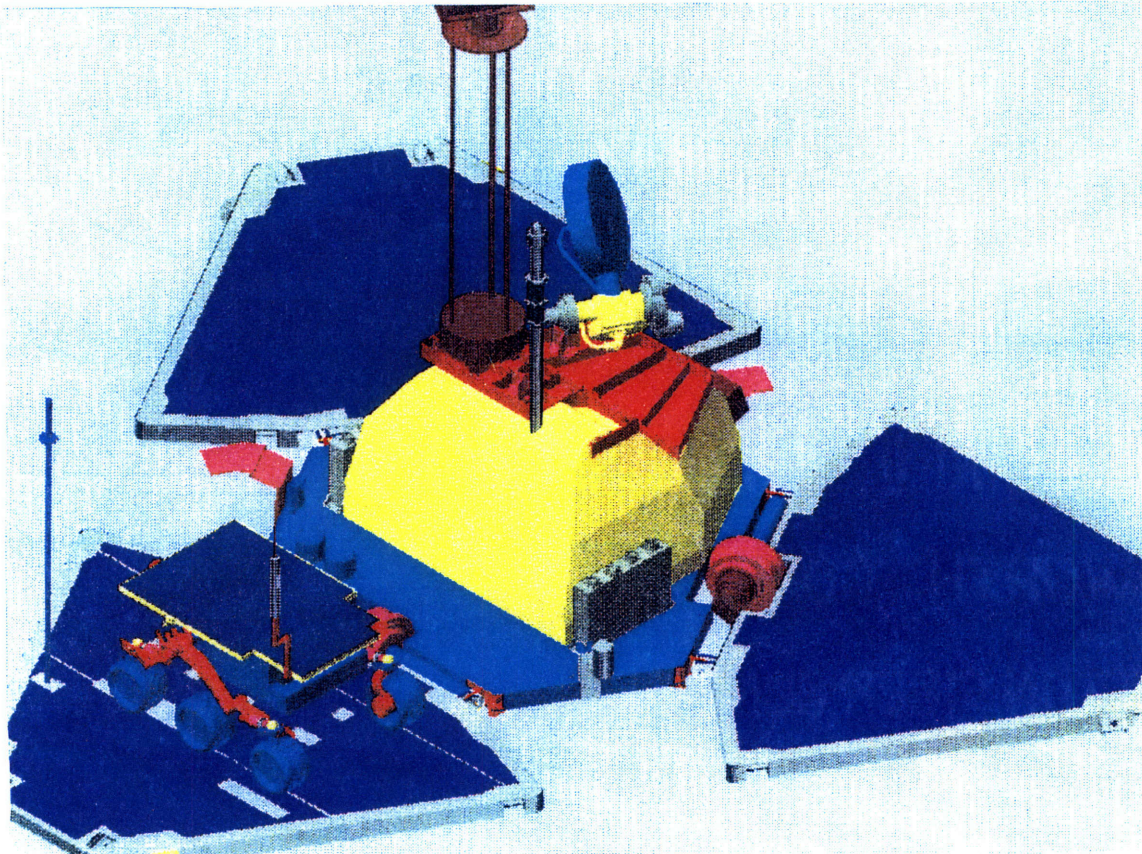
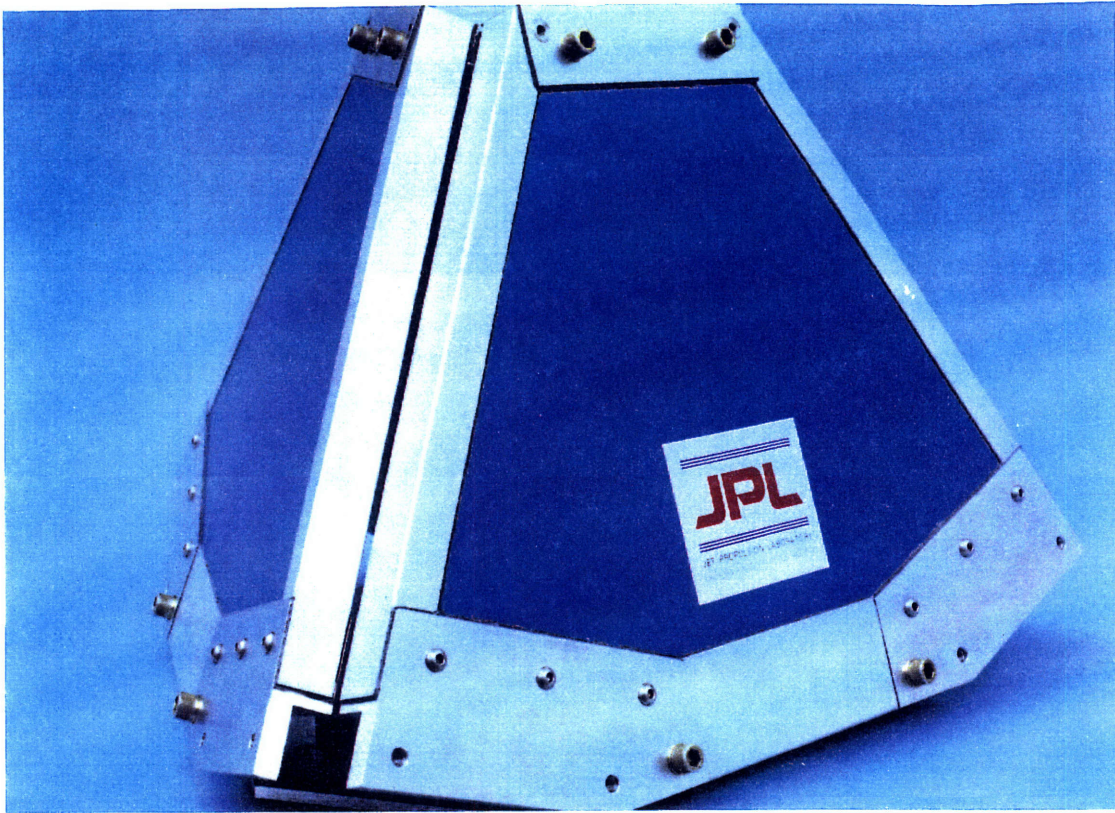


Figure 3. Mars Pathfinder, Exploded View.



Figures 4 and 5. The Lander, Closed (above) and Open (below) Configurations.

PRIORITY OF AIRBAG DEVELOPMENT

The Pathfinder Flight System is a blend of available and new technology. It uses the existing equipment and designs from Cassini, Magellan Star Scanner, Adcol Sun Sensors, Viking heritage aeroshell and parachute designs, and Department of Defense-developed RAD (Rocket Assisted Deceleration) technology and altimeters. Pathfinder's new technologies include a free ranging rover with on-board autonomous navigation, a solid state X-band power amplifier, a RAD-hardened IBM RS 6000 32 bit flight computer, lander image data compression, and airbags for use in Mars' atmosphere. With the entry, descent, and landing comprising 50% of the entire mission's objective, the Pathfinder airbag subsystem requires major development, while the rest of the subsystems have been proven technologies for use in other areas of the space program.

BACKGROUND INFORMATION

Cues were taken from two fields that directly relate to the folding and inflation of airbags: parachute rigging and the automotive airbag industry. The search for better folding methods did not stop at these two, but the baseline theories were formulated using them simply because of the amount of information that was available pertaining to these topics. Hints for improving upon folding schemes were taken from everything from the topics mentioned above, to musical instruments (such as an accordion), to party favors.

PARACHUTE RIGGING

It was found that the parachute drag-area, which is the surface area of the parachute that the air acts on in order to inflate the parachute, increases from zero to one hundred percent during inflation. The drag-area-versus-time increase -- whether it be

linear, convex, concave, or random -- is well known and has proven to be constant for known parachute shapes. The drag-area-versus-time increase for various parachutes is shown below in Figure 6. Descriptions of the parachute types that come closest to the Pathfinder airbag subsystem are given in Figures 7 and 8. The shape of the drag-area

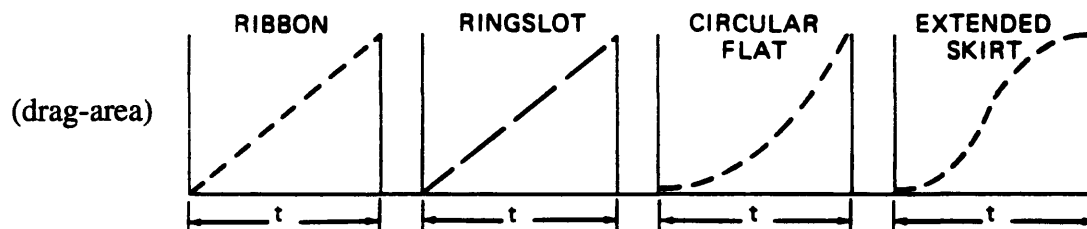


Figure 6. Typical Drag-area Versus Time for Various Parachute Types.
(Courtesy of *Parachute Recovery Systems Design Manual*.)

TYPE	CONSTRUCTED SHAPE		$\frac{D_c}{D_o}$	INFLATED SHAPE $\frac{D_p}{D_o}$	DRAG COEF C_{D_o} RANGE	OPENING FORCE COEF C_x (INF MASS)	AVERAGE ANGLE OF OSCILLATION, DEGREES	GENERAL APPLICATION
	PLAN	PROFILE						
FLAT (FIST) RIBBON			1.00	0.67	0.45 TO 0.50	-1.05	0 TO ±3	DROGUE, DESCENT, DECELERATION, OBSOLETE
CONICAL RIBBON			0.95 TO 0.97	0.70	0.50 TO 0.55	-1.05	0 TO ±3	DESCENT, DECELERATION, 0.1 < M < 2.0
CONICAL RIBBON (VARIED POROSITY)			0.97	0.70	0.55 TO 0.60	1.05 TO 1.30	0 TO ±3	DROGUE, DESCENT, DECELERATION, 0.1 < M < 2.0
RIBBON ¹ (HEMISFLO)			0.62	0.62	0.30 ¹ TO 0.46	1.00 TO 1.30	±2	SUPERSONIC, DROGUE, 1.0 < M < 3.0
RINGSLOT			1.00	0.67 TO 0.70	0.56 TO 0.65	-1.05	0 TO ±5	EXTRACTION, DECELERATION, 0.1 < M < 0.9
RINGSAIL			0.84	0.69	0.75 TO 0.86	-1.10	±5 TO ±10	DESCENT, M < 0.5
DISC-GAP-BAND			0.73	0.66	0.52 TO 0.58	-1.30	±10 TO ±15	DESCENT, M < 0.5

Figure 7. Slotted Parachutes.
(Courtesy of *Parachute Recovery Systems Design Manual*.)

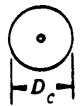
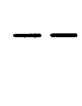
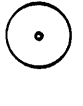
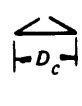
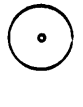

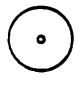


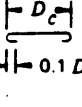

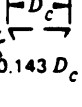
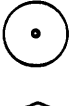







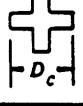

TYPE	CONSTRUCTED SHAPE		$\frac{D_c}{D_o}$	INFLATED	DRAG COEF C_{D_o}	OPENING FORCE COEF C_X (INF MASS)	AVERAGE ANGLE OF OSCILLATION, DEGREES	GENERAL APPLICATION
	PLAN	PROFILE		SHAPE $\frac{D_p}{D_o}$				
FLAT CIRCULAR			1.00	0.67 TO 0.70	0.75 TO 0.80	~1.7	±10 TO ±40	DESCENT, OBSOLETE
CONICAL			0.93 TO 0.95	0.70	0.75 TO 0.90	~1.8	±10 TO ±30	DESCENT, M < 0.5
BICONICAL			0.90 TO 0.95	0.70	0.75 TO 0.92	~1.8	±10 TO ±30	DESCENT, M < 0.5
TRICONICAL POLYCONICAL			0.90 TO 0.95	0.70	0.80 TO 0.96	~1.8	±10 TO ±20	DESCENT, M < 0.5
EXTENDED SKIRT 10% FLAT			0.86	0.66 TO 0.70	0.78 TO 0.87	~1.4	±10 TO ±15	DESCENT, M < 0.5
EXTENDED SKIRT 14.3% FULL			0.81 TO 0.85	0.66 TO 0.70	0.75 TO 0.90	~1.4	±10 TO ±15	DESCENT, M < 0.5
HEMISPHERICAL			0.71	0.66	0.62 TO 0.77	~1.6	±10 TO ±15	DESCENT, M < 0.5, OBSOLETE
GUIDE SURFACE (RIBBED)			0.63	0.62	0.28 TO 0.42	~1.2	0 TO ±2	STABILIZATION, DROGUE, 0.1 < M < 1.5
GUIDE SURFACE (RIBLESS)			0.66	0.63	0.30 TO 0.34	~1.4	0 TO ±3	PILOT, DROGUE, 0.1 < M < 1.5
ANNULAR			1.04	0.94	0.85 TO 0.95	~1.4	<±6	DESCENT, M < 0.5
CROSS			1.15 TO 1.19	0.66 TO 0.72	0.60 TO 0.85	1.1 TO 1.2	0 TO ±3	DESCENT, DECELERATION

Figure 8. Solid Textile Parachutes.
(Courtesy of *Parachute Recovery Systems Design Manual*.)

versus time curves may be somewhat drawn out or compressed by reefing, changes in porosity distribution in the canopy, wide slots, or other means, but the basic configuration of the curve is maintained for a particular type of parachute. As can be seen in Figures 7 and 8, the parachute that most closely resembles the shape of an airbag such as Mars Pathfinder's is the ribbon parachute. Although the inflation of a compactly folded airbag by a gas generator does not exactly mimic air flowing up into a folded parachute, it was certainly a similar enough situation to warrant the exploration of some folding ideas given in parachute rigging manuals.

AUTOMOTIVE AIRBAGS

The automotive airbag industry abounds with literature on airbag models, studies, and analyses. The inflation of an airbag is a complex thermochemical process for which numerous mathematical models have been developed. Simulations of everything from the airbag's deployment loads to the transient, thermochemical events associated with ignition and combustion of pyrotechnic automotive gas generators have been attempted by industry and academia. Because Thiokol Corporation's gas generator that will be inflating Mars Pathfinder's airbag subsystem is similar in many aspects to automotive inflators, the information obtained from these studies proved to be useful in understanding the deployment dynamics of Pathfinder's airbag subsystem.

The cross section of a typical automotive airbag inflator, as interpreted for modeling purposes, is shown on the following page in Figure 9. For comparison, a cross section of Thiokol's proposed gas generator is shown in Figure 10. Some fundamental

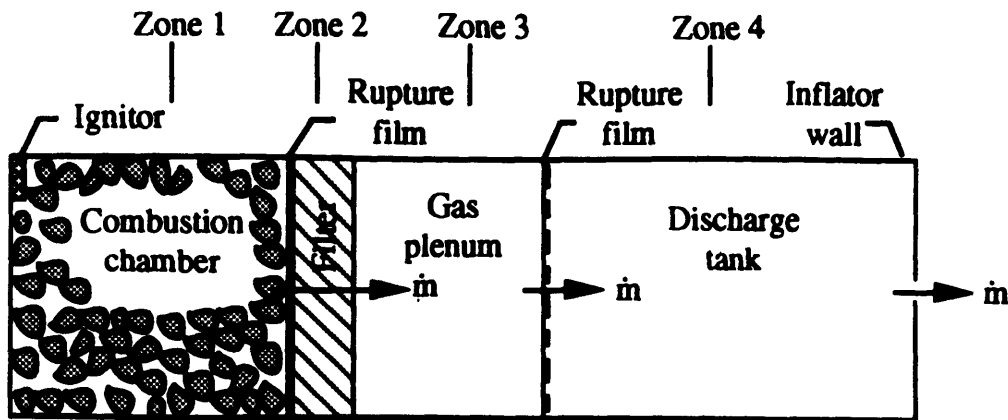


Figure 9. Cross section of automotive airbag gas generator for modeling purposes.
 (Courtesy of P. Barry Butler, Jian Kang, and Herman Krier.)

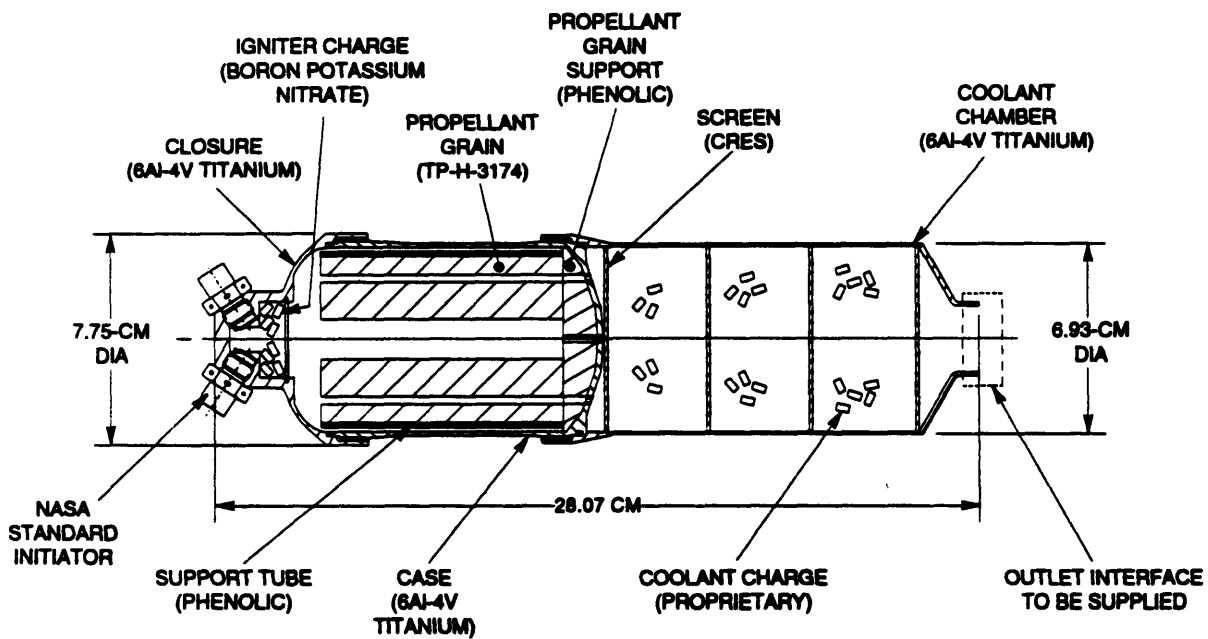


Figure 10. Cross section of Thiokol gas generator for modeling purposes.
 (Courtesy of ILC Dover, Incorporated.)

assumptions made in most automotive airbag models are also applicable to the model of Pathfinder's airbags. These include (but are not limited to) the following.

- In each zone of Figure 9, the gas phase and condensed phase are well mixed, respectively, and gas phase species are ideal and condensed phase species are incompressible.
- The filter does not accumulate gas phase species, but it can accumulate solid/liquid particles.
- The filter is not selective to the condensed phase product species (i.e. it collects species mass in the same proportions as the condensed phase material flowing through it).
- Gas and condensed phases are composed of multiple species with temperature-dependent specific heats. Specific heats of hardware components are also a function of temperature.
- Chemical reactions are restricted to the combustion chamber (zone 1).

The equations gleaned from models with the above assumptions that show up in airbag deployment literature include the same mass and energy conservation principles as those proposed for Mars Pathfinder's airbag subsystem. The warm-gas mathematical model for Thiokol's generator is shown on the following page in Figure 11. Note the predicted pressure versus time plot at the bottom of Figure 11. This is what Pathfinder's pressure in the subsystem versus time is predicted to be using the models shown in Figure 12. The mass flow rates out of the propellant chamber versus time, shown in Figure 13,

WARM-GAS MATH MODEL GENERAL METHODOLOGY

	<h3>Chained Control Volume Approach</h3> <ul style="list-style-type: none"> • Balance of mass flow rates between control volume (CV) boundaries • Energy equation, equation of state for each CV • Refinements <ul style="list-style-type: none"> -Dynamic model for moving components -Heat-transfer model as a function of mass flow -Variable specific heat -Pressure drops as a function of mass flow
<h3>Simulink®-Based Network Analysis of Warm-Gas Math Model</h3>	
<ul style="list-style-type: none"> • 36 states • PC-386-33 with coprocessor • Windows 3.1 platform 	

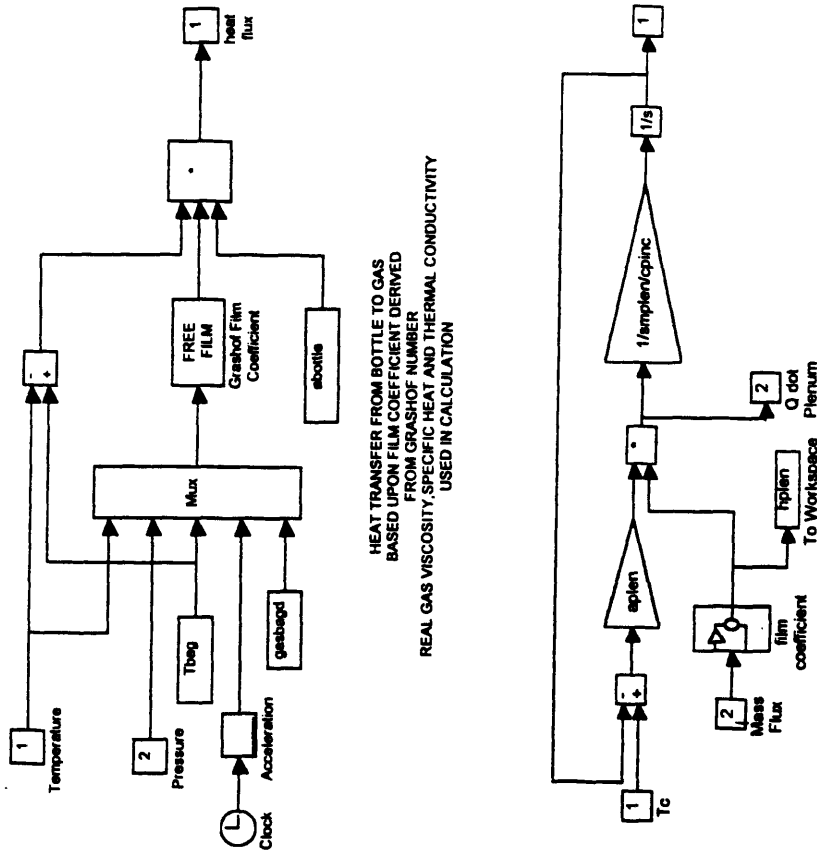
V0763148 [108]

WARM-GAS MATH MODEL SUBSYSTEM APPROACH – GENERATOR

<p>BURNING RATE, WEB</p>	<h3>Generator Model</h3> <ul style="list-style-type: none"> • Balance of mass generated, discharged, and stored • Energy equation with heat loss terms derive thermodynamic properties for next control volume • Propellant parameters and geometric parameters as input
<p>V0763171</p> <h4>Pressure vs Time</h4>	<p>V0763168</p> <h4>Heat Loss vs Time</h4>

Correlated to measured pressure

Figure 11. Mars Pathfinder Mathematical Model for Gas Generator.
(Courtesy of ILC Dover, Incorporated.)



HEAT TRANSFER FROM BOTTLE TO GAS
 BASED UPON FILM COEFFICIENT DERIVED
 FROM GRASHOF NUMBER
 REAL GAS VISCOSITY, SPECIFIC HEAT AND THERMAL CONDUCTIVITY
 USED IN CALCULATION

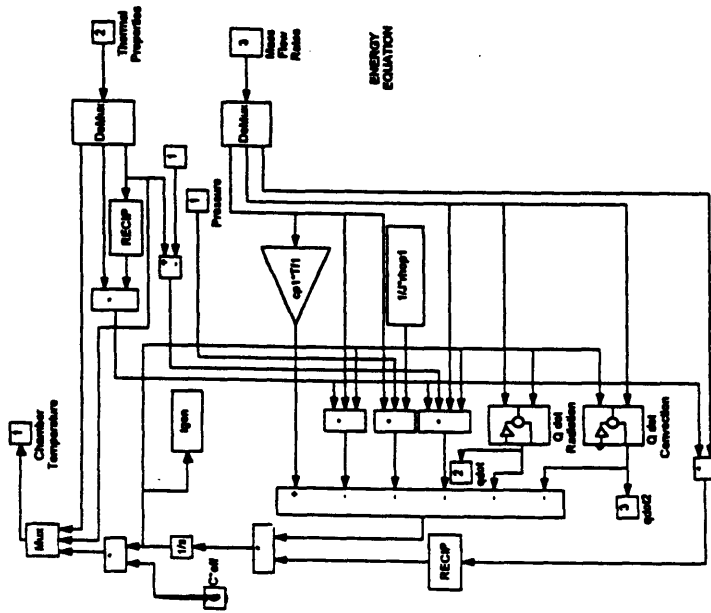


Figure 12. Mars Pathfinder Gas Generator Thermal Models.
 (Courtesy of ILC Dover, Incorporated.)

and out of the coolant chamber versus time (Figure 14), are directly analogous to typical automotive airbag gas generator mass flow rate versus time curves for the combustion and discharge chambers (Figure 15). As can be seen, the dynamics of the first one hundred milliseconds are similar enough between the two models to allow for the use of findings from the automotive industry pertaining to inflation and deployment forces to be used for the Mars Pathfinder folding schemes.

The automotive airbag models, however, cease to be similar to Pathfinder's after the first one hundred milliseconds, which is why the information from them can only be used for folding scheme ideas, and not the entire deployment process. Automotive airbags deflate rapidly soon after the half of a second, whereas Pathfinder's airbags remain inflated. Also, the information about deployment loads and the unfurling of material is only marginally useful, because automotive airbags can be folded up without any constraints, while Pathfinder's airbags have complex internal and external hardware that needs to be oriented properly.

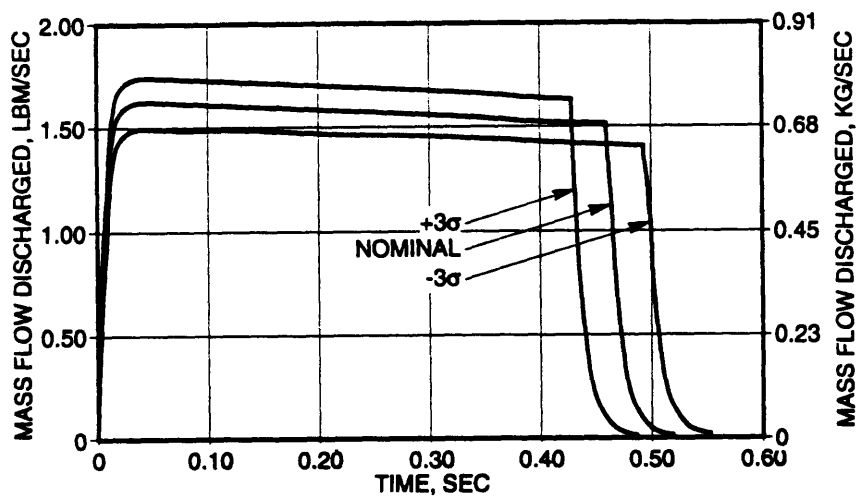


Figure 13. Mass Flow Rate out of the Propellant Chamber versus Time, Pathfinder.
(Courtesy of ILC Dover, Incorporated.)

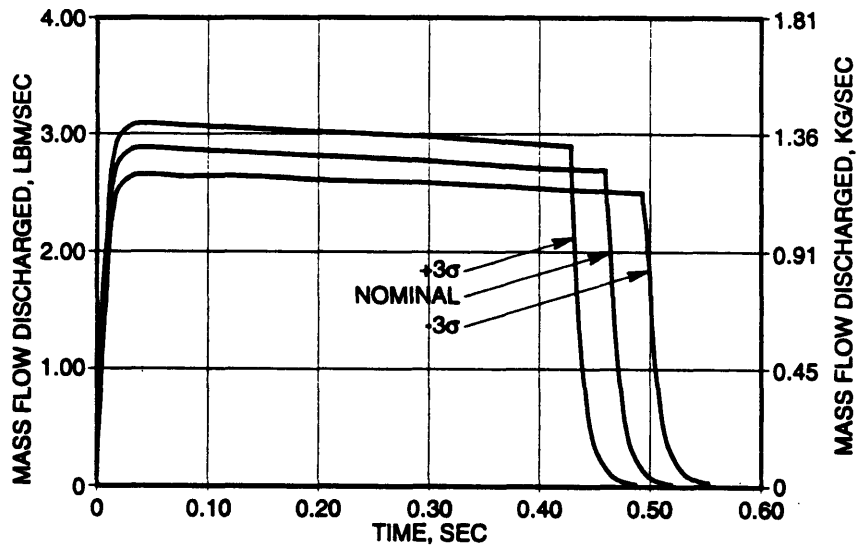


Figure 14. Mass Flow Rate out of the Coolant Chamber versus Time, Pathfinder.
(Courtesy of ILC Dover, Incorporated.)

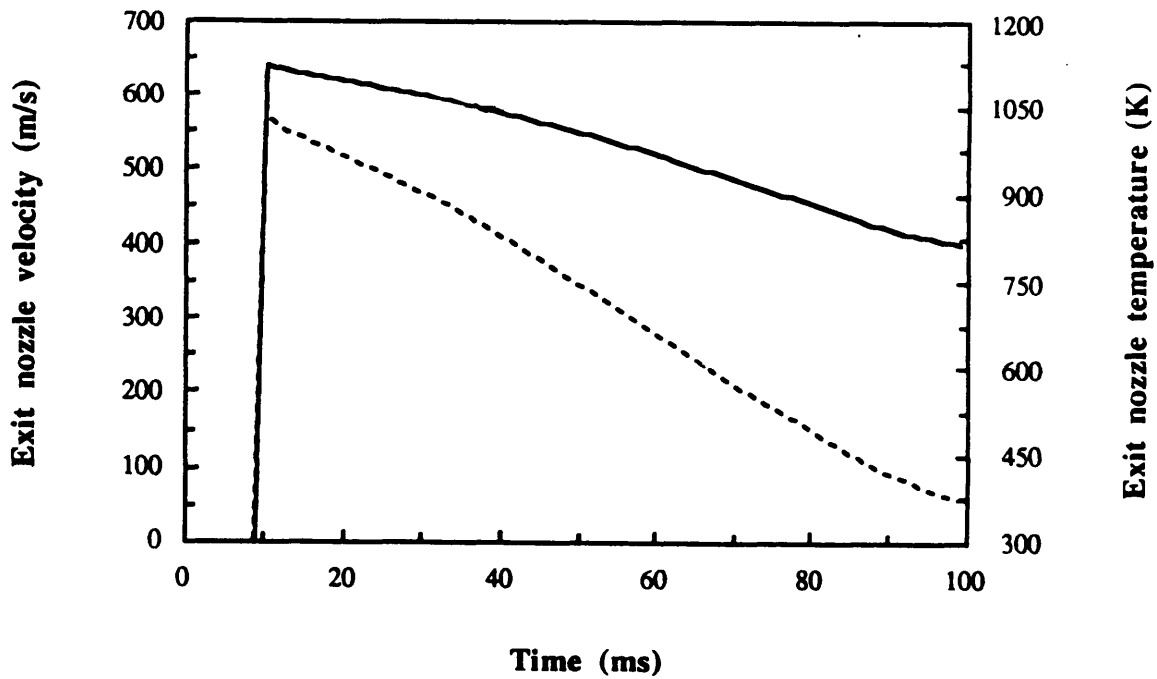


Figure 15. Mass Flow Rates out of the Combustion Chamber (continuous line) and Discharge Chamber (dotted line), Typical Automotive Airbag Gas Generator Model.
(Courtesy of P. Barry Butler, Jian Kang, and Herman Krier.)

GUIDE TO THIS THESIS

Chapter One of this thesis has introduced the Mars Pathfinder mission and the background areas that were researched to gain knowledge in the areas of gas generators, inflation models, airbag folding methods, and general airbag deployment. Chapter Two will describe the test equipment, the airbag, and the scale model used in the experiments, and Chapter Three explains the operating procedure. The four different folding schemes and trials completed in the experiments are also detailed in Chapter Three. Results of the folding schemes and the different diffusers and deflectors are given in Chapter Four, and Chapters Five and Six discuss the results and summarize the work done, respectively.

Chapter Two: Apparatus

A quarter scale mock-up of one of Mars Pathfinder's four lander petals, the associated airbag subsystem for that petal, and the other necessary test apparatus were fabricated and set up in a testing room at the Jet Propulsion Laboratory.

GENERAL TEST HARDWARE

The general test hardware included two major pieces. A base structure supporting a thirty-two gallon tank, a test bed, and a pipe connecting the tank to the test bed was the first piece, and a Lexan safety shield was the second. Figure 16 below shows a top view of the base structure and the shield. The base structure is pictured horizontally, with all units in inches, while the shield is the vertical I-shaped member. Side and front views follow on the next page in Figures 17 and 18, respectively.

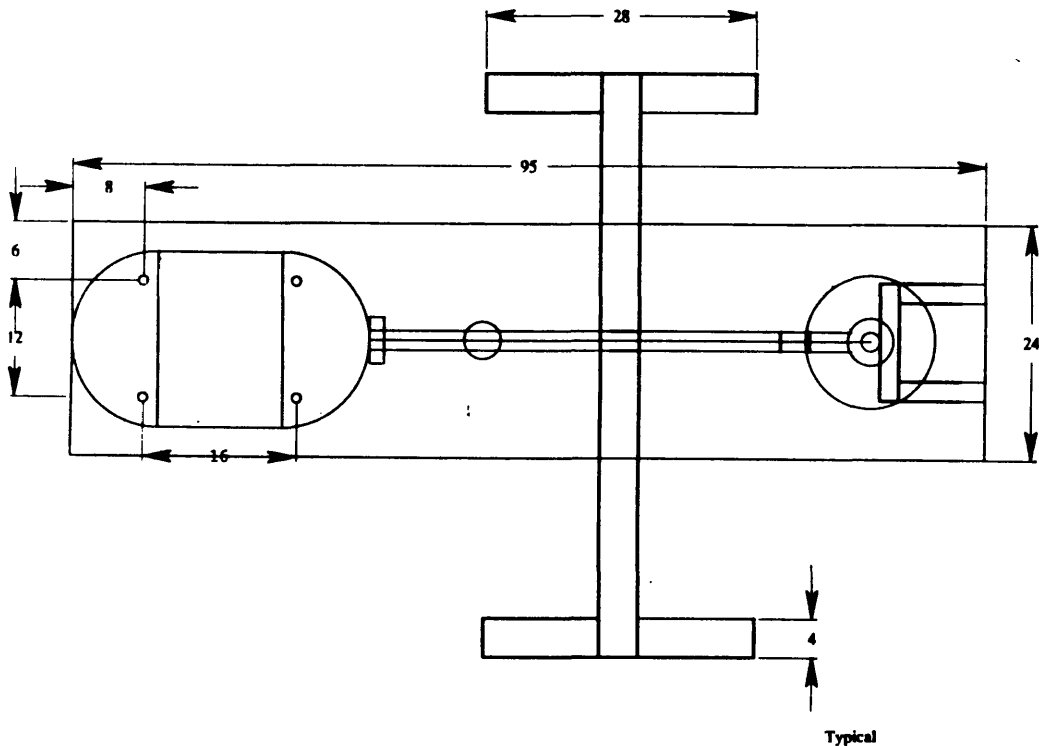


Figure 16. Base Structure and Shield, Top View.

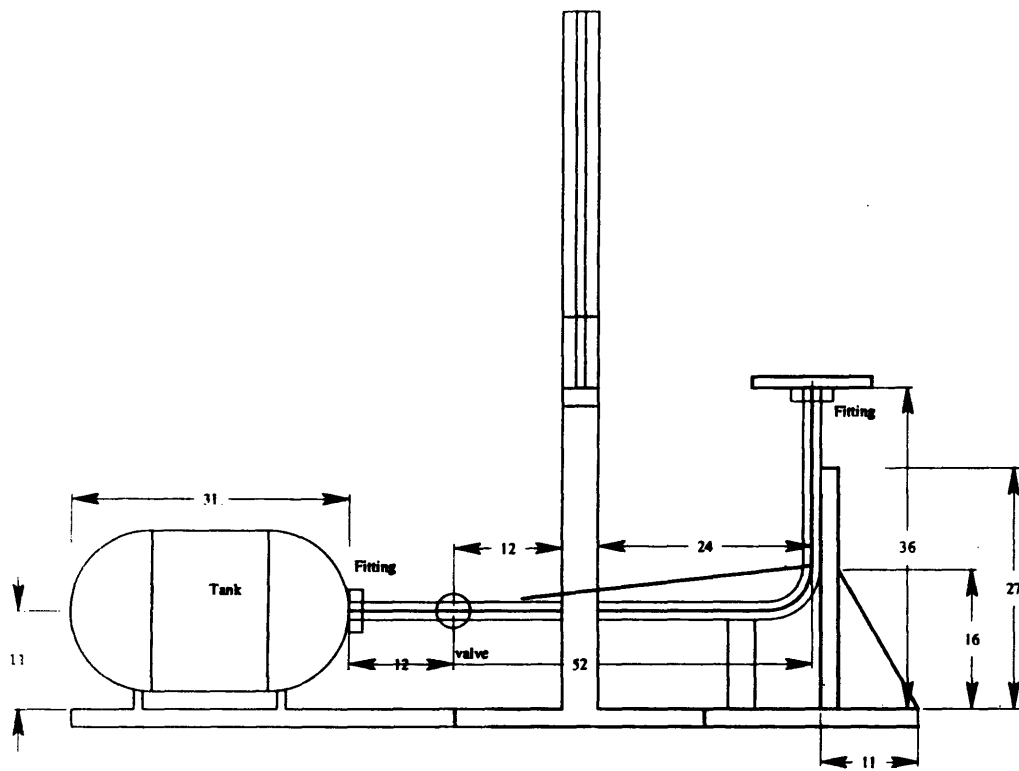


Figure 17. Base Structure and Shield, Side View.

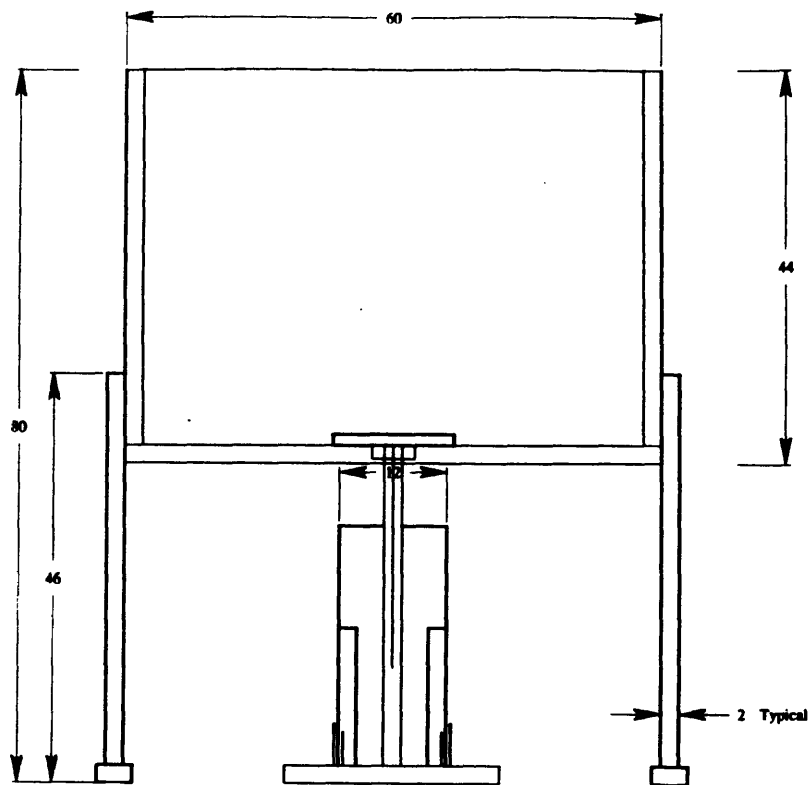


Figure 18. Base Structure and Shield, Front View.

Not pictured in the previous three figures are the inlet hose and the test bed. These are shown in the pictures of the test hardware from the front side toward the rear, and then vice versa, in Figures 19 and 20, respectively. In the view from the front, a

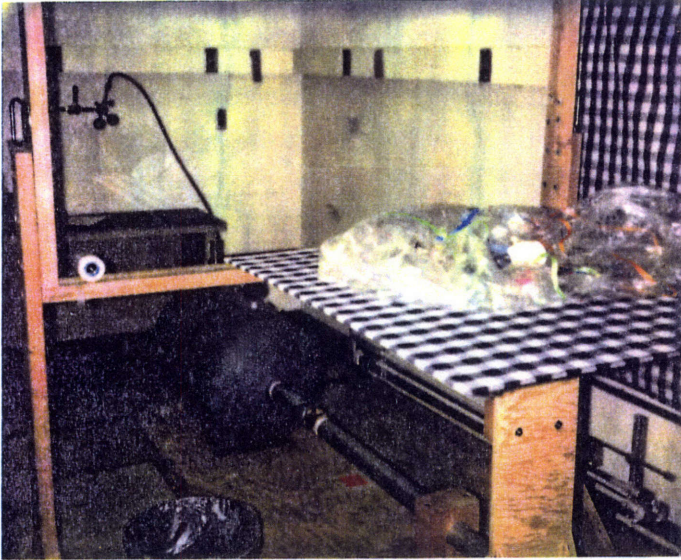


Figure 19. Test Hardware,
View from Front.



Figure 20. Test Hardware,
View from Rear.

valve can be seen against the back wall. When open, air was pumped from the source behind the wall through the valve (where the two gauges can be seen) and then through the tubing down into the back side of the gray thirty-two gallon tank. In this same picture, a pipe extends forward from the tank and curves up at a ninety degree elbow.

Half-way between the tank and the point at which the pipe curved up was a butterfly valve. This was used to release tank pressure, thereby inflating the airbag, which was located on the horizontal test bed above the vertical section of pipe that stemmed up from the ninety degree elbow. A flange at the top of the vertical pipe section mated with the forty inch square masonite test bed, which was covered with checkered cloth for a spatial reference while filming from above. A flow orifice plate was used to regulate the mass flow rate into the airbag. It was sandwiched between the pipe flange and the test bed, and cannot be seen in the picture.

MARS PATHFINDER AIRBAG

The airbag, which is shown fully inflated in Figure 21 on the following page, was a quarter scale mock-up of the Mars Pathfinder airbag. The mock-up, though made of different materials than the full scale airbag, was equipped with the full internal and external tendon assemblies and hardpoint attachments to the lander petal. For a scale reference, each square of the checkered pattern is one and a quarter inches square. Figure 22 shows an early version of the airbag that had only three lobes, whereas the current design has six, but the hardware in both designs is essentially the same. The internal and external tendons, which on the mock-up were simply ribbons fixed at their endpoints by grommets, are routed throughout the inside and outside of the airbag in directions that

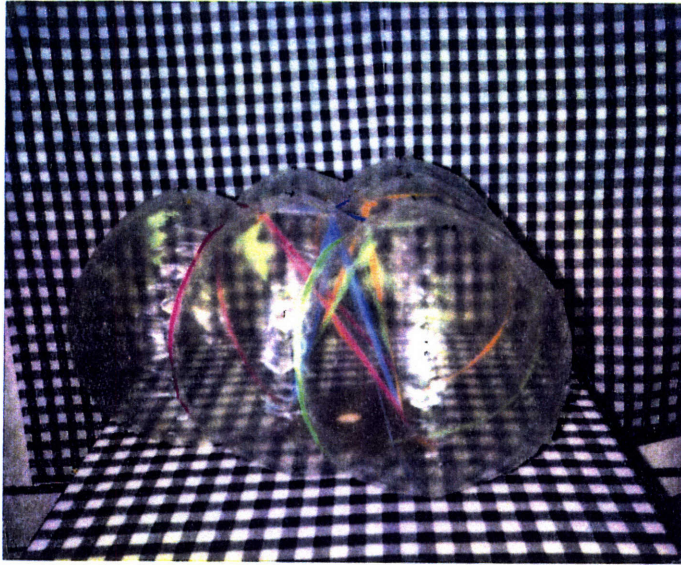


Figure 21. Quarter Scale Mars Pathfinder Airbag, Fully Inflated.

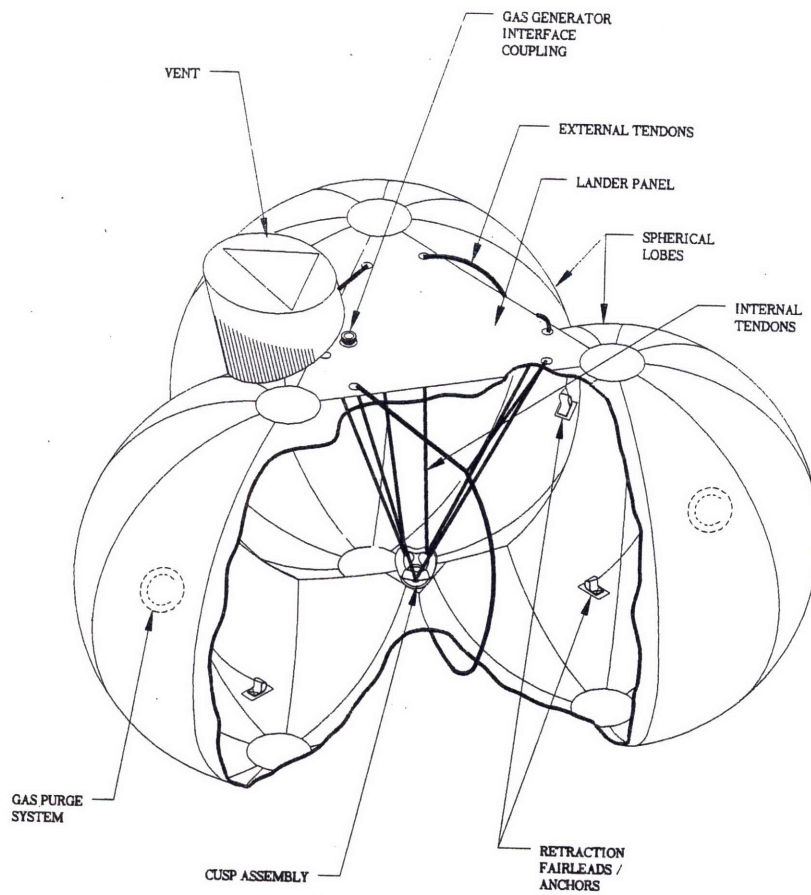


Figure 22. Mars Pathfinder Airbag Internal and External Hardware.
(Courtesy of ILC Dover, Incorporated.)

provide rigidity and tension when the airbag is loaded from any direction. The six lobe design has four cusp assemblies instead of one (shown as darkened circles in Figure 23 below), placed at the intersections of the six lobes. This new design allows for better cushioning when the lander hits the surface and for more airbag coverage over the lander petals. The quarter scale airbag was thirty-six inches along each side of the equilateral triangle formed when spread out flat on the test bed.

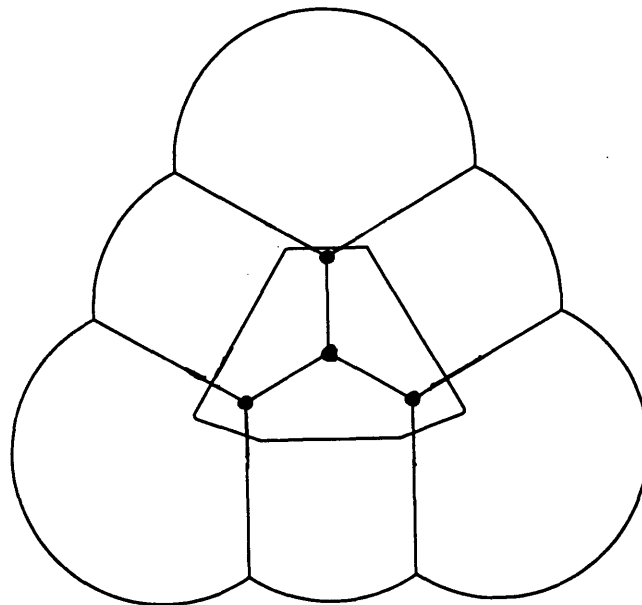


Figure 23. Six Lobe Airbag Design, Top View.

MARS PATHFINDER LANDER PETAL

The quarter scale mock-up lander petal, made of one-eighth inch thick masonite, was fixed to the quarter scale airbag at the hardpoints as shown previously in Figure 22. The petal was representative of any of the four petals on the lander, as they are all similarly shaped. It's shape and dimensions are shown in Figure 24. The petal bolted to

the pipe flange through the four bolt holes shown in the middle area of the petal, and the airbag attached to the petal on the opposite (upper) side at the small holes around it's perimeter. All dimensions in Figure 24 are in inches.

Though the placement of the gas inlet hole shown in this diagram is in the center, the most recent design change in the petal put the inlet in the lower section of the triangular petal, which is where it was for the filmed inflations included with this document. Because of the nature of the design process at the Jet Propulsion Laboratory,

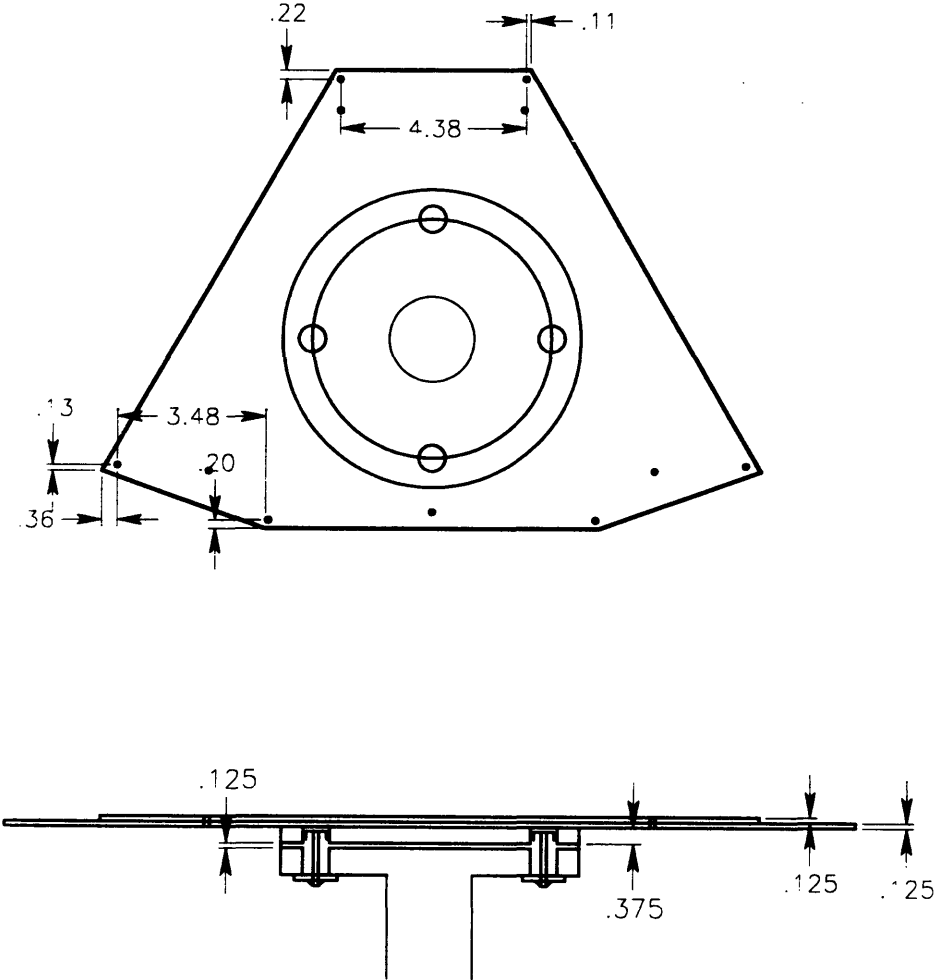


Figure 24. Quarter Scale Lander Petal, Top and Side Views.

the inlet hole position changed numerous times over this six month project. Consider Figure 24 to be for general illustrative purposes and petal dimensions only, as the inlet hole position currently being considered for the lander petal, which was the one used in the inflations for this project, was actually closer to the lower bolt hole.

FLOW DIFFUSION AND REDIRECTION

There were two primary variables of interest in this project, one of which was the folding scheme used for a given inflation. The other variable, which was of equal importance, was the method of inflation. The two different methods of inflation used were the diffusion of the airflow entering the airbag inlet hole and the deflection of it.

DIFFUSERS

A swatch of material, either high or low porosity, depending on the desired inflation duration, was clamped over the diffuser/deflector flange to regulate the air flow into the airbag. The diffuser/deflector flange, which was simply an aluminum tube with lipped edges that accommodated both diffusers and deflectors, bolted directly to the orifice plate. The airflow redirection devices were clamped with a hose clamp to the diffuser/deflector flange. The air flow entered the airbag after traveling first through the orifice plate at the end of the pipe, then through the diffuser/deflector flange, then through whatever flow redirection device was attached to the diffuser/deflector flange. The diffusers, swatches of material with different porosities, are shown in Figure 25. If slow inflation was the objective of a particular trial, low porosity satin was clamped to the diffuser/deflector flange. If rapid inflation was desired, high porosity cotton was used.

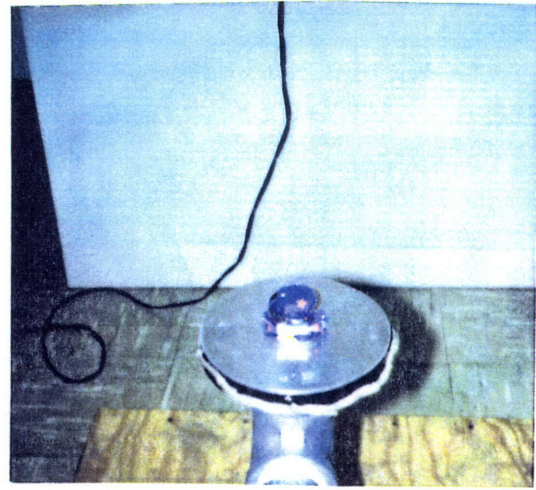
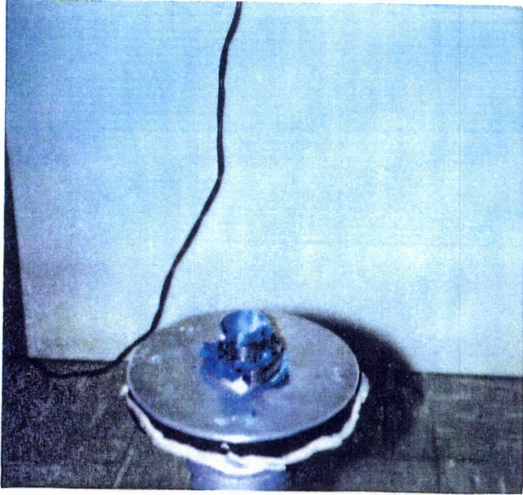


Figure 25. Diffusers. Low Porosity (left) and High Porosity (right).

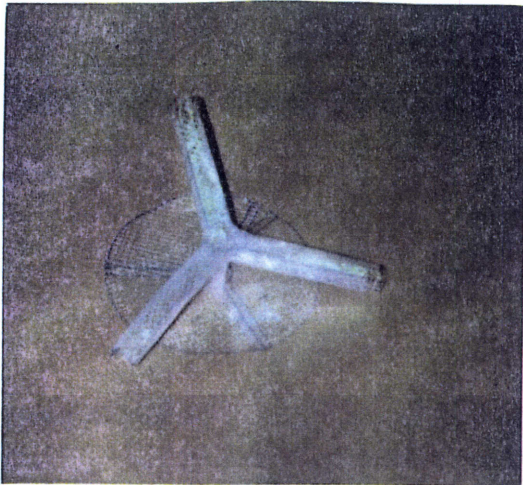


Figure 26. Deflectors. Tri-chute (left) and Redirection Sock (right).

DEFLECTORS

Figure 26 displays a tri-chute deflector and a flow redirection tube. The tri-chute deflector split the air flow in three directions angled one hundred twenty degrees apart. A simple flow redirection sock is pictured in Figure 26. With both of these deflectors, the air flow was not diffused in any manner, and entered the airbag in a direct stream from the vertical pipe through the diffuser/deflector flange

The reasons for the use of each of the different diffusers and deflectors will be detailed in the explanation of the trials. Note that the test bed (the masonite square covered with checkered cloth onto which the mock-up lander petal and airbag are bolted) has been removed from Figures 25 and 26 so that the orifice plate and flow diffusion and redirection devices may be seen clearly.

DATA RECORDING MEDIA

Data recording devices used for the folding schemes and inflations in this thesis include a Polaroid camera, a Sony Handycam video recorder, and a handwritten fold form. Each fold of each of the four folding schemes was video taped as it was being performed, and a Polaroid shot was taken at the end of each fold. Also used to record folding schemes was a paper form of recording folds that has sections for both verbally and visually explaining how each fold was made and what the resulting geometry was after completing the fold. The inflations for the varying flow inlet conditions and the four different folding schemes were all video taped.

Chapter Three: Procedure

The deliverable of this thesis was a document to ILC Dover, Incorporated outlining the processes by which four folding schemes were completed and their resulting inflation dynamics. Folding schemes are sets of individual folds, done one at a time, that when done in the proper order result in a certain folded geometry. Deployment dynamics, which are basically the characteristics of an inflation (such as “smooth,” “even,” or “lopsided”) that can be used to describe or define it, are dictated by the original folded geometry of the airbag. The packaged geometry of an airbag, when paired with a particular choice of air flow diffusion or redirection, entirely determines the deployment dynamics.

In this set of experiments, the folding process and the particular order in which the folds were made were of utmost importance, while diffuser and deflector design were of secondary importance, to the Jet Propulsion Laboratory and ILC Dover, Incorporated. ILC Dover, Incorporated will be designing, fabricating, and packaging the Mars Pathfinder Airbag Subsystem, and will be using the quarter scale experiments described in this thesis to help direct their efforts to produce an optimal folding scheme and optimal gas inlet conditions. Because the actual folding process and the particular folds that comprise each folding scheme were both of primary interest, the conveyance of not just the results of the inflations done with the quarter scale test setup, but also the operating procedures leading up to those results, was the main objective of this project.

OPERATING PROCEDURE

PREPARATION

For each individual step of a folding scheme the fold was video taped as it was being made; a Polaroid picture of the fold was taken after it was performed; and then the resultant shape of the airbag was recorded on a fold form (which will be described below). For example, the first step of each of the four folding schemes was always to vacuum all of the air out of the airbag. Then the “hand hole,” a small slit in the side of one of the airbag’s lobes through which the internal airbag hardware could be accessed, was taped shut. Finally, the airbag was spread out into a flat, triangular shape on the test bed.

This preparatory step of each scheme was recorded as Step A of whichever folding scheme was being performed. The individual folds were lettered, so the second step of every scheme was labeled Step B of that scheme, the third C, and so on. The folding schemes, which were specific collections of steps performed in a certain order, were numbered one through four. Each of the four folding schemes was paired up with each of the methods of air flow modification described in the previous chapter to produce different trials, all of which were numbered. For example, Folding Scheme One paired with the low porosity diffuser was Trial One, while Folding Scheme Two paired with that same method of air diffusion was a separate numbered trial -- Trial Two, in this case.

BEFORE EACH FOLD

Because of the importance of reproducibility of these folding schemes to ILC Dover, Incorporated, a fold form was devised so that the series of folds comprising each

folding scheme could be repeated on the full scale airbag to produce the same packaged geometry (to achieve the same inflation dynamics) as that which was achieved with the quarter scale mockup. Each fold was described in detail, with explicit directions as to how to proceed before and after that particular fold. An example of a fold form for Step A of Scheme Two is shown below in Figure 27.

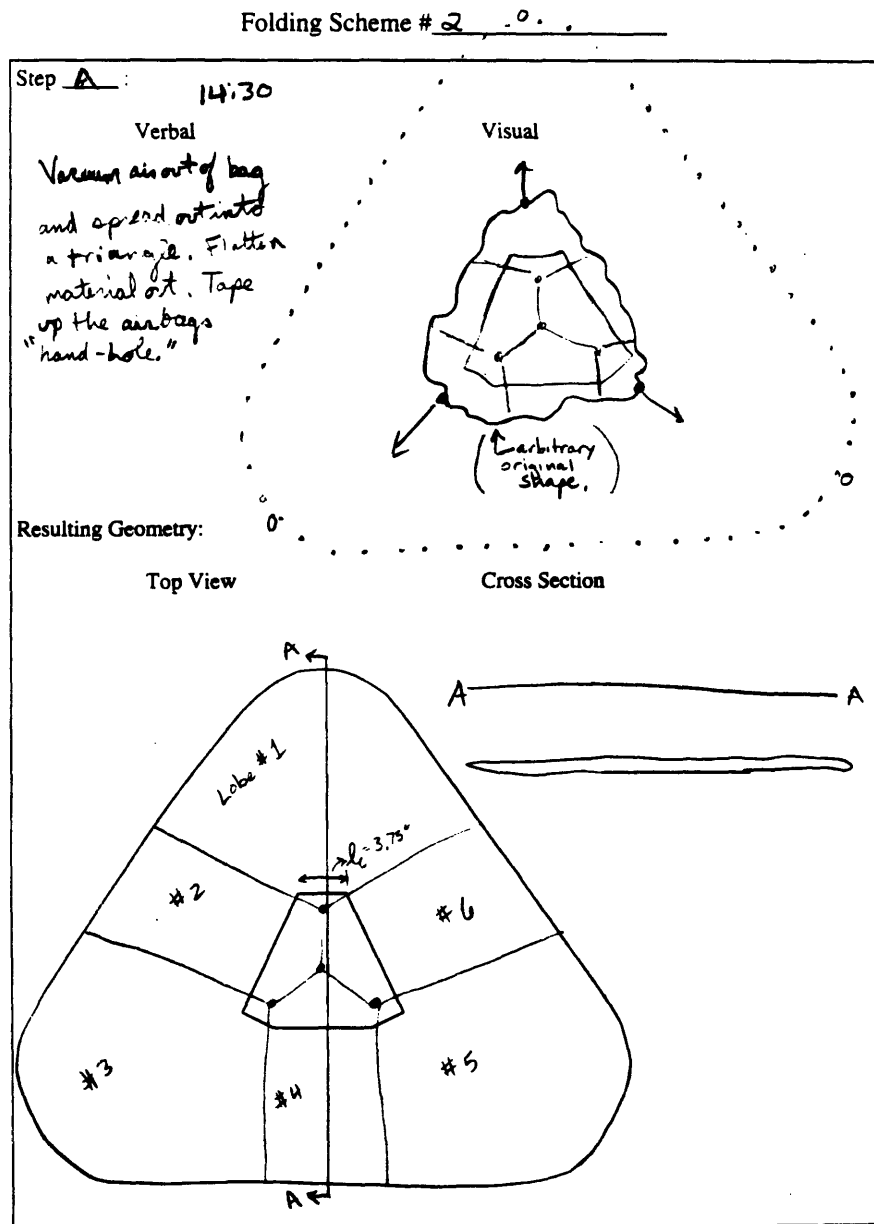


Figure 27. Fold Form for Step A of Scheme Two.

The top half of the fold form describes both verbally and visually how the fold was to be made. In this case, the operation being performed was not exactly a fold, but this first step's simplicity allows the four areas of the fold form and the information they contain to be displayed in a format that is easy to understand.

The left half of the upper portion of the fold form describes verbally how to perform the upcoming fold, and the right describes it visually. In the visual sketch, bold lines indicate the current perimeter of the airbag, while dotted indicate where the perimeter will lie once the fold has been made. The dark, filled-in circles indicate "grab points" -- suggested places to hold the airbag material as the fold is being made -- and open circles indicate where the material at the grab points should be after the fold is complete. Arrows show the motion or direction that one moves the grab points to achieve that particular fold. After filling out the upper half of the fold form, the fold was then carried out while being video taped.

AFTER EACH FOLD

A Polaroid picture was taken after the fold was done on the airbag. The lower half of the fold form, which shows both a top view sketch and a cross section of the airbag after the fold described in the upper half of the form has been made, is then filled out. To allow for easier reproduction of these folding schemes with the ILC Dover, Incorporated full scale airbags, all dimensions that characterized a fold were measured in characteristic lengths, which, in these folding schemes, was chosen arbitrarily to be the distance between the two hardpoints on the upper edge of the lander petal. This distance on the quarter scale mock-up was 3.75 inches.

On the first fold form of each scheme the airbag lobes were numbered so that they could be referred to in folding instructions. Because the folding schemes got more complex with each fold made, drawing all previous folds in the sketch cluttered the view from the top and proved to be more of a hindrance than a help, so the airbag was treated as being opaque, and only the most recent fold and the perimeters of that fold as seen from above were drawn.

INFLATION

After each folding scheme had been performed and documented with the fold forms, Polaroid pictures, and video tape, its inflation was then filmed. For each inflation the thirty-two gallon tank was pressurized up to twenty-two pounds per square inch. This was found to be just enough air to unfurl all the folds and allow the airbag to assume its full shape, but not so much air that excessive forces were placed on the tendons or that the bag was damaged in any way. The butterfly valve in the pipe connecting the tank to the airbag was pushed to an open position allowing the tank to release the pressurized air, which then inflated the airbag.

FOLDING SCHEMES

FOLDING SCHEME ONE

Scheme One was intended to be an example of a “bad” scheme. There were several folds that entirely covered other folds, which caused unnecessarily large deployment loads. Large deployment loads are responsible for not only violent motions when folds of a scheme unfurl, but also damage to the airbag when the forces on the inner surface of the airbag exceed those required to unfurl a fold. Each step of Folding Scheme

One had very large portions of material left overhanging the lander petal edges, which means that with each successive fold unfurled, the internal forces required to unfurl the flaps of material were very large compared to other types of folds used in later schemes. The larger the flap of material that extends beyond the fold line, the more difficult it is to unfurl and inflate for the blast of air trying to unfold it.

Folding Scheme One is described both verbally and visually in the fold forms that follow in Figure 28. The pictures that were taken after each fold are shown in Figure 29. Only pictures of Steps A through G are included because the pictures beyond that point do not convey enough information about the folds. If attempting to recreate this folding scheme, the fold forms and the video tape should be used. The still pictures beyond the first few folds are of marginal value because of the added complexity that the folding scheme takes on with each successive fold. The time-stamped video tape included with this thesis shows the entire succession of folds that comprise Folding Scheme One. The segment begins at about eight and a half minutes into the tape and lasts for roughly five minutes.

Folding Scheme # 1

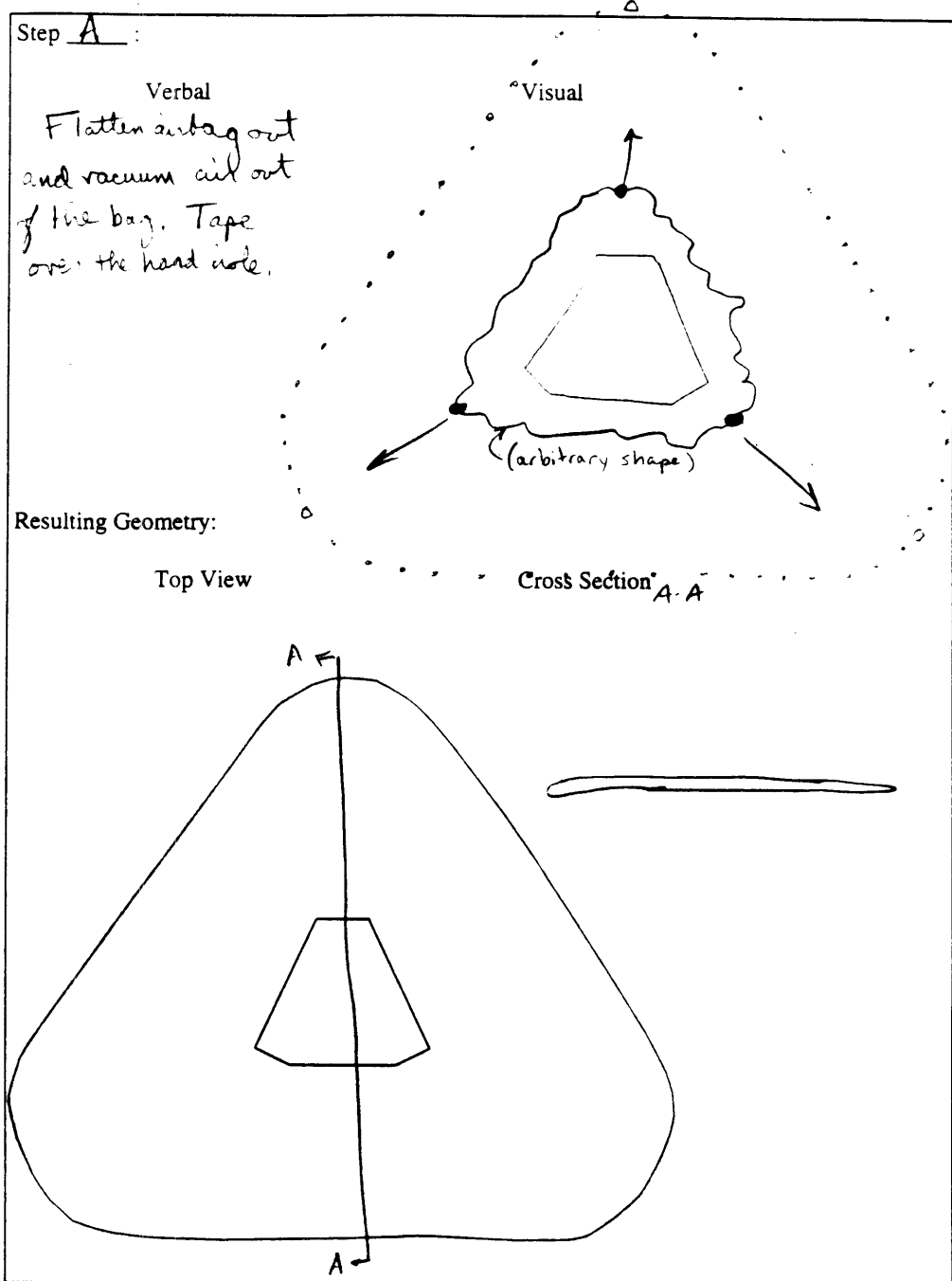


Figure 28. Fold Forms for Folding Scheme One.
Step A.

Folding Scheme # 1

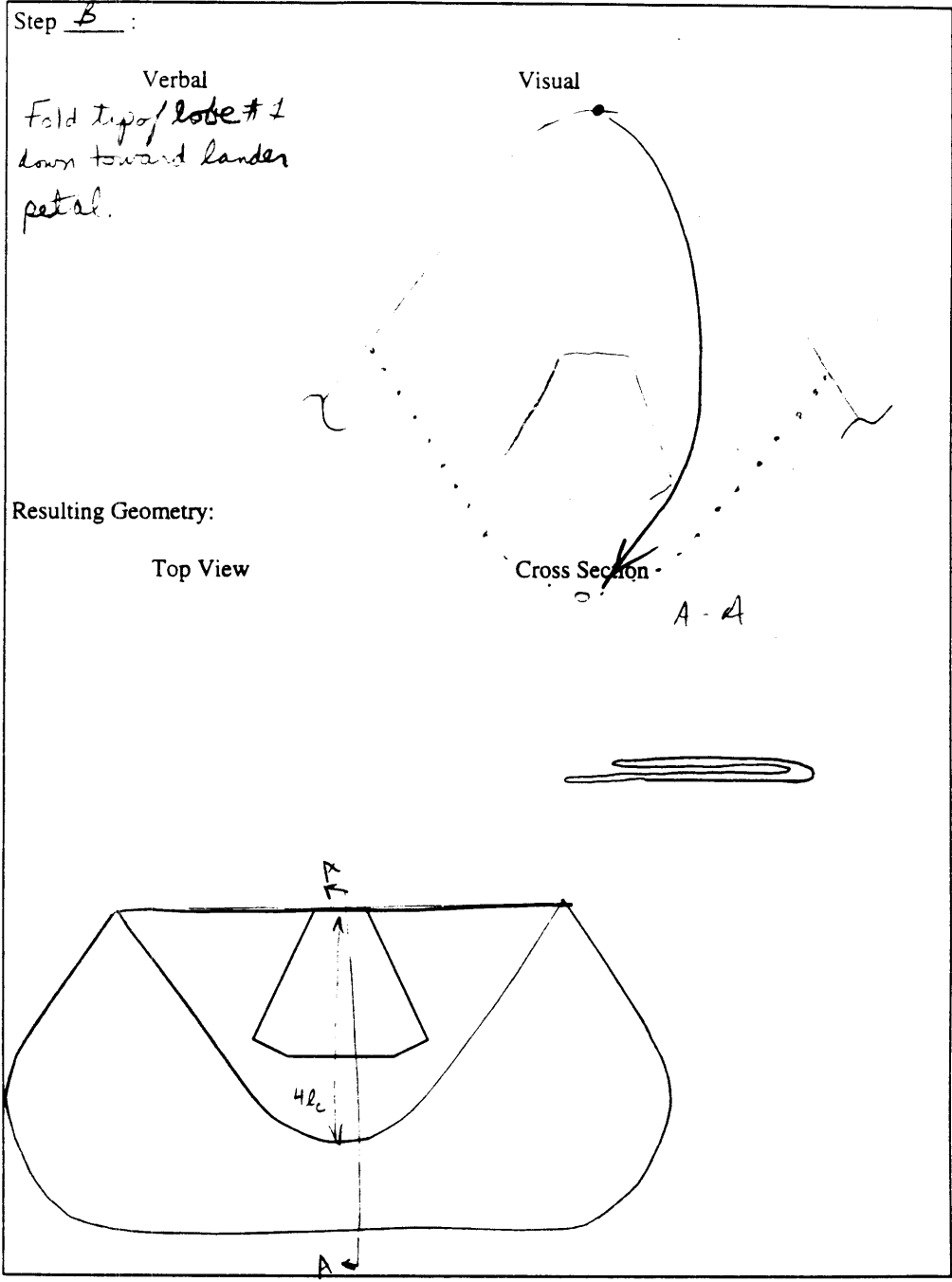


Figure 28. Fold Forms for Folding Scheme One, Continued.
Step B.

Folding Scheme # 1

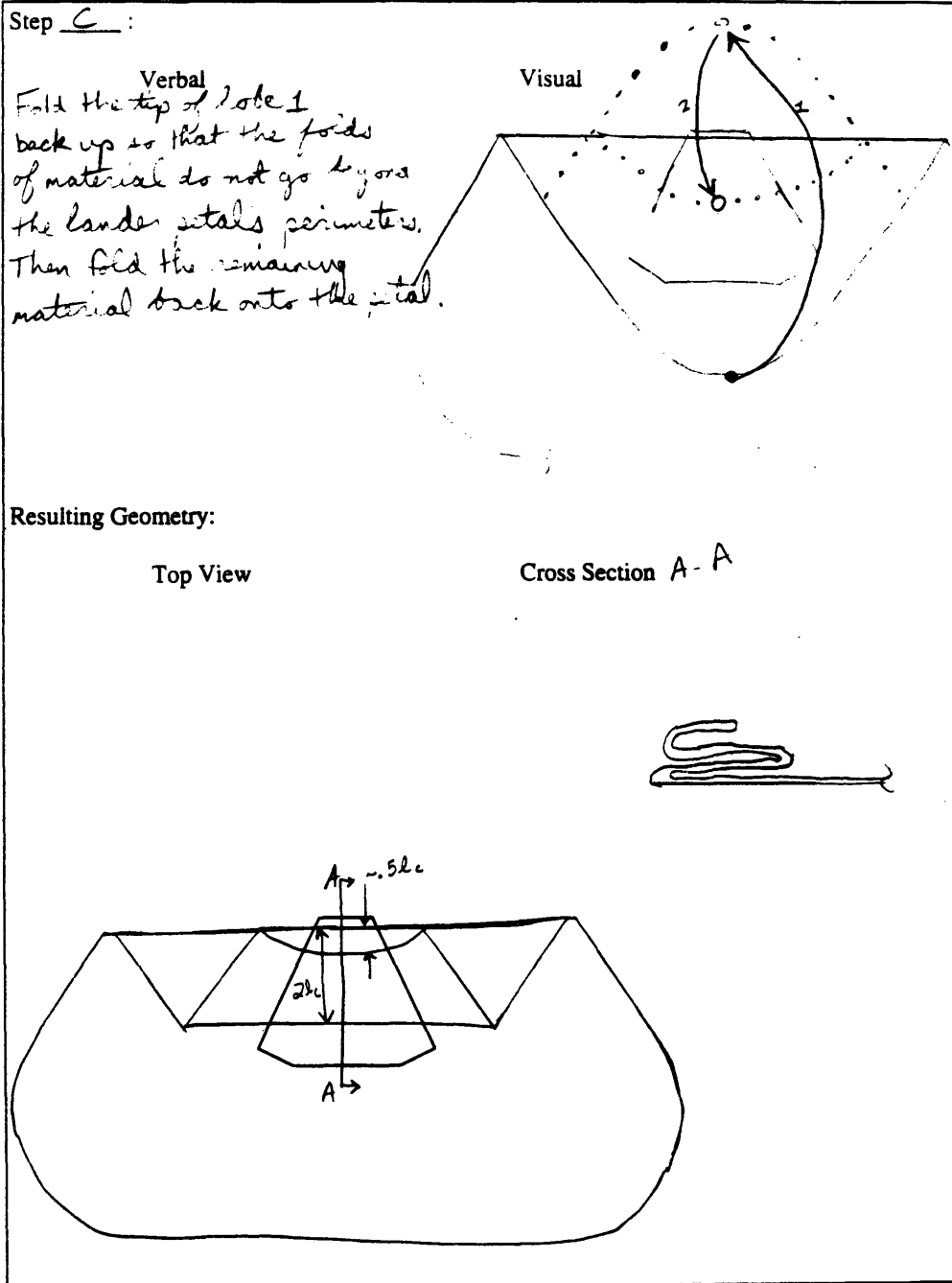


Figure 28. Fold Forms for Folding Scheme One, Continued.
 Step C.

Folding Scheme # 1

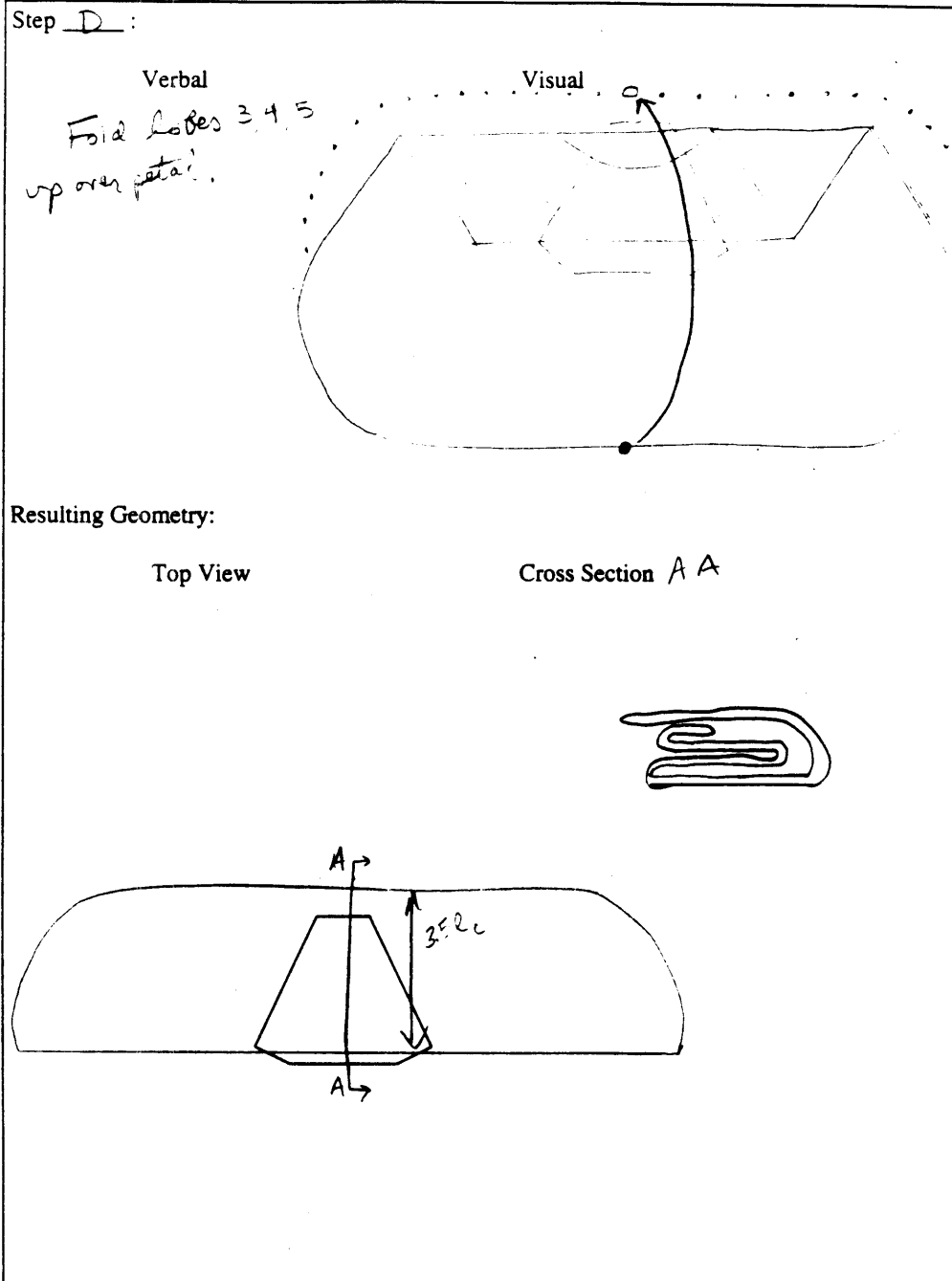


Figure 28. Fold Forms for Folding Scheme One, Continued.
Step D.

Folding Scheme # 1

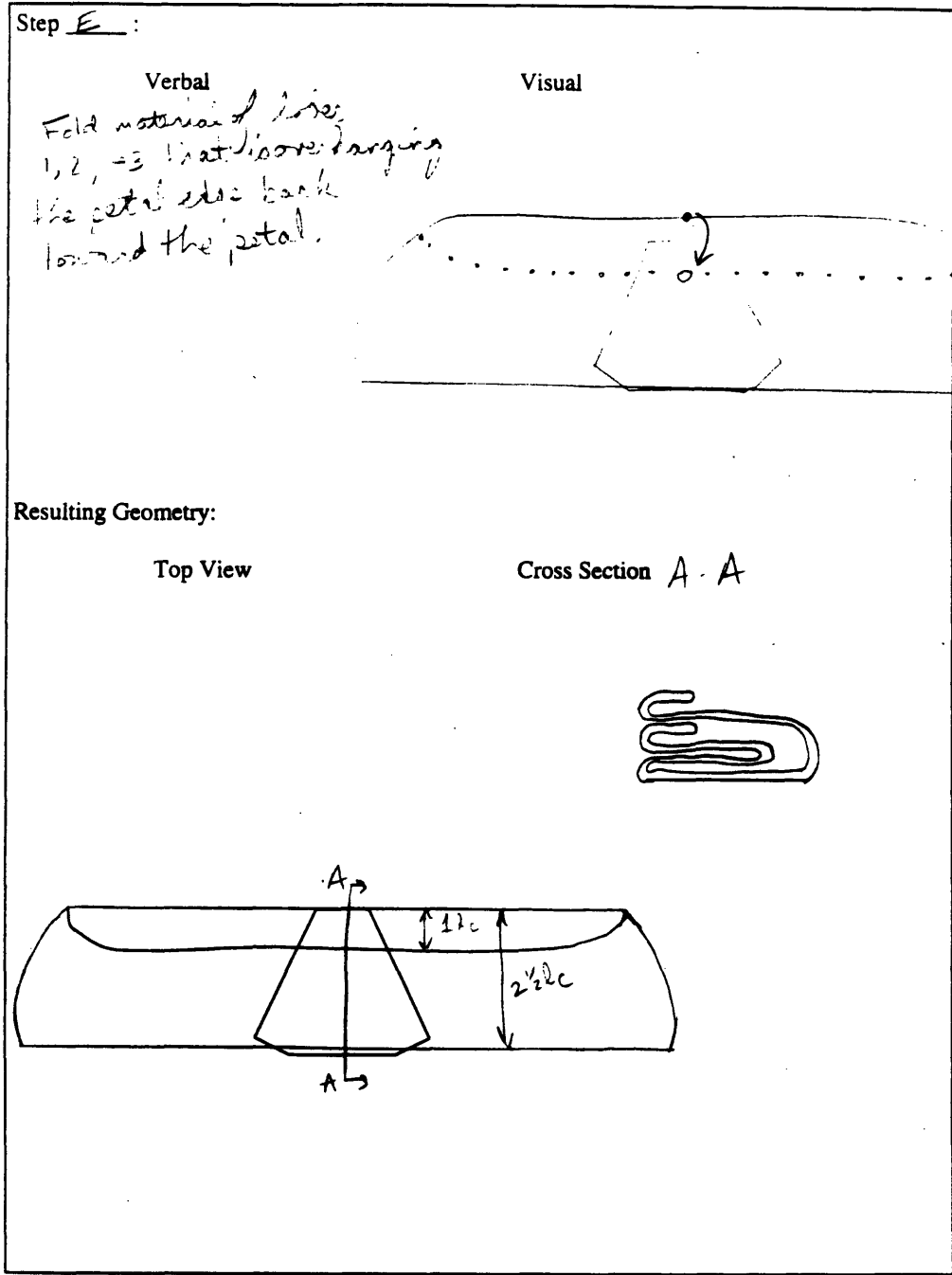


Figure 28. Fold Forms for Folding Scheme One, Continued.
Step E.

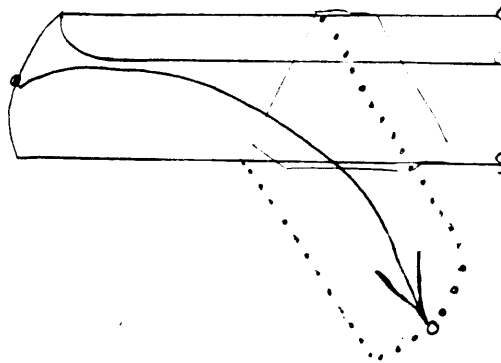
Folding Scheme # 1

Step F:

Verbal

Fold the flap containing
leaves 1, 2, and 3 (the
LEFT flap) down and
to the right lower corner
so that the fold line
is parallel to the left
petal edge.

Visual



Resulting Geometry:

Top View

Cross Section A-A

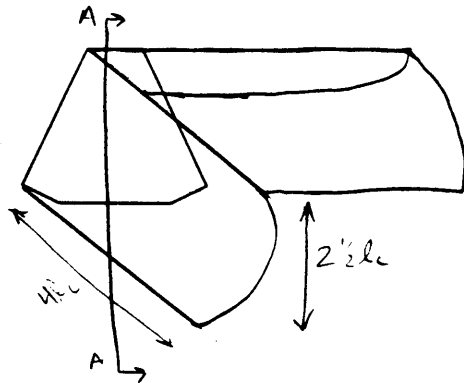
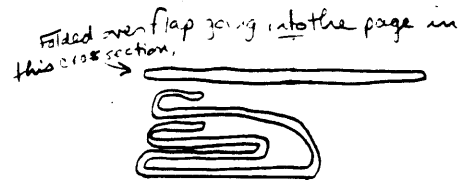


Figure 28. Fold Forms for Folding Scheme One, Continued.
Step F.

Folding Scheme # 1

Step G :

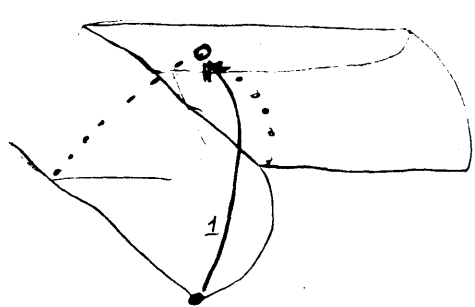
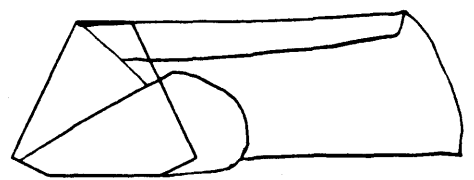
<p>Verbal Fold portion of flap containing folded 2 and 3 back up toward petal. Fold along line at base of petal.</p>	<p>Visual</p> 
<p>Resulting Geometry:</p>	
<p>Top View</p>	<p>Cross Section</p>
	

Figure 28. Fold Forms for Folding Scheme One, Continued.
Step G.

Folding Scheme # 1

Step ~~H~~ :

Verbal	Visual
<i>Fold the remaining flap of material back to the left over the petal.</i>	

Resulting Geometry:

Top View	Cross Section
	<hr/>

Figure 28. Fold Forms for Folding Scheme One, Continued.
Step H.

Folding Scheme # 1

Step I :

Verbal	Visual
<p>Fold right flap containing edges 1, 6 and 5 inward toward the left corner. Fold along the petals edge.</p>	
Resulting Geometry:	
Top View	Cross Section

Figure 28. Fold Forms for Folding Scheme One, Continued.
Step I.

Folding Scheme # 1

Step I:

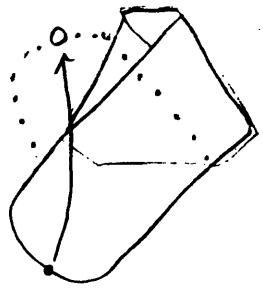
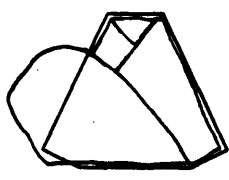
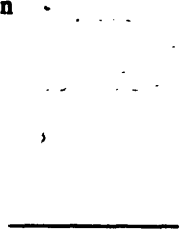
<p>Verbal</p> <p>Fold the remaining material below the petal upwards using the petal's lower edge as a fold line.</p>	<p>Visual</p> 
<p>Resulting Geometry:</p>	
<p>Top View</p>	<p>Cross Section</p>
	

Figure 28. Fold Forms for Folding Scheme One, Continued.
Step J.

Folding Scheme # 1

Step K :

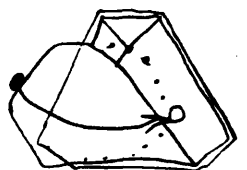
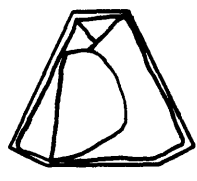
<p>Verbal</p> <p><i>Fold the material overhanging the petal base on the left back toward the petal's center.</i></p>	<p>Visual</p> 
<p>Resulting Geometry:</p>	
<p>Top View</p>	<p>Cross Section</p>
	<hr/>

Figure 28. Fold Forms for Folding Scheme One, Continued.
Step K.

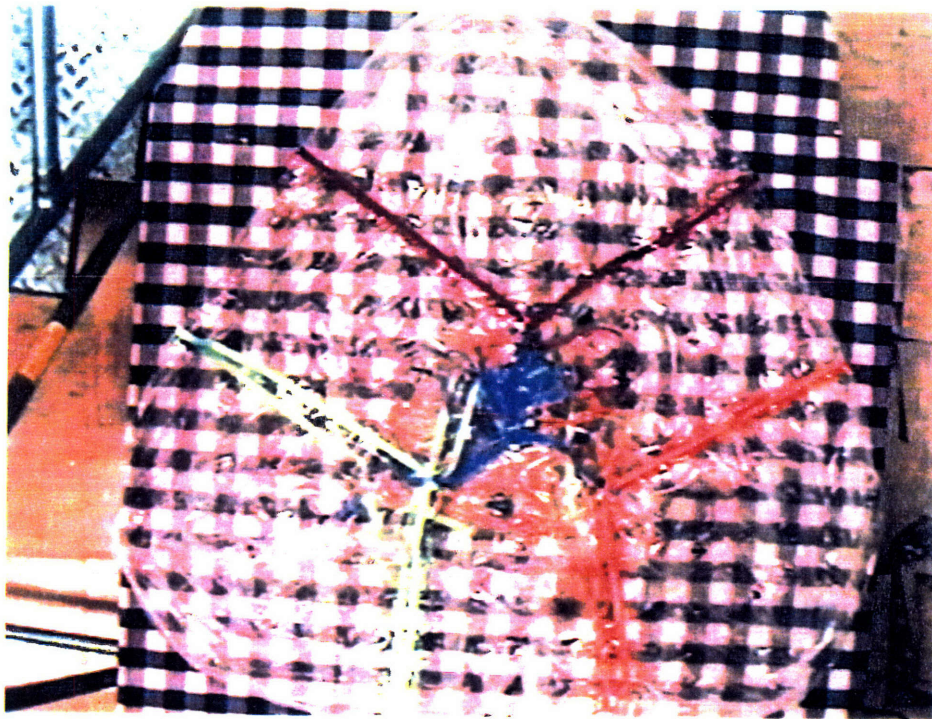


Figure 29. Pictures of the Steps of Folding Scheme One.
Step A (below).

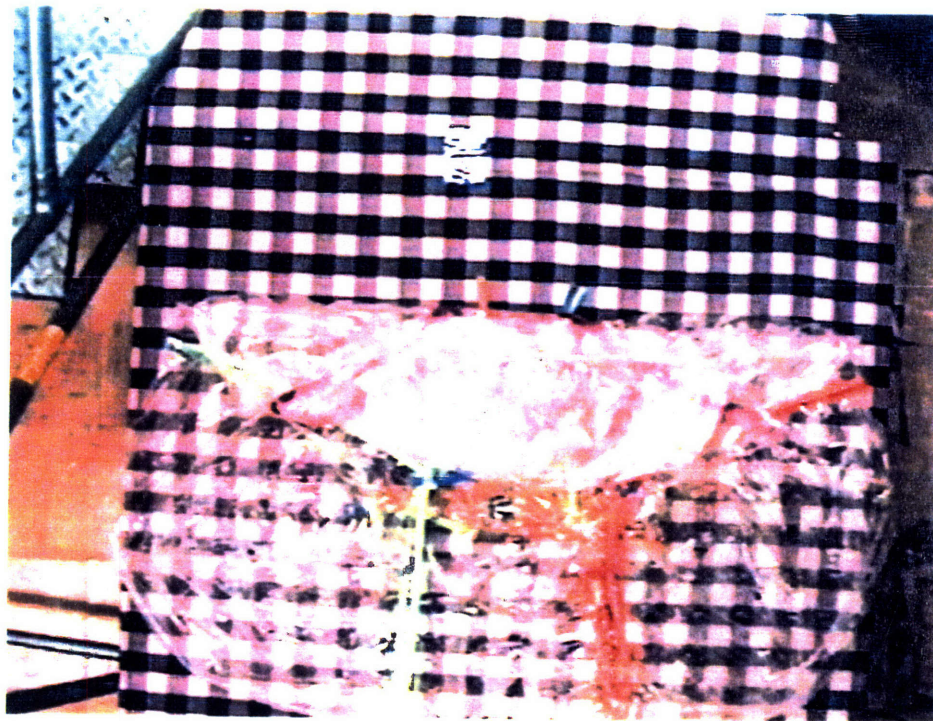
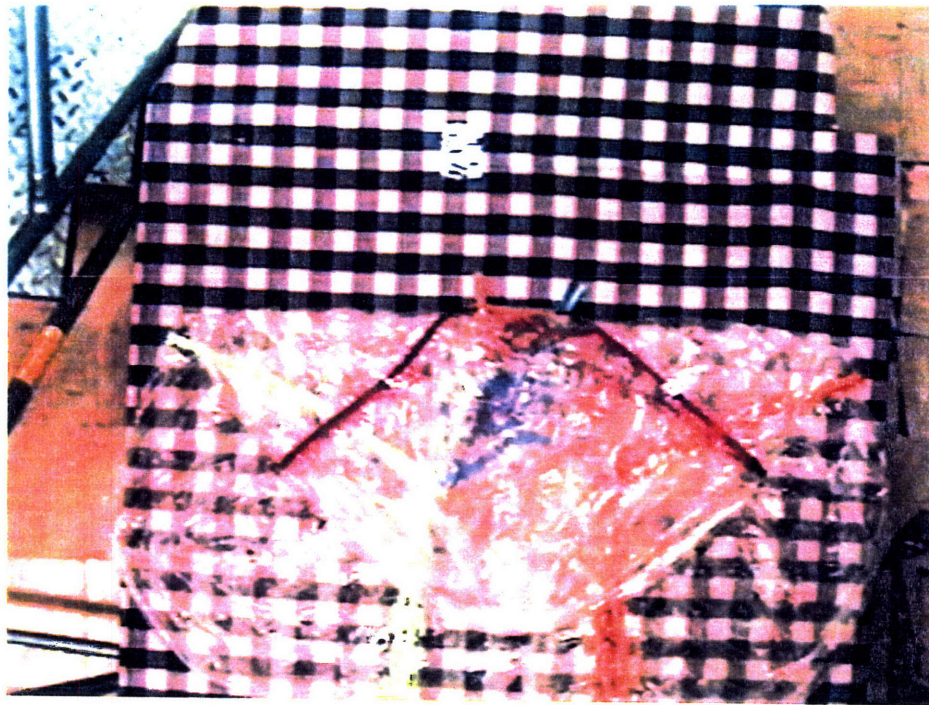


Figure 29. Pictures of the Steps of Folding Scheme One, Continued. Steps B (above) and C (below).

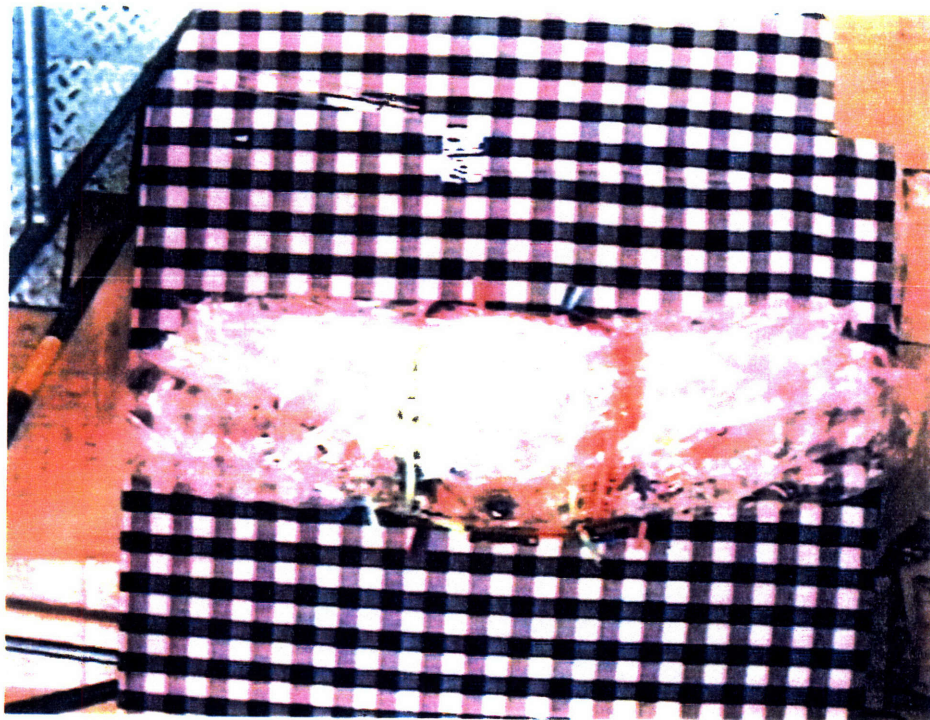
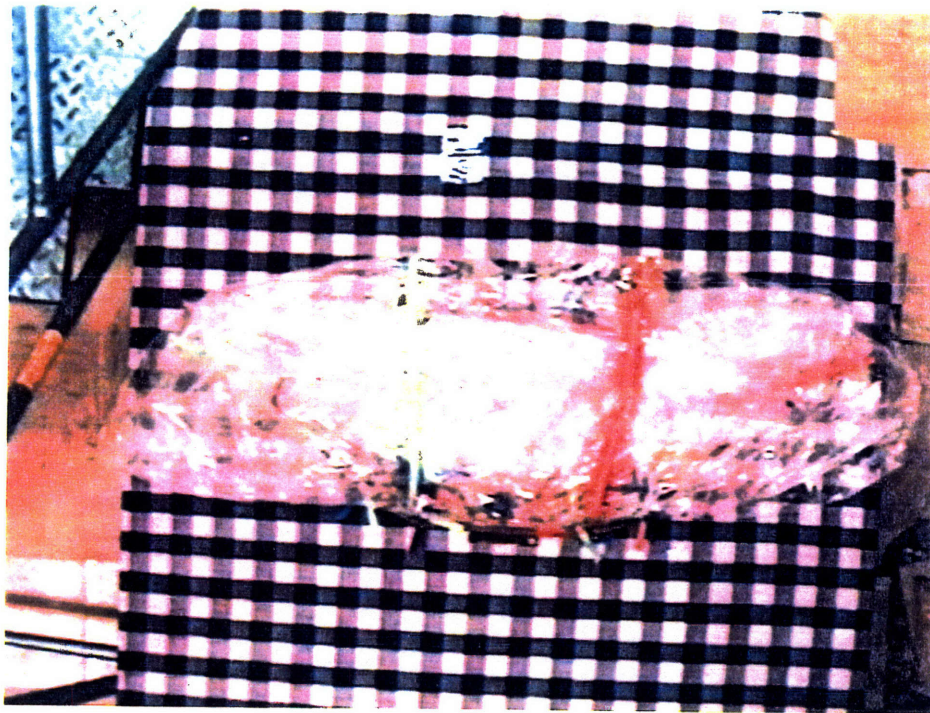


Figure 29. Pictures of the Steps of Folding Scheme One, Continued.
Steps D (above) and E (below).

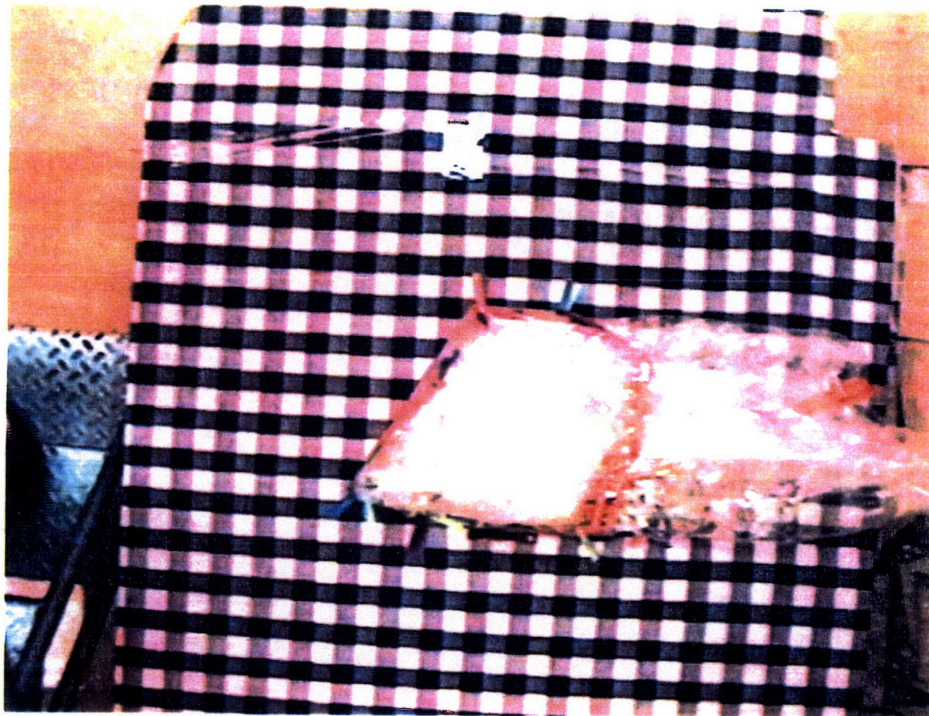


Figure 29. Pictures of the Steps of Folding Scheme One, Continued.
Steps F (above) and G (below).

FOLDING SCHEME TWO

Scheme Two is a design that could best be described as continuous helical accordion fold. It begins at the base of the airbag making “S” shaped folds that spiral clockwise and upward in a helical pattern. After the first fold was made on the lower side of the lander petal (Step B), the same fold was performed along the petal edge to the left of the base. Then the same “S” shaped accordion fold was done along the petal edge to the left of that, and so on, until the material leading up to the top of the airbag was completely folded up within the bounds of the lander petal edges, with the exception of the three flaps of material overhanging the edges. The fold forms for Folding Scheme Two are included in Figure 30 and pictures of the first few steps can be found in Figure 31. The five minute video segment showing the steps of Folding Scheme Two can be seen on the video tape after the fifteen minute marker.

Folding Scheme # 2 . 0 .

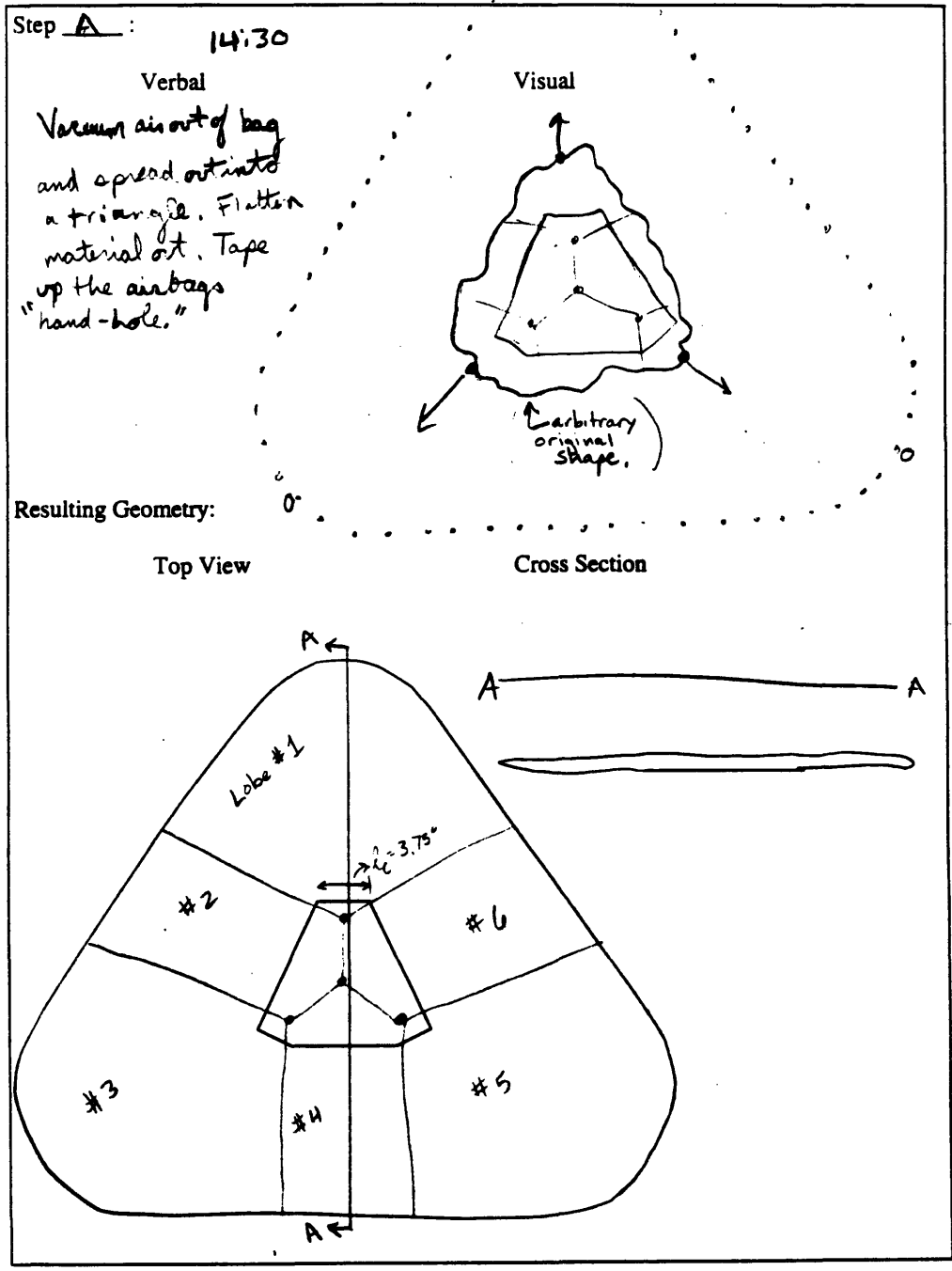


Figure 30. Fold Forms for Folding Scheme Two.
 Step A.

Folding Scheme # 2

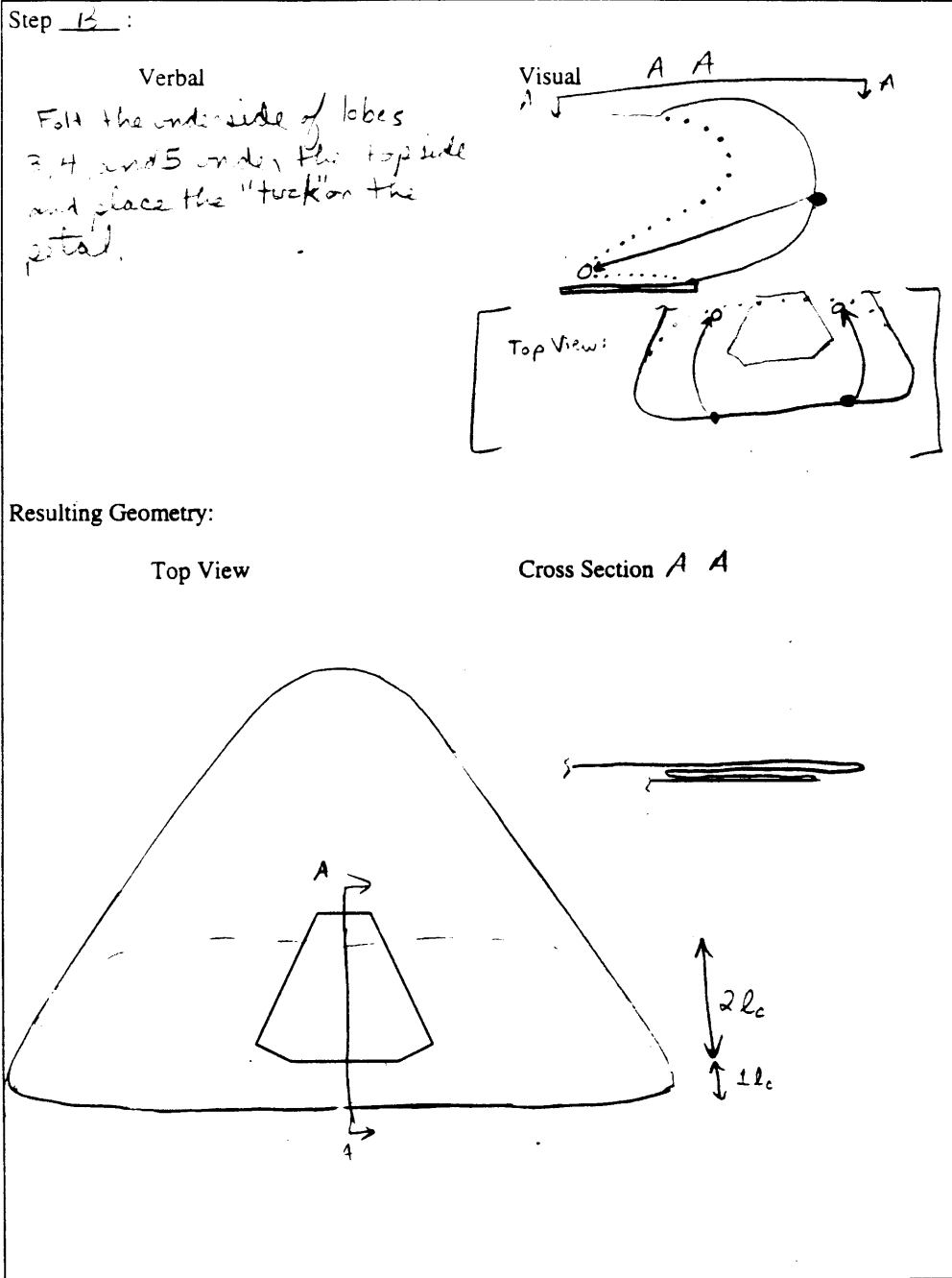


Figure 30. Fold Forms for Folding Scheme Two, Continued.
 Step B.

Folding Scheme # 2

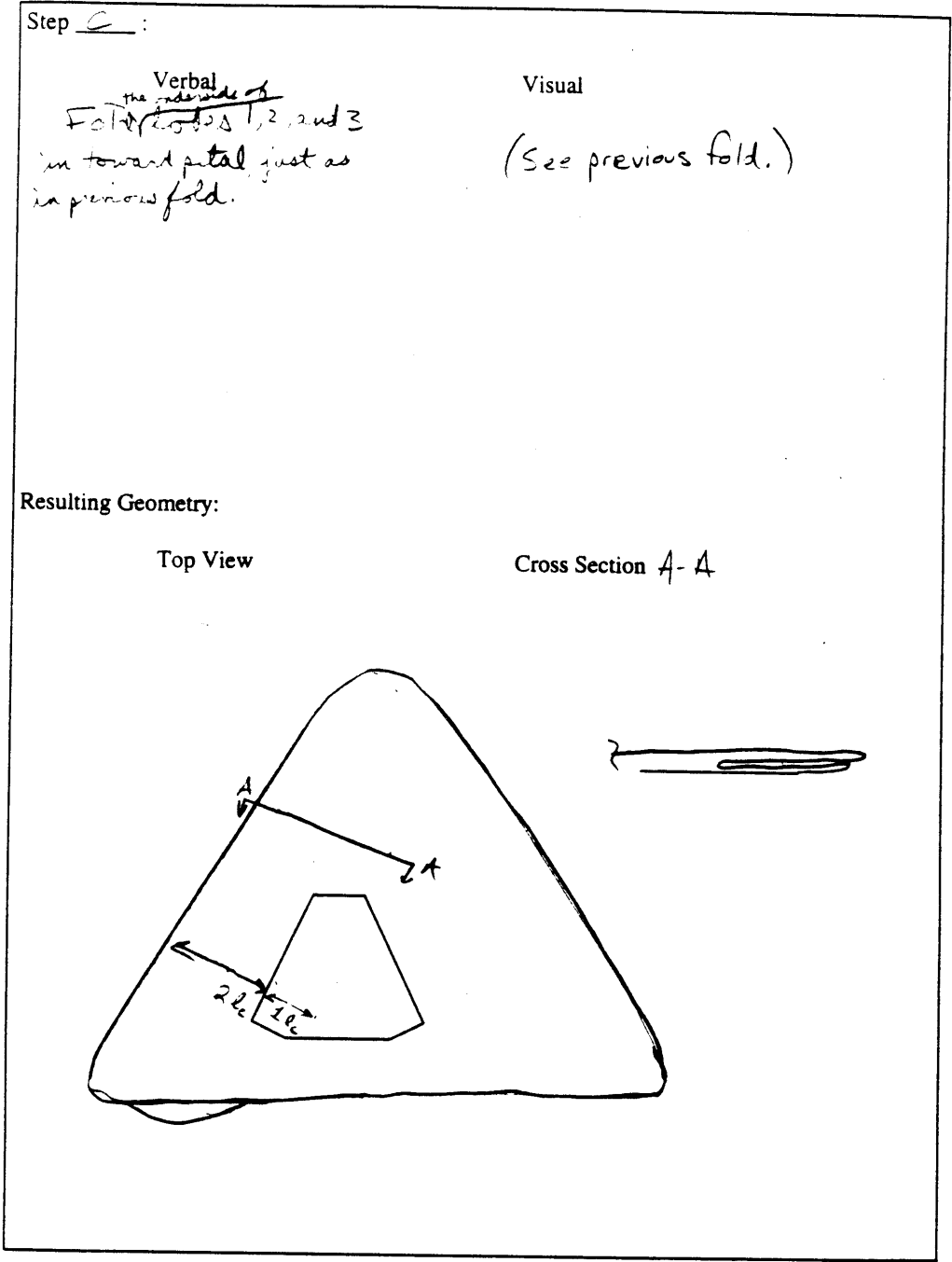


Figure 30. Fold Forms for Folding Scheme Two, Continued.
Step C.

Folding Scheme # 2

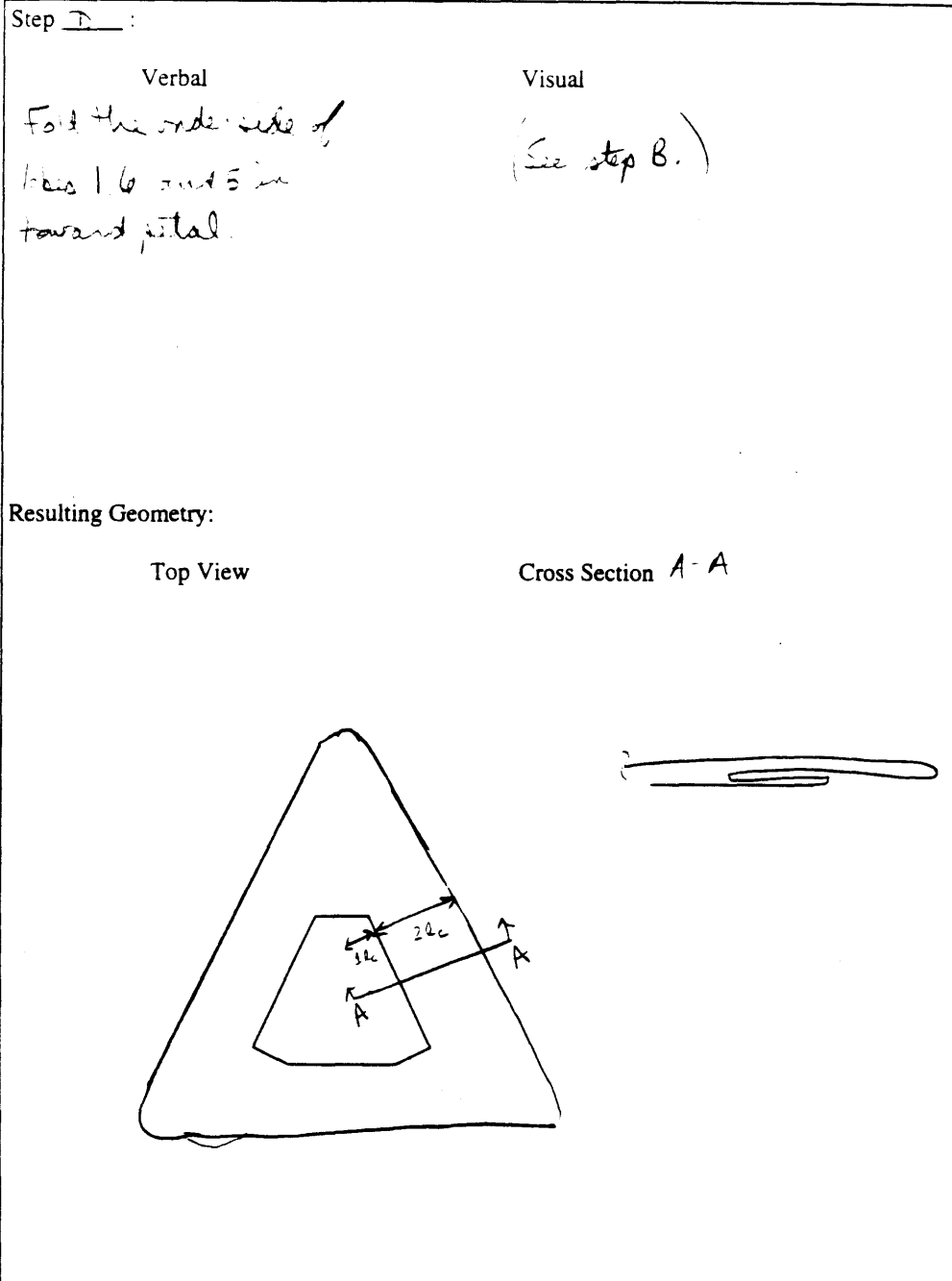


Figure 30. Fold Forms for Folding Scheme Two, Continued.
Step D.

Folding Scheme # 2

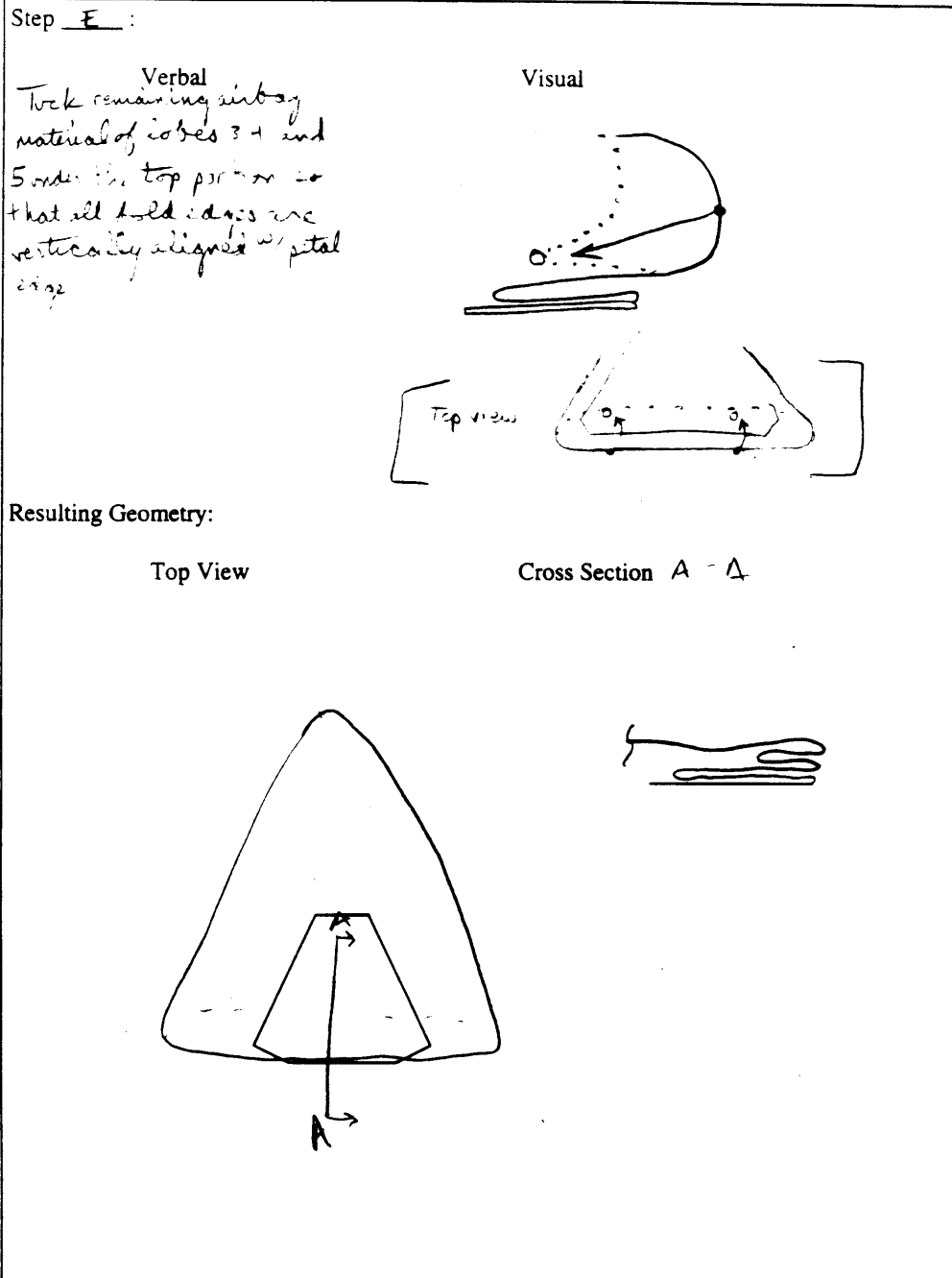


Figure 30. Fold Forms for Folding Scheme Two, Continued.
 Step E.

Folding Scheme # 2

Step F :

<p>Verbal</p> <p>Repeat previous Fold (E) on remaining material along edges 1, 2, and 3.</p>	<p>Visual</p> <p>(See previous Fold.)</p>
--	---

Resulting Geometry:

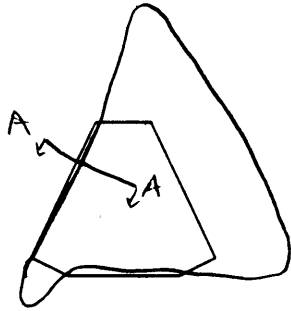

<p>Top View</p> 	<p>Cross Section A-A</p> 
---	---

Figure 30. Fold Forms for Folding Scheme Two, Continued.
Step F.

Folding Scheme # 2

Step G :

Verbal	Visual
<i>Repeat previous fold lines lobes 1, 2, and 3.</i>	<i>(See fold E.)</i>

Resulting Geometry:

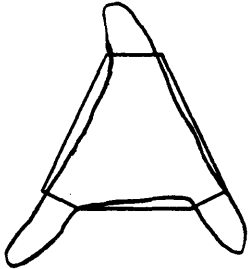

Top View	Cross Section
	

Figure 30. Fold Forms for Folding Scheme Two, Continued.
Step G.

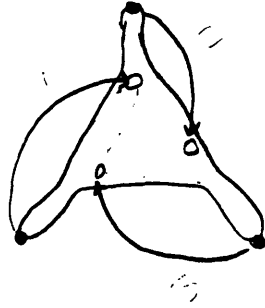
Folding Scheme # 2

Step H :

Verbal

Fold in remaining
"flaps" of material
in a clockwise
direction. Anchor
w/ weights to hold
folds until inflation.

Visual



Resulting Geometry:

Top View

Cross Section

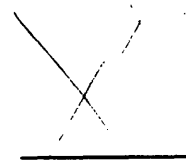


Figure 30. Fold Forms for Folding Scheme Two, Continued.
Step H.

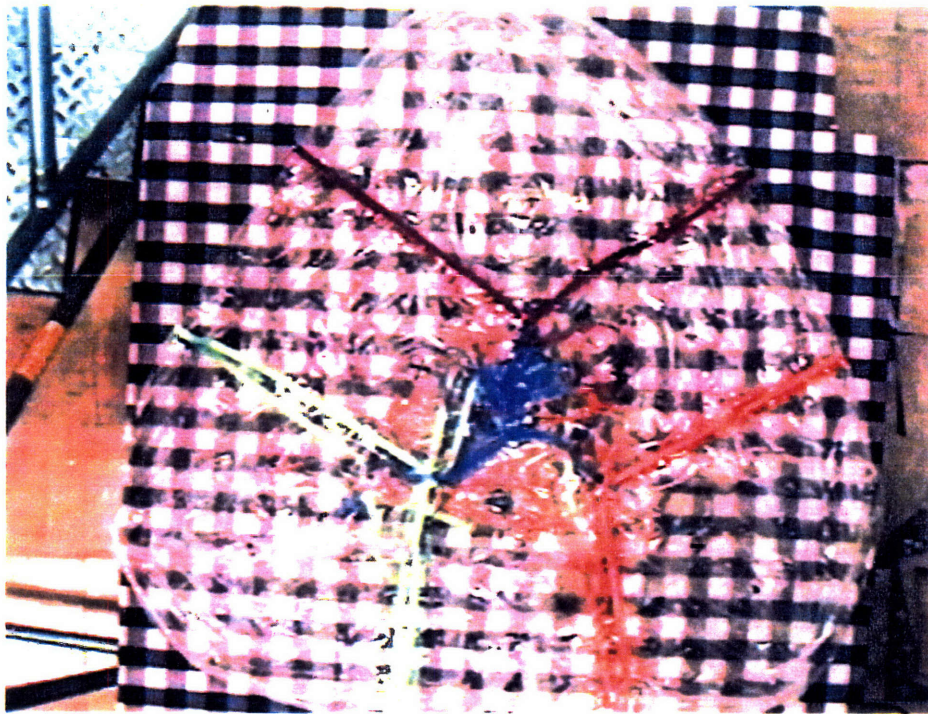


Figure 31. Pictures of the Steps of Folding Scheme Two.
Step A.

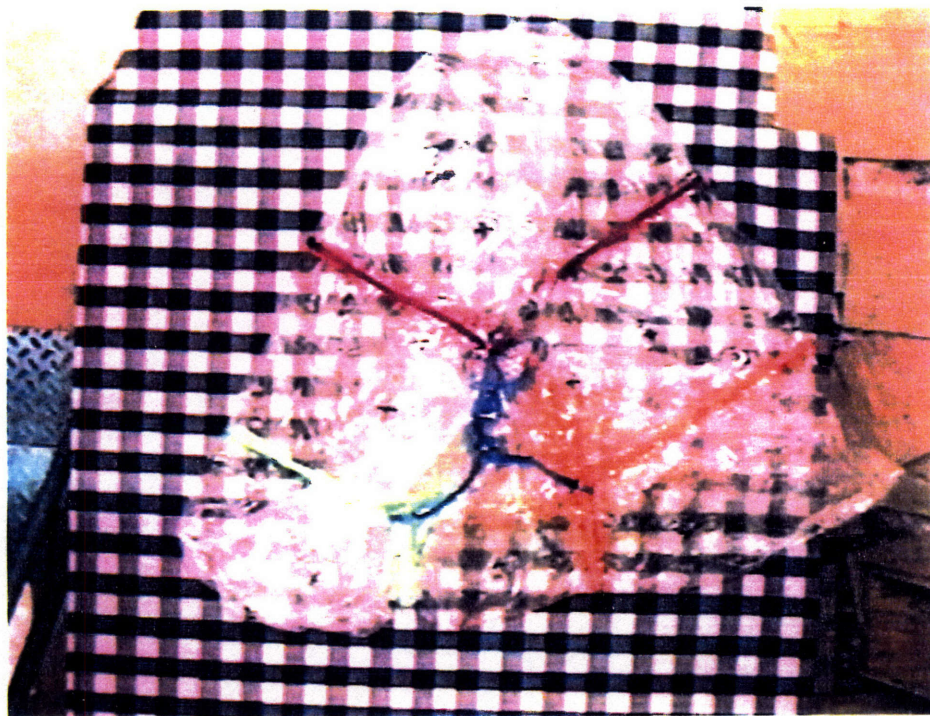
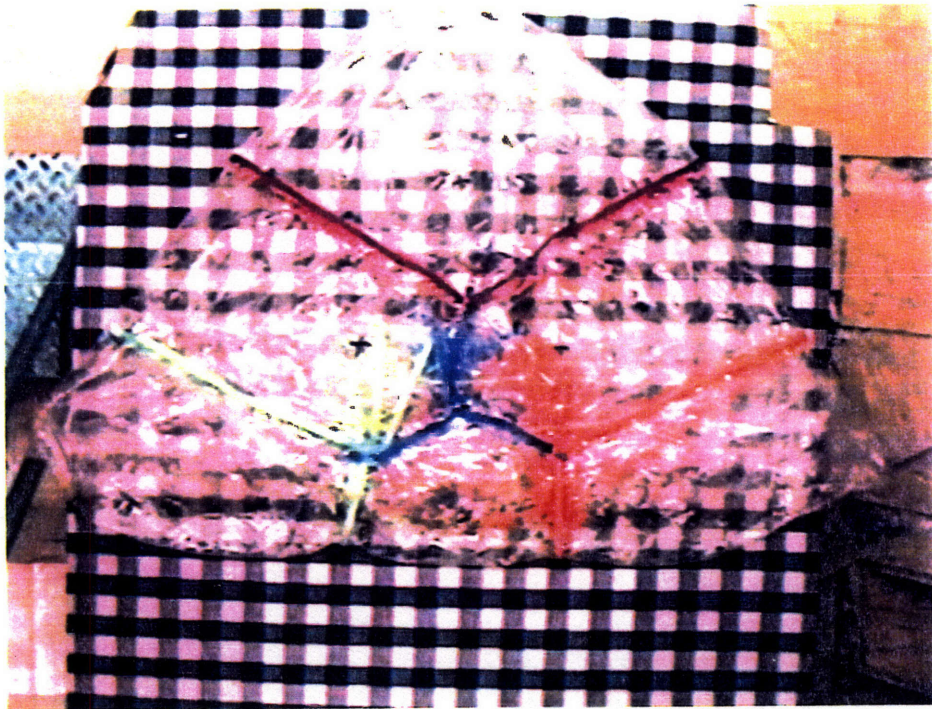


Figure 31. Pictures of the Steps of Folding Scheme Two, Continued.
Steps B (above) and C (below).



Figure 31. Pictures of the Steps of Folding Scheme Two, Continued.
Steps D (above) and E (below).



Figure 31. Pictures of the Steps of Folding Scheme Two, Continued.
Steps F (above) and G (below).

FOLDING SCHEME THREE

Scheme Three was an attempt to get rid of the last three flaps of material left overhanging the lander petal edges after most of the material was folding inward. Both Scheme One and Scheme Two had these leftover flaps, and the unfolding of Scheme Two would have been entirely smooth if those three flaps could have been eliminated. The lobes of the airbag that made up the majority of the material left overhanging the petal edges (lobes one, three, and five) were folded inward on top of themselves first (as opposed to Schemes One and Two where they were folded inward last) and then the remaining lobes were folded in toward their respective petal edges in a stacked accordion pattern. Fold forms and pictures for Scheme Three are shown in Figures 32 and 33, respectively, and the video taped segment showing the steps of Folding Scheme Three begins at twenty-six minutes.

Folding Scheme # 3

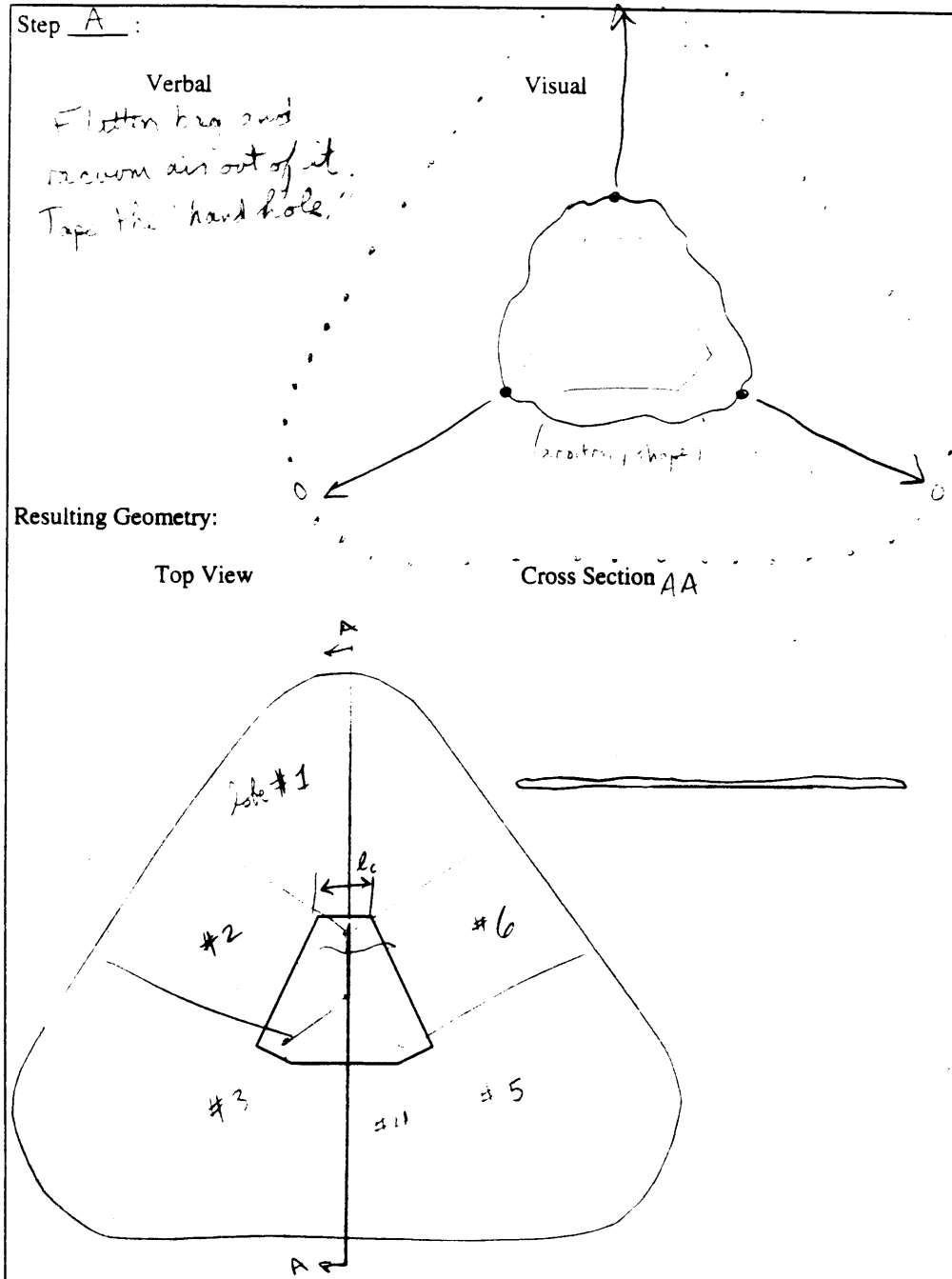


Figure 32. Fold Forms for Folding Scheme Three.
Step A.

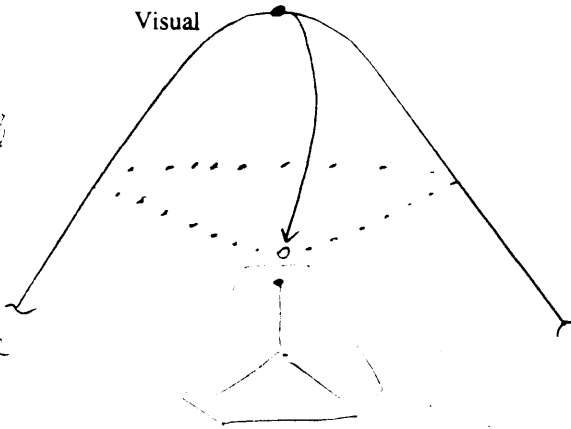
Folding Scheme # 3

Step B :

Verbal

Tuck in the portion of lobe 1 that lies above an imaginary horizontal line drawn between the two external tendons that delineate lobe #1 and tuck that material in toward the center of the petal.

Visual



Resulting Geometry:

Top View

Cross Section A-A

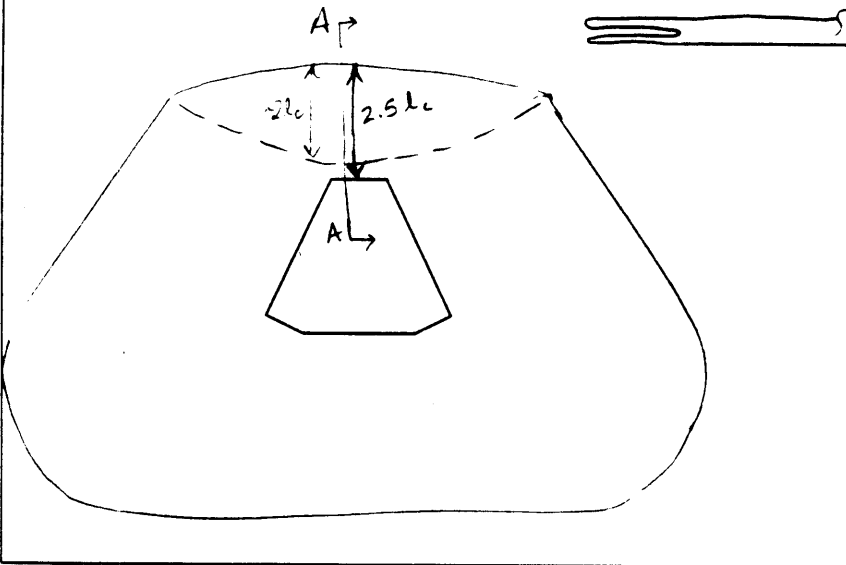


Figure 32. Fold Forms for Folding Scheme Three, Continued.
Step B.

Folding Scheme # 3

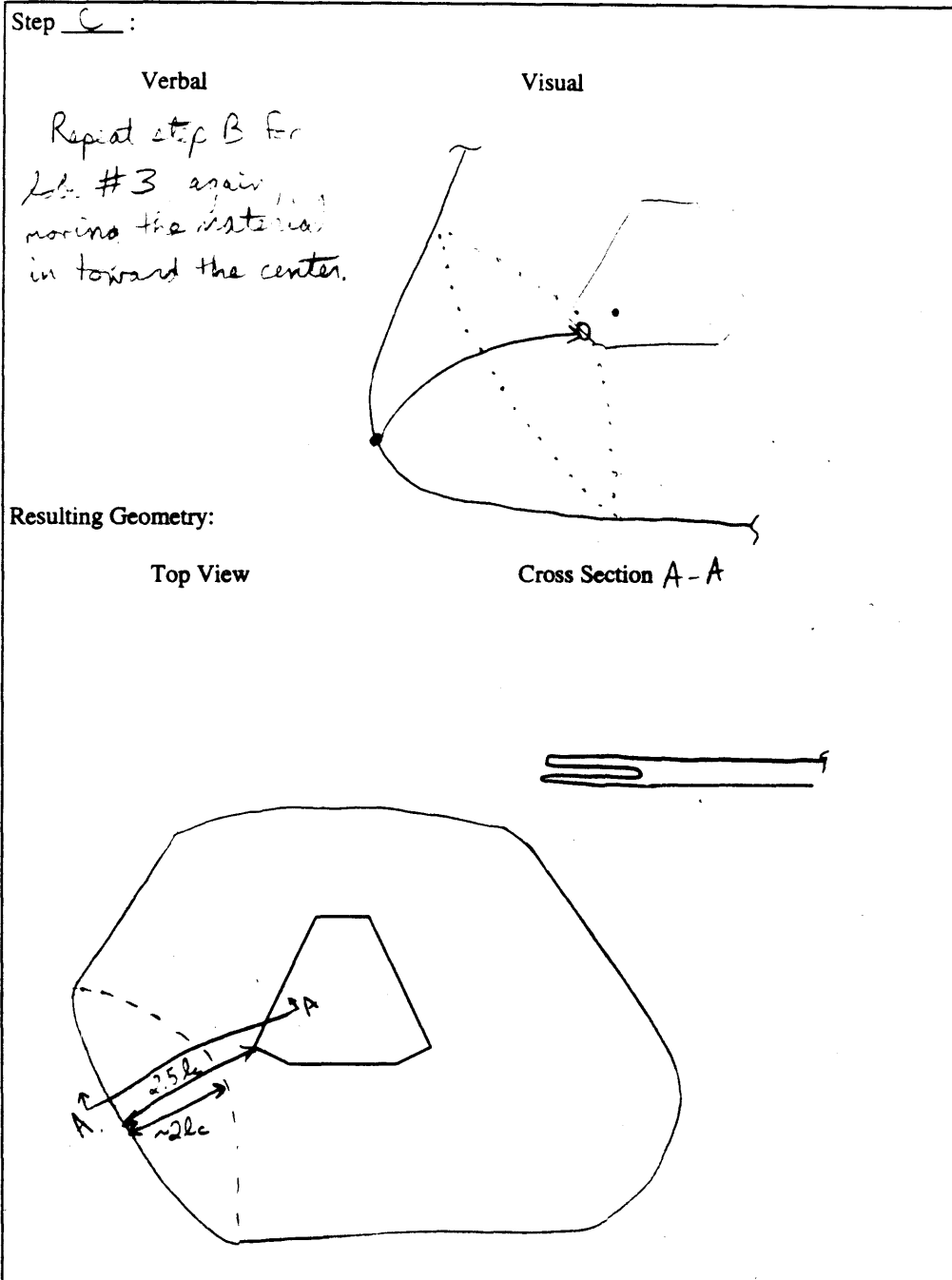


Figure 32. Fold Forms for Folding Scheme Three, Continued.
Step C.

Folding Scheme # 3

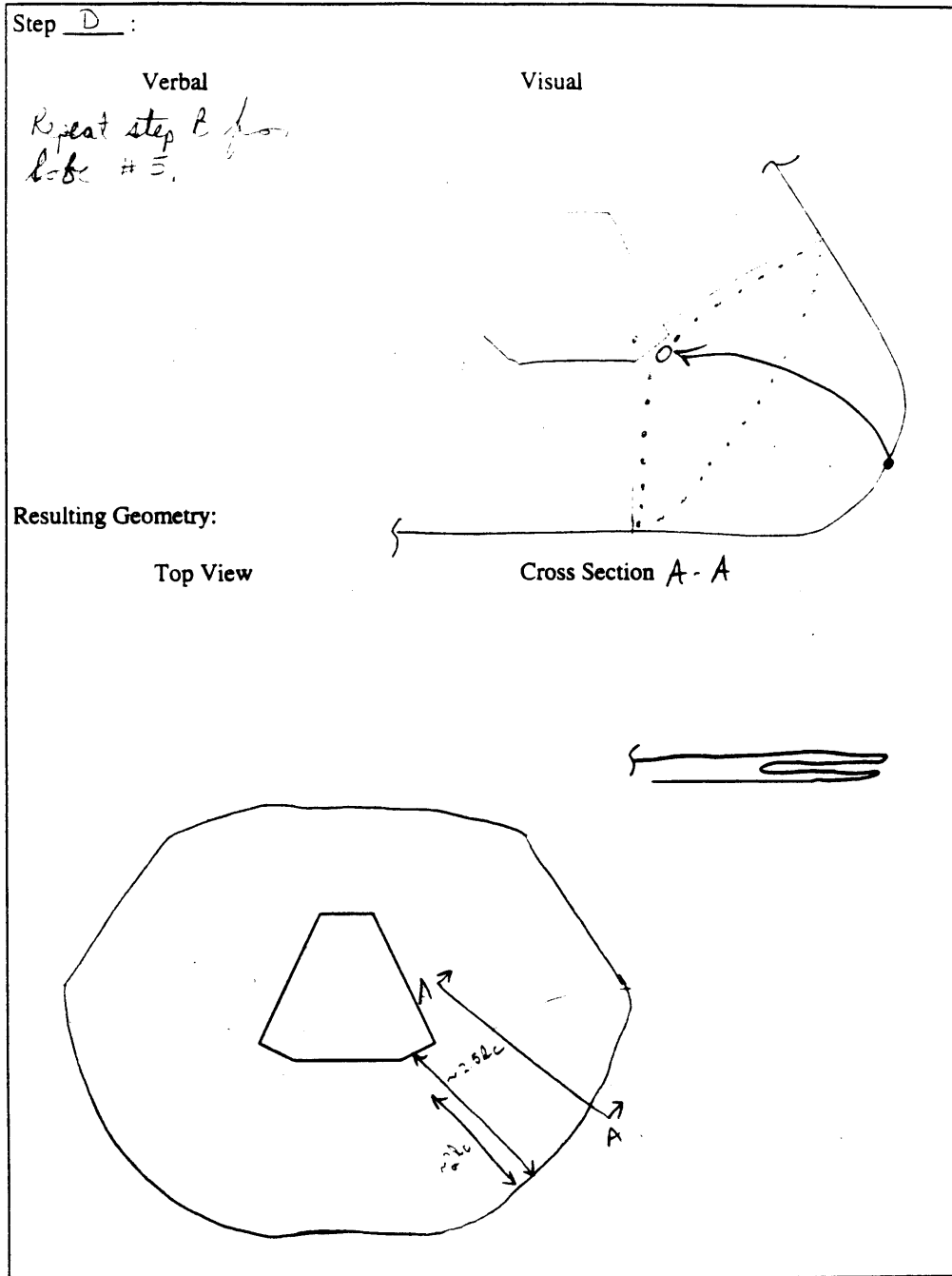
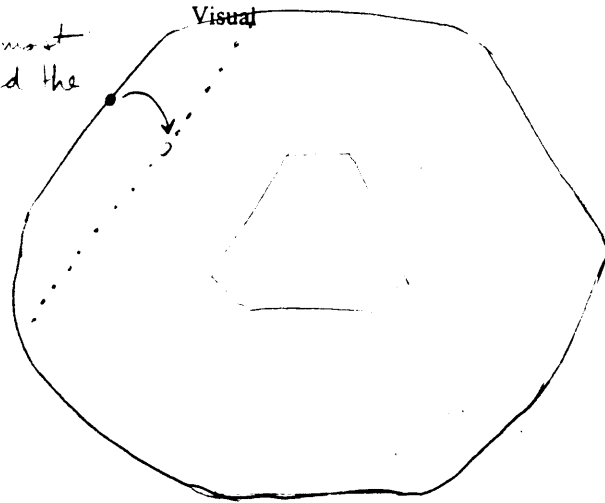


Figure 32. Fold Forms for Folding Scheme Three, Continued.
Step D.

Folding Scheme # 3

Step E :

Verbal
Fold one L_2 of the outermost
edge of lobe 2 toward the
center.



Resulting Geometry:

Top View

Cross Section A A

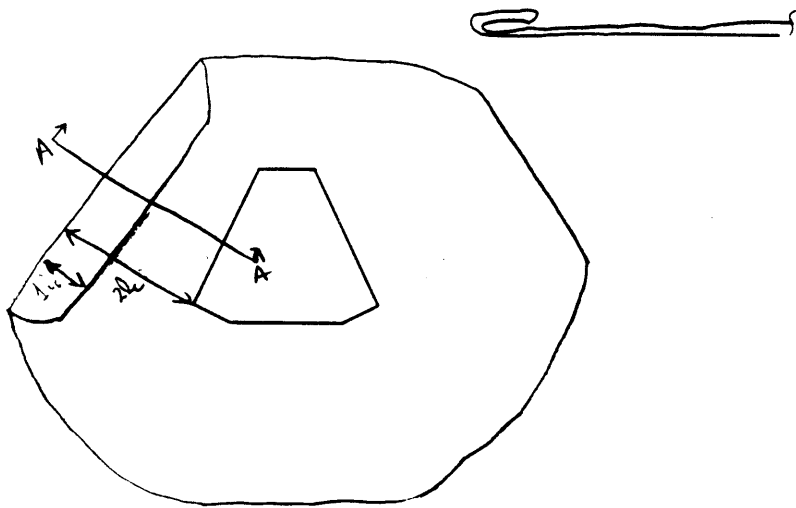


Figure 32. Fold Forms for Folding Scheme Three, Continued.
Step E.

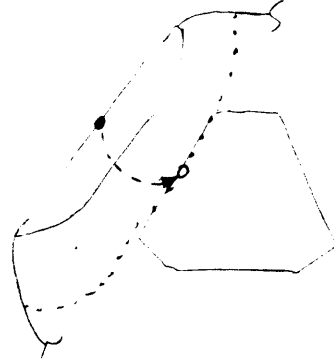
Folding Scheme # 3

Step F:

Verbal

Fold the material from
Step E and the material
underneath it UNDER
and toward the center
of the petal.

Visual



Resulting Geometry:

Top View

Cross Section A A

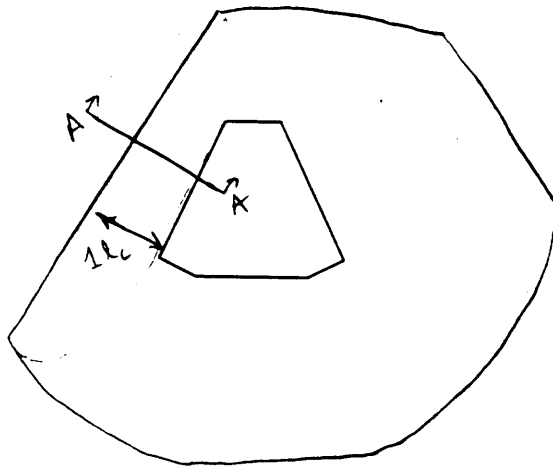


Figure 32. Fold Forms for Folding Scheme Three, Continued.
Step F.

Folding Scheme # 3

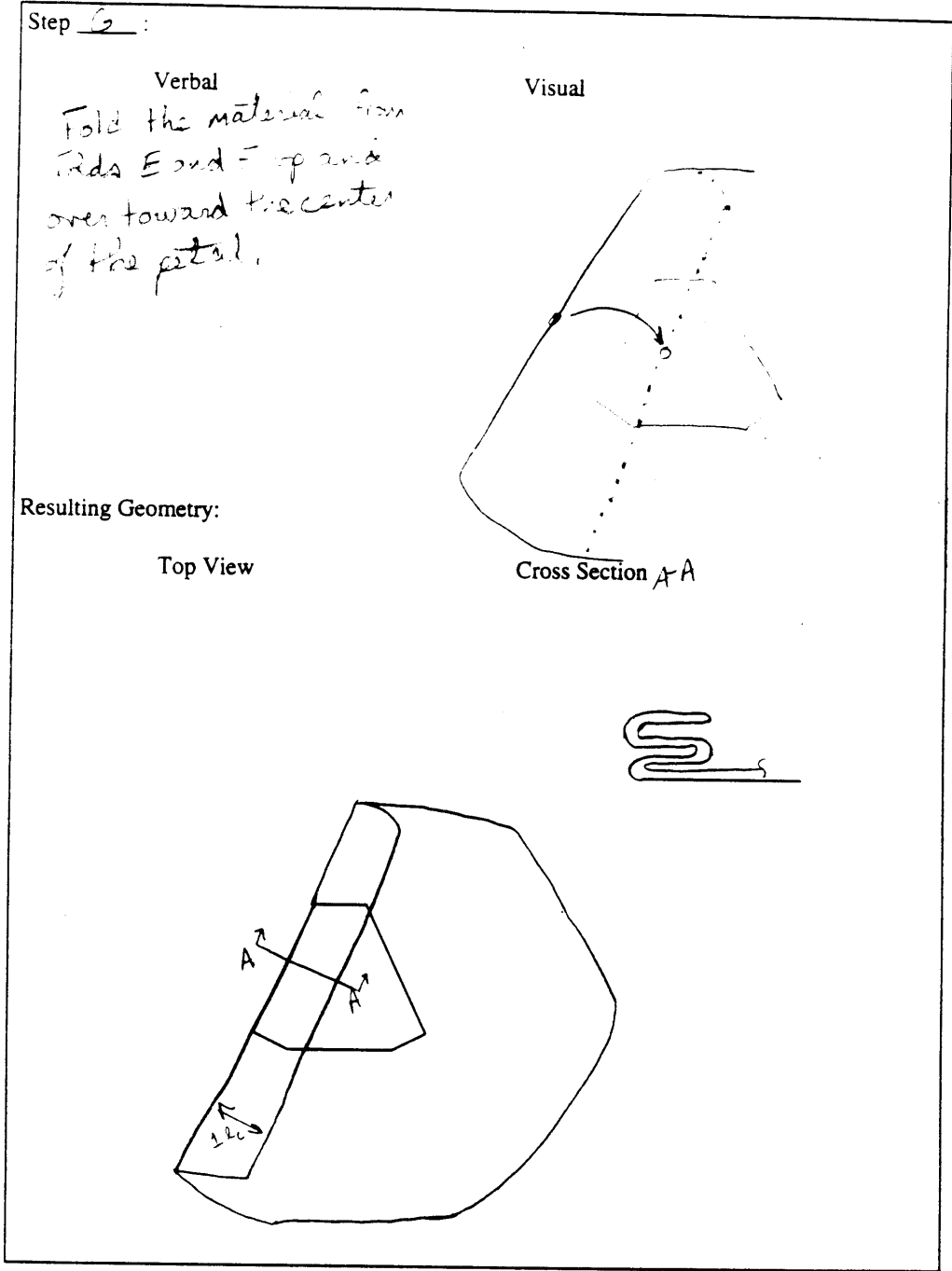


Figure 32. Fold Forms for Folding Scheme Three, Continued.
Step G.

Folding Scheme # 3

Step H :

Verbal

Repeat steps E, F,
and G for lobe #6.

Visual

(See previous folds -
E, F, G.)

Resulting Geometry:

Top View

Cross Section A-A

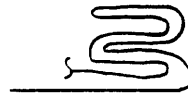
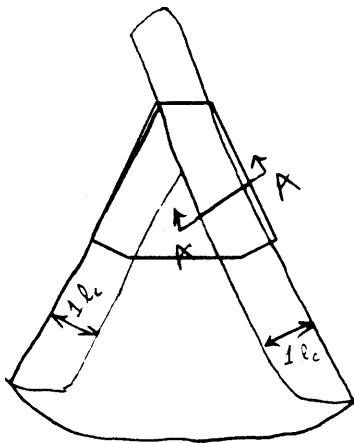


Figure 32. Fold Forms for Folding Scheme Three, Continued.
Step H.

Folding Scheme # 3

Step I :

Verbal

Repeat steps E, F, G
for lobe 4.

Visual

(See previous (131)-
E, F, G)

Resulting Geometry:

Top View

Cross Section AA

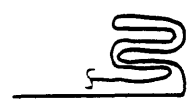
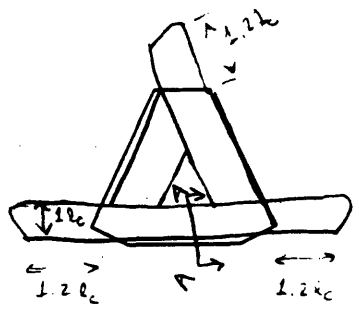


Figure 32. Fold Forms for Folding Scheme Three, Continued.
Step I.

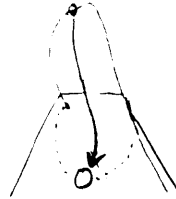
Folding Scheme # 3

Step J :

Verbal

Fold top flap (lobe #1)
down ~~so that~~ so
that all of the material
is on the plate.

Visual



Resulting Geometry:

Top View

Cross Section

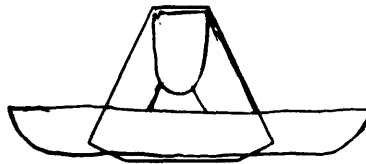


Figure 32. Fold Forms for Folding Scheme Three, Continued.
Step J.

Folding Scheme # 3

Step K :

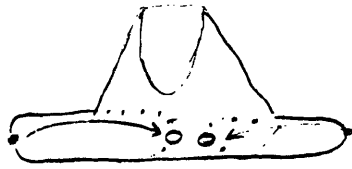
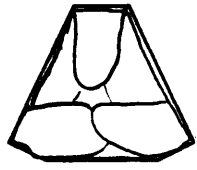

<p>Verbal Fold left flap (lobe 3), in toward petal center. Repeat for right flap (lobe 5).</p>	<p>Visual</p> 
<p>Resulting Geometry:</p>	
<p>Top View</p>	<p>Cross Section</p>
	

Figure 32. Fold Forms for Folding Scheme Three, Continued.
Step K.

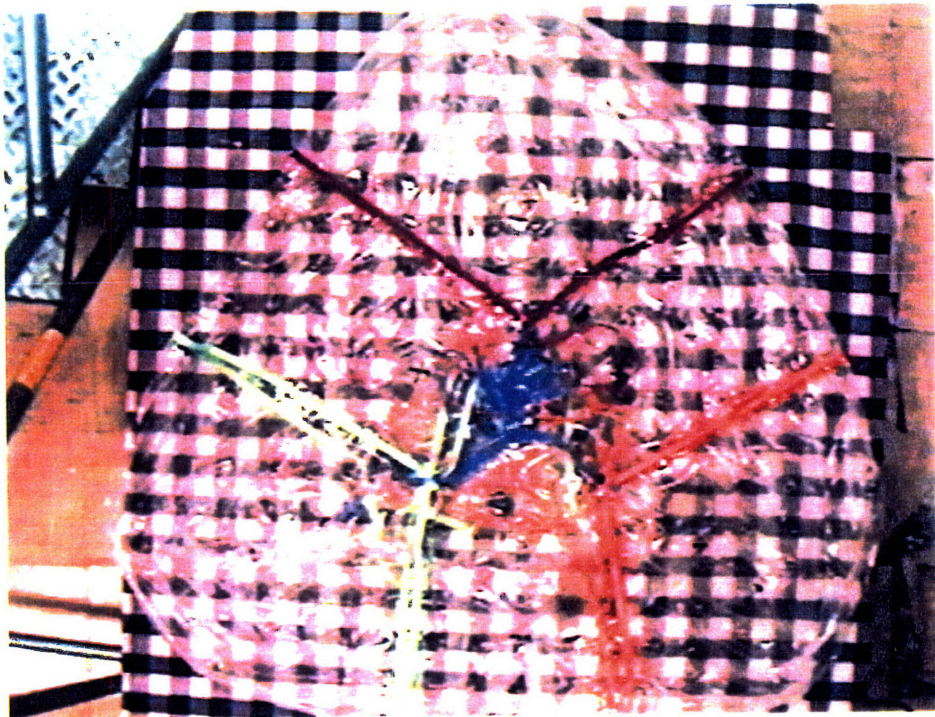


Figure 33. Pictures of the Steps of Folding Scheme Three.
Step A.

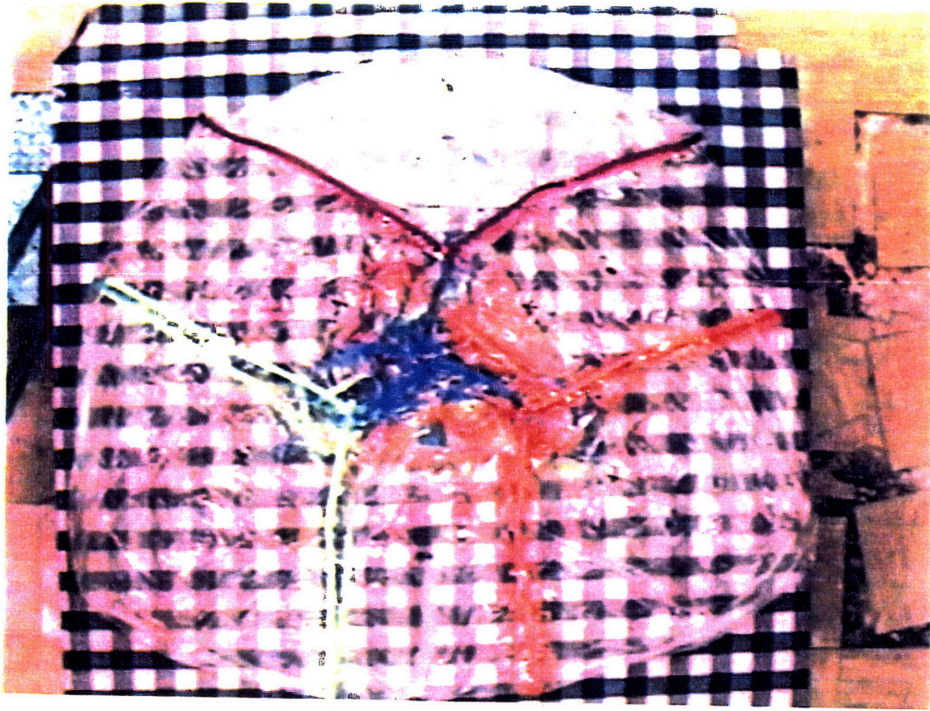


Figure 33. Pictures of the Steps of Folding Scheme Three, Continued.
Steps B (above) and C (below).

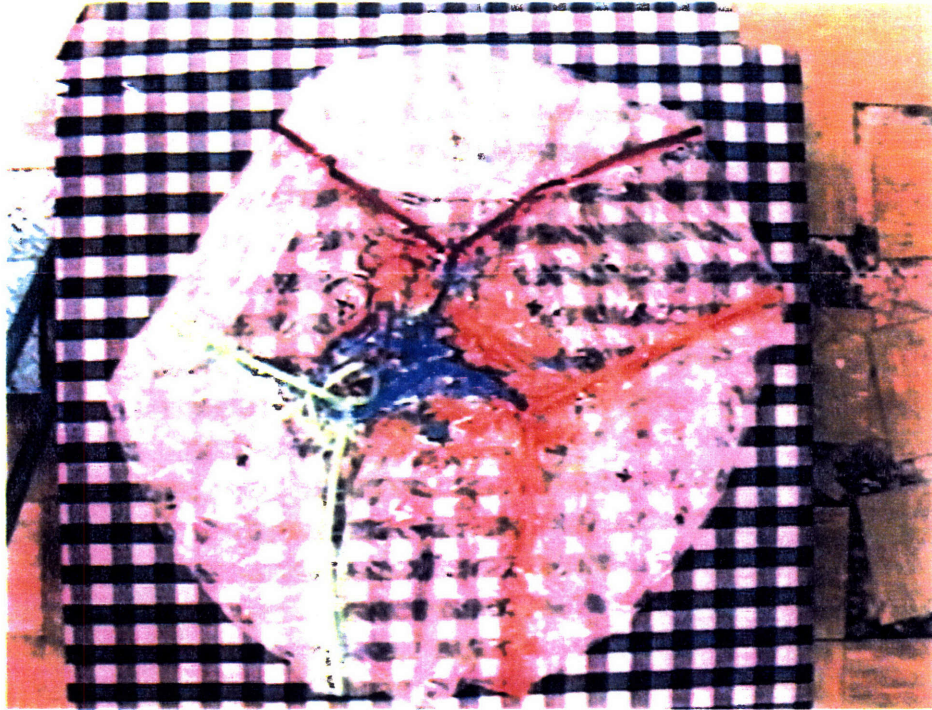
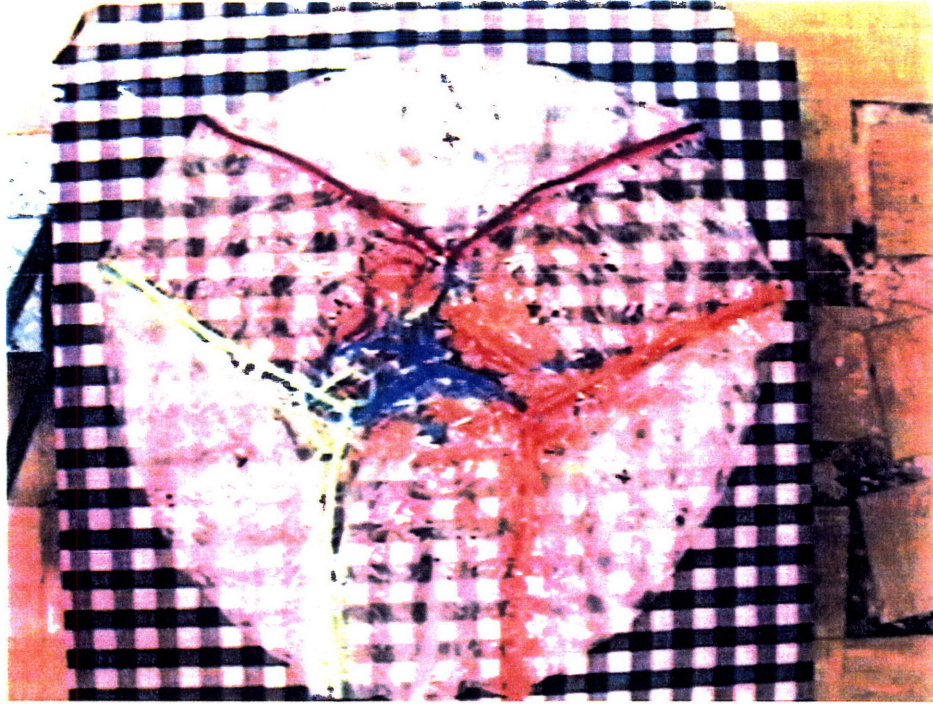


Figure 33. Pictures of the Steps of Folding Scheme Three, Continued.
Steps D (above) and E (below).

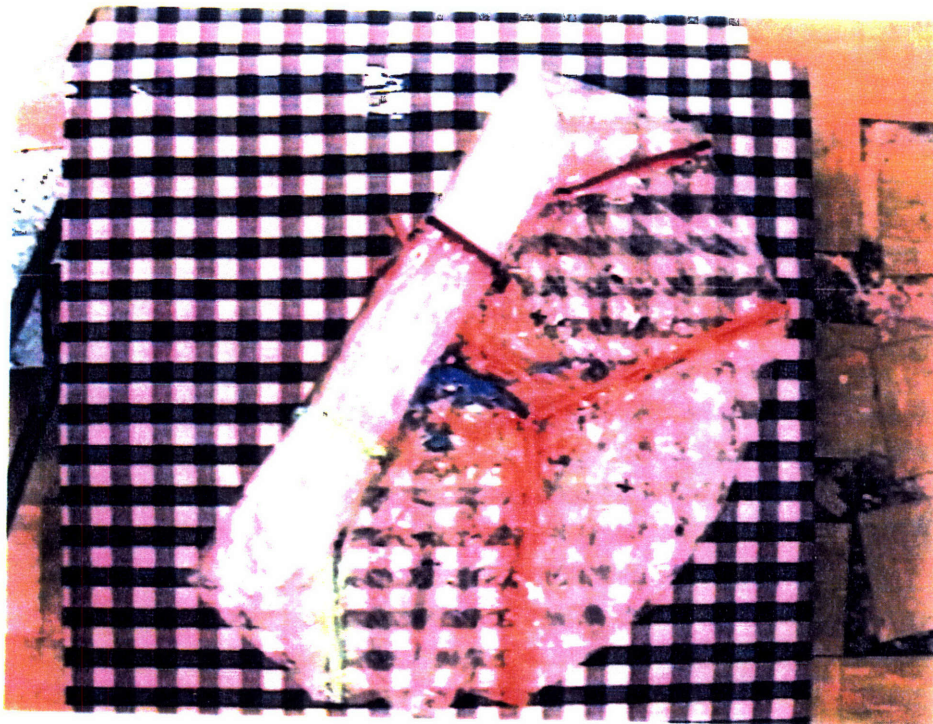
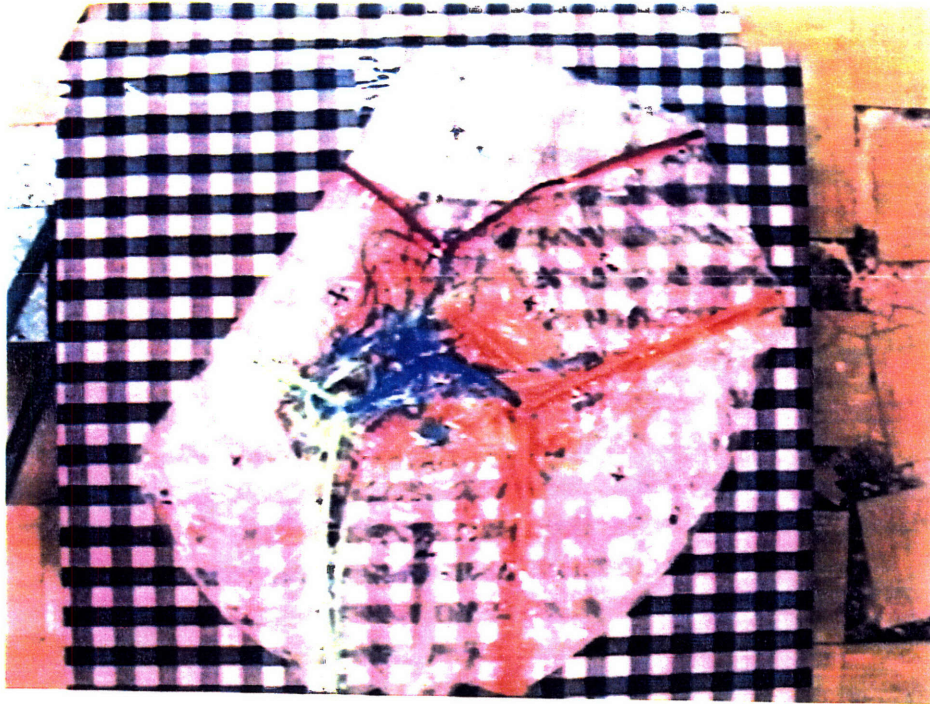


Figure 33. Pictures of the Steps of Folding Scheme Three, Continued.
Steps F (above) and G (below).

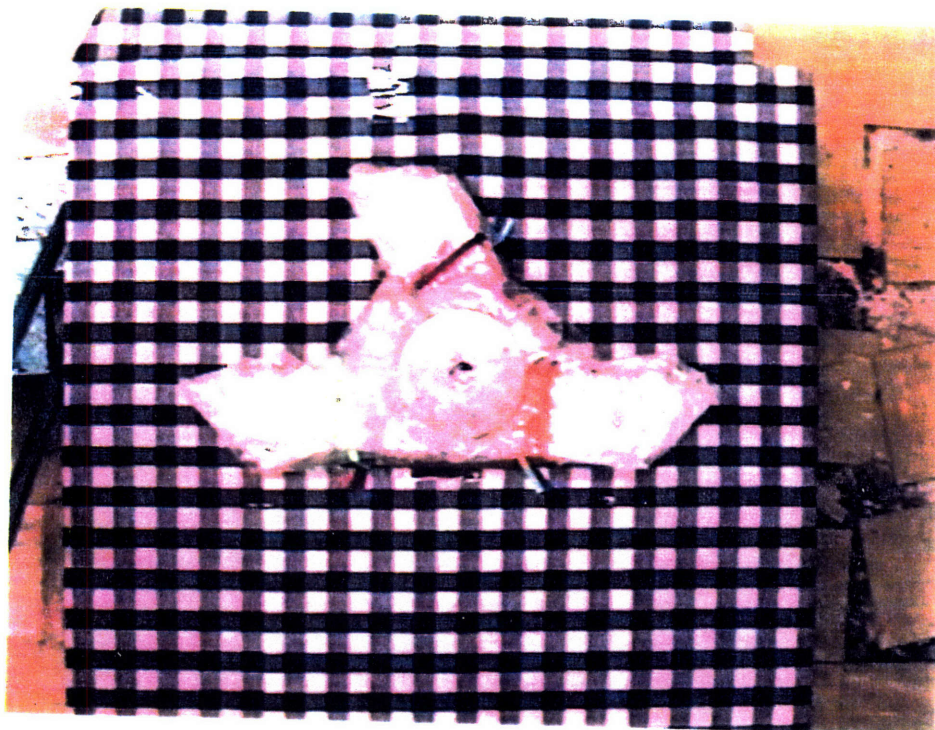
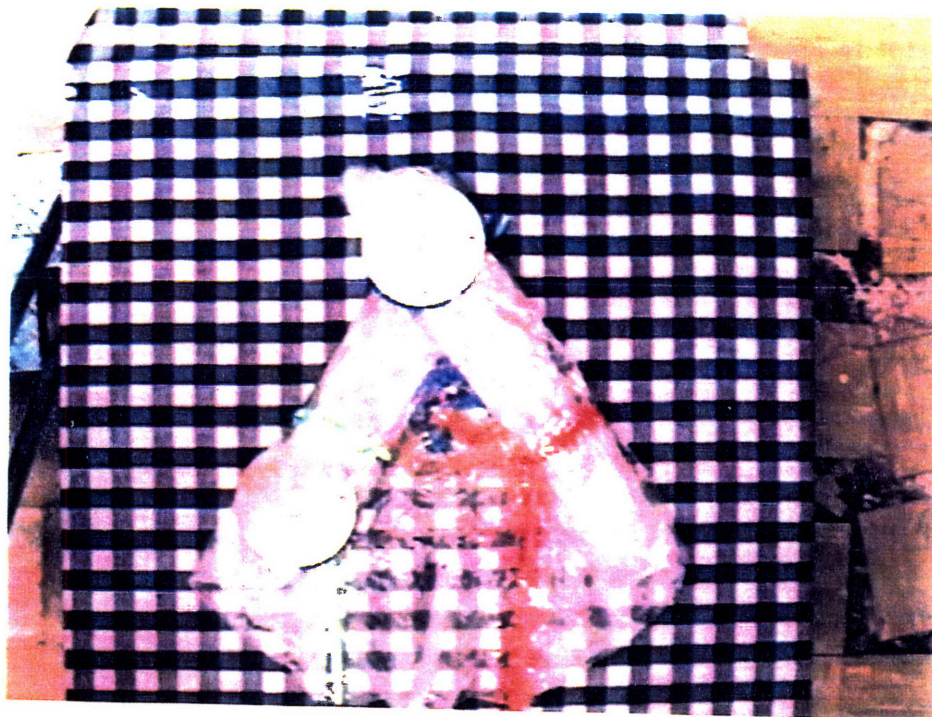


Figure 33. Pictures of the Steps of Folding Scheme Three, Continued.
Steps H (above) and I (below).

FOLDING SCHEME FOUR

Scheme Four was the design most recently proposed for Mars Pathfinder's airbag subsystem folding scheme by ILC Dover, Incorporated. Fold forms have not been included because of its similarity to JPL's Folding Scheme Two. The only notable differences were the order in which the folds were performed. As seen in Figure 34, the "S" folds are stacked vertically along one edge of the petal, proceeding from the bottom fold up to the top along each edge. The vertical stack of three accordion folds is completed along each petal edge before moving to the next edge and beginning another vertical stack along the second edge, as opposed to Folding Scheme Two in which the first layer of each of the three stacks was folded all the way around the petal, then the second layer, and finally the third. Folding Scheme Four built the folds in the airbag up each side of the triangular petal, whereas the design of Folding Scheme Two wrapped the airbag material in a helical pattern from the base up toward the top.

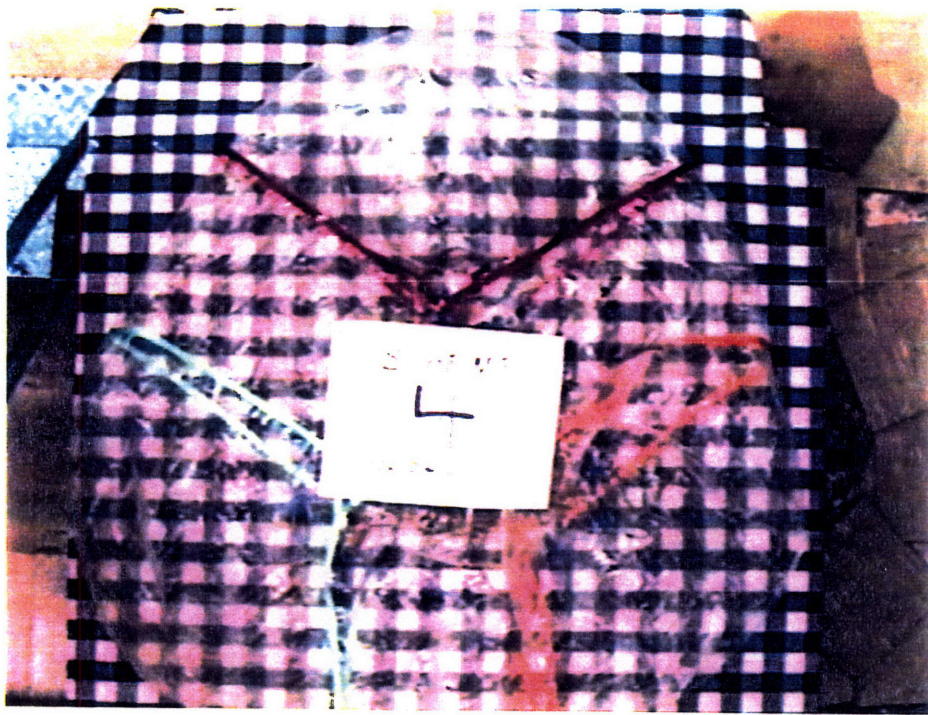


Figure 34. Pictures of the Steps of Folding Scheme Four.
Step A.

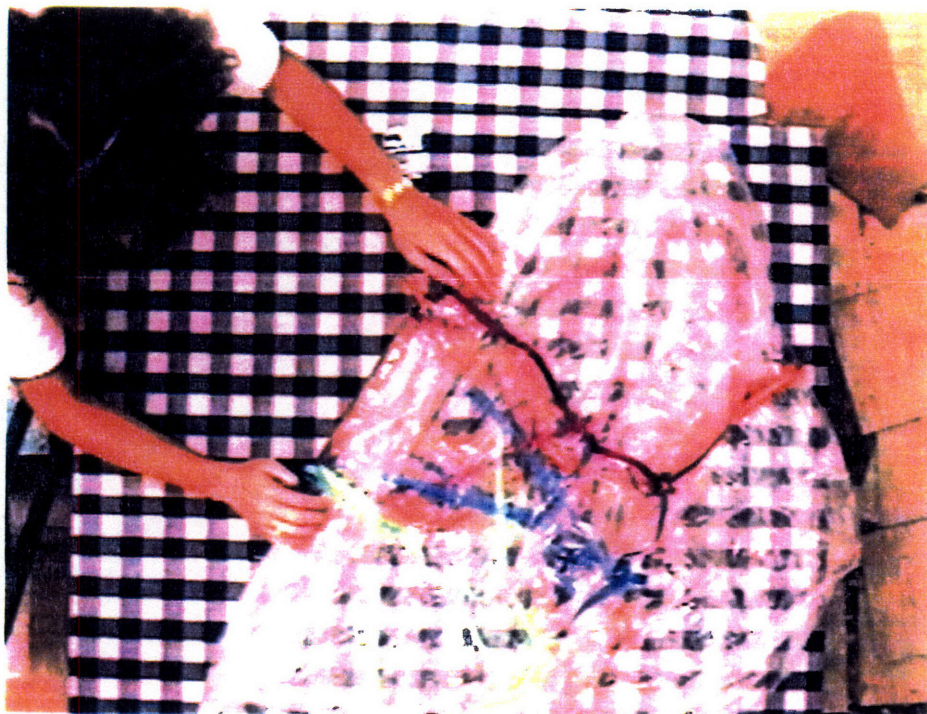
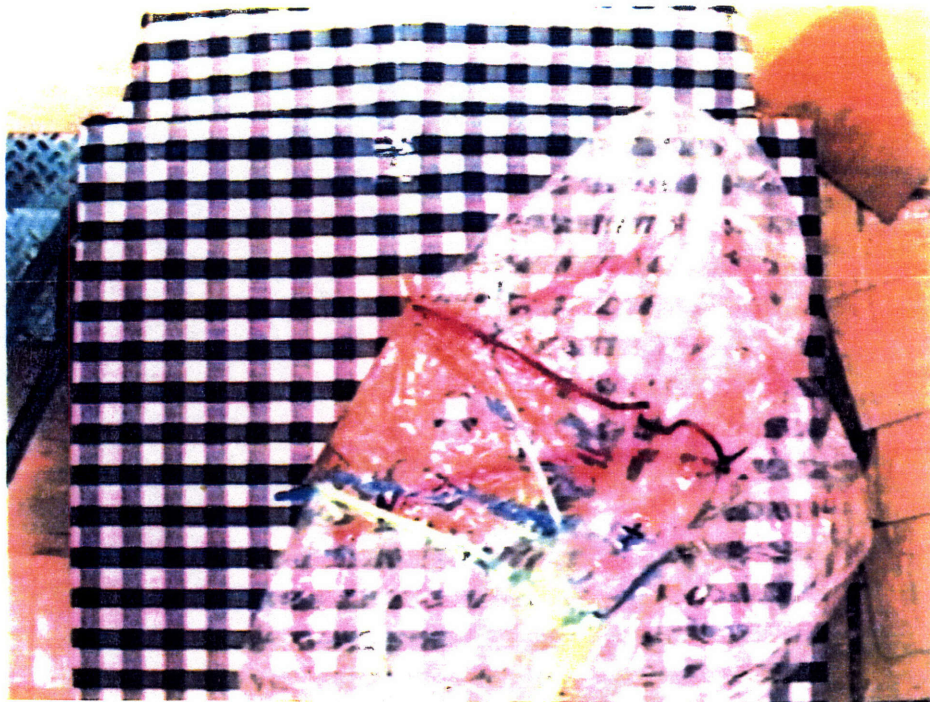


Figure 34. Pictures of the Steps of Folding Scheme Four, Continued.
Steps B (above) and C (below).

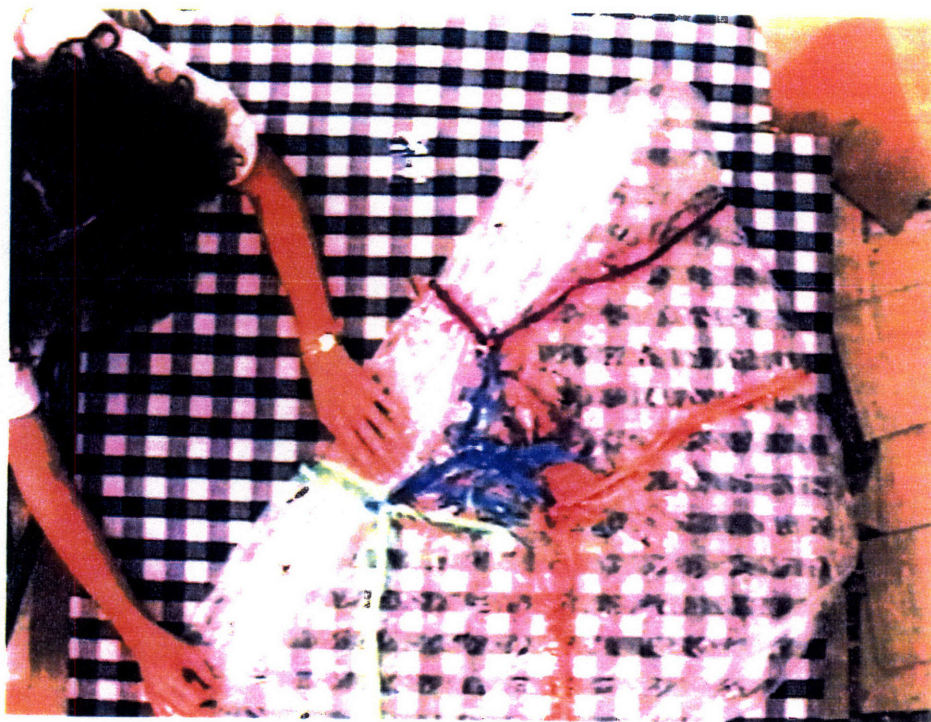
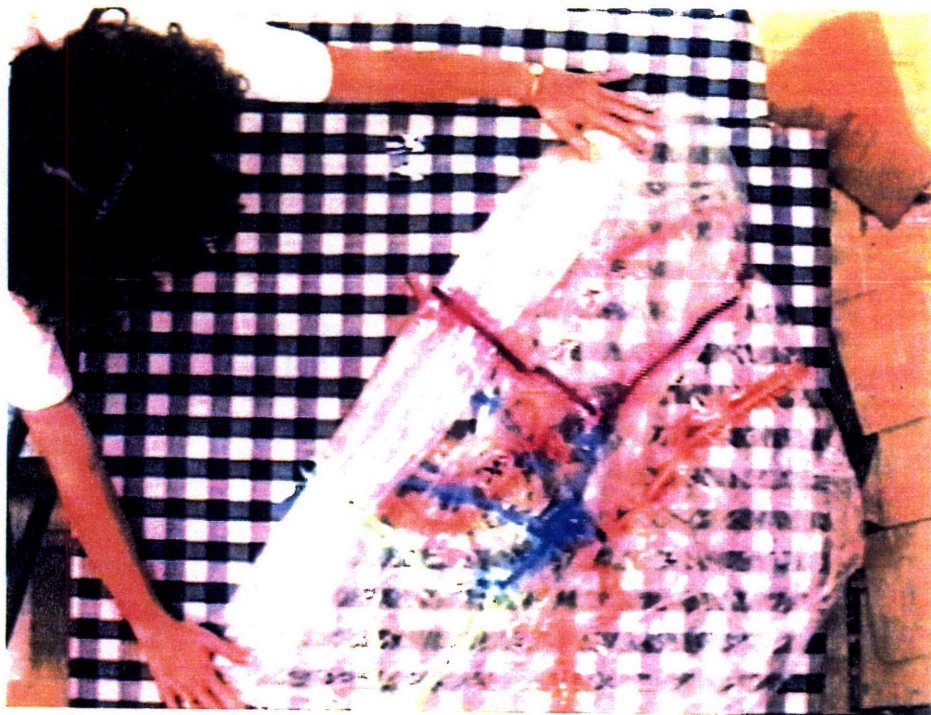


Figure 34. Pictures of the Steps of Folding Scheme Four, Continued.
Steps D (above) and E (below).

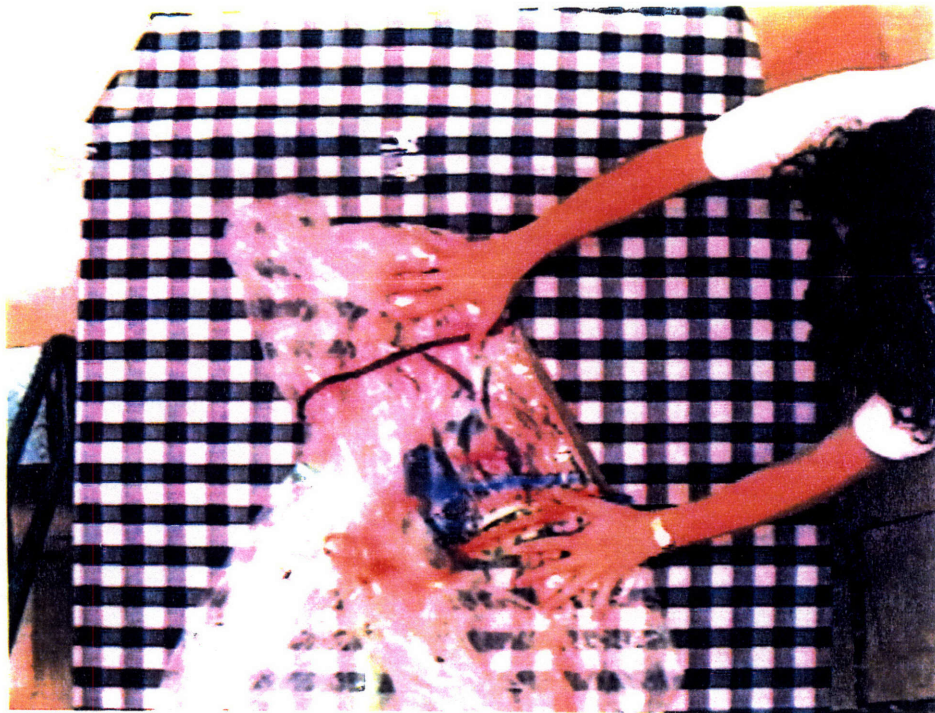


Figure 34. Pictures of the Steps of Folding Scheme Four, Continued.
Steps F (below) and G (above).

TRIALS

TRIALS ONE THROUGH SIX

A trial consisted of one of the four folding schemes paired with one of the two available diffusers or two deflectors in an inflation. Trials One through Three consisted of the first three folding schemes described in the previous section inflated with the low porosity diffuser (Figure 25, Chapter Two) and with a three-sixteenths inch orifice plate. Trials Four through Six had all the same conditions as Trials One through Three, but were inflated with a half-inch orifice instead. Trials One through Three can be seen on the video tape within the first eight and a half minutes. Trials Four through Six follow on the tape up to the thirty-eight minute marker, each one following the folding of each of the three folding schemes.

TRIALS SEVEN THROUGH TEN

Trials Seven through Ten, which involved all four of the folding schemes paired with the high porosity diffuser, are the ones highlighted in pictures in the results section of Chapter Four, because their inflation times were shorter than the times associated with the low porosity diffuser of the first six trials. These rapid inflations were much better indicators than the previous trials of the true inflation dynamics that will be experienced with the full scale airbags. The inflation dynamics and times of the quarter scale mock-up with the high porosity diffuser installed were closer to those expected of the full-scale airbag subsystem's than the low porosity trials, so the remainder of the trials used the high porosity diffuser.

Another reason for the use of the high porosity diffuser instead of the low porosity one used in the first six trials was because it provided a simple baseline for the unfurling of each folding scheme without any added factors, such as flow redirection, the spring rate of the material as it unfolds, and diffusing the mass flow so much that the value of the inflation data is questionable. The inflation of Trials Seven through Nine can be viewed on the video tape within the forty to forty-five minute range, and Trial Ten begins at around fifty minutes.

TRIALS ELEVEN THROUGH FOURTEEN

Because of findings from the first few inflations, a tri-chute deflector was designed, fabricated, and tested without the airbag. No inflation data was recorded because the deflector was later blown apart during its first inflation with the airbag. (Details follow in the Results chapter.) Another deflector was fabricated, this one being a simple flow redirection device (Figure 25) that effectively moved the gas inlet hole closer to the center of the lander petal. It routed the air from the lower section of the petal toward the center with a tube in hopes of achieving a more evenly distributed gas flow for smoother deployment. Trials Eleven through Fourteen, which take up the remainder of the video tape, were Folding Schemes One through Four paired up with the flow redirection sock.

Chapter Four: Results

The results of the four airbag subsystem packaging designs, their subsequent inflations, and the effects of the flow diffusion and redirection devices are best described visually on the video tape. Due to the rapid nature of the inflations, the pictorial results in the pages that follow, though accurate, do not capture as much information as the video tape.

FOLDING SCHEMES

FOLDING SCHEME ONE

Scheme One was intended to be an example of a “bad” scheme. The larger the flap of material that extended beyond the fold line, the more difficult it was to unfurl and inflate for the blast of air trying to unfold it, and almost every fold of Scheme One was made with large portions of material left overhanging the fold lines.

One positive attribute of Folding Scheme One was that it did not have three long, thin flaps of material left overhanging the lander petal edge like Schemes Two through Four. It did, however, have two very broad flaps toward the end of the folding procedure that presented the same unfolding problems as the three thin flaps. The gas rushing into the airbag “punched” out the flaps violently before undoing the rest of the folds and inflating the airbag. Ideally, the gas would have smoothly unfurled the folds and inflated the airbag such that the drag-area versus time increased in a more linear fashion.

The inflation of Folding Scheme One is shown in Figure 35. The first flap to unfurl was the one containing lobes four, five, and six. It sprang out to the right, as seen in the first four pictures. The next three show the left flap, the bottom fold, and the top

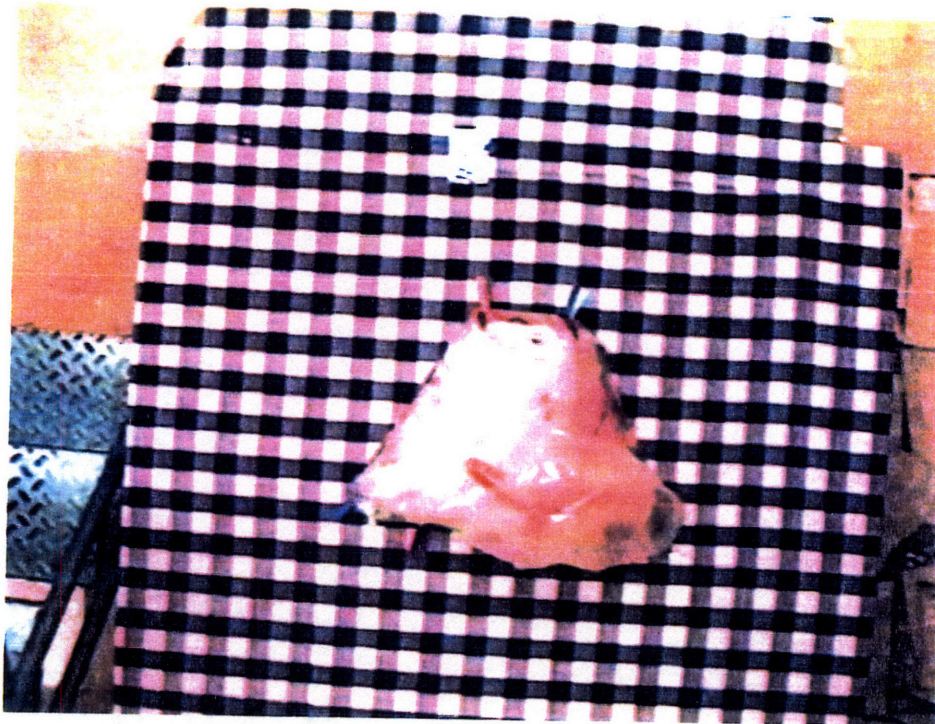


Figure 35. Inflation of Folding Scheme One.

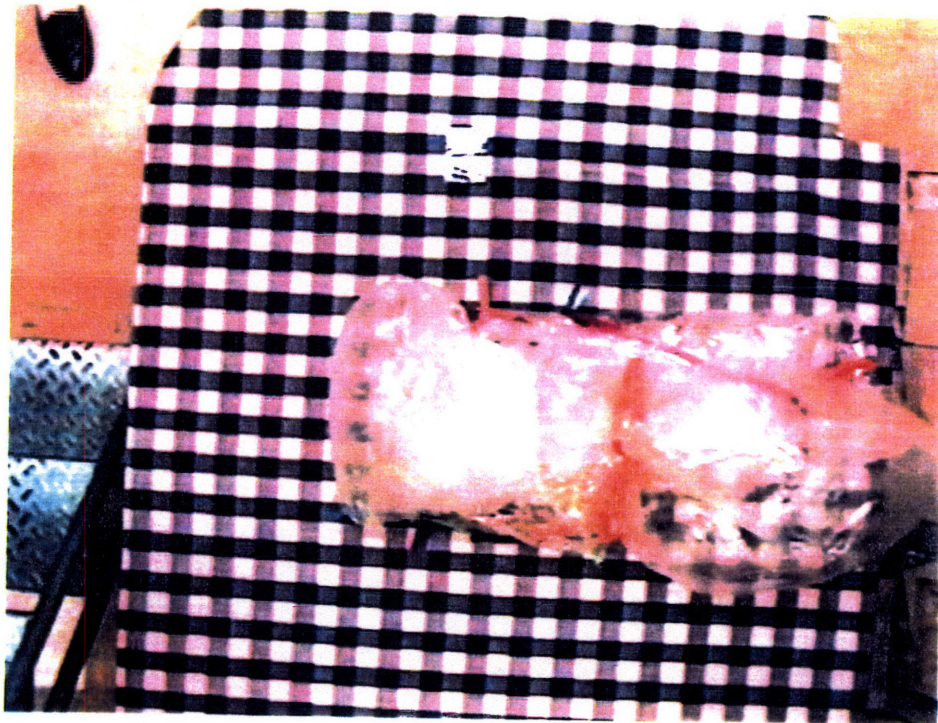
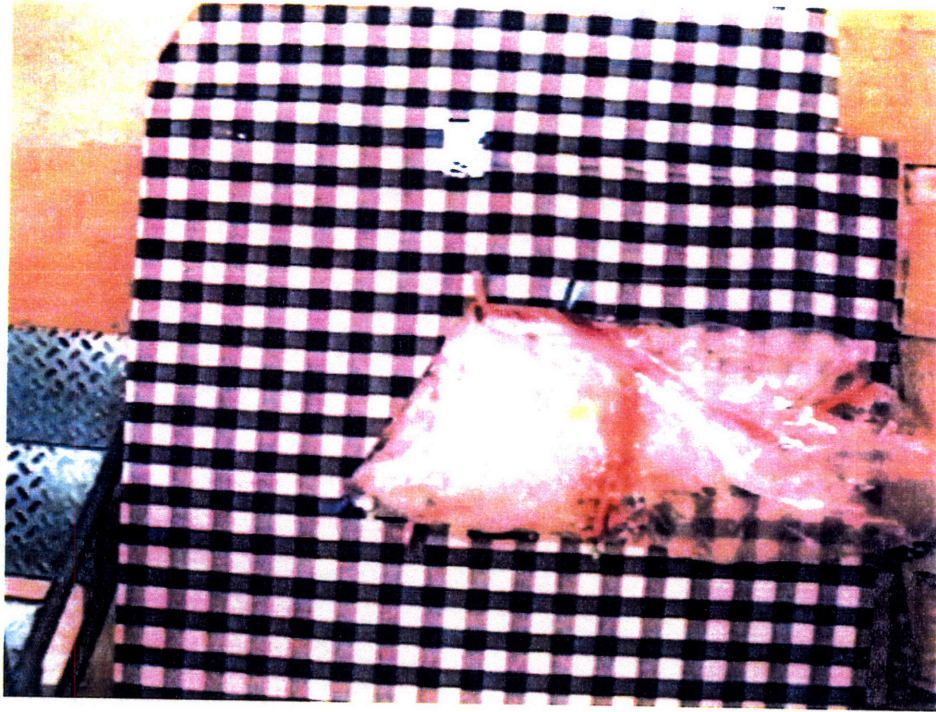


Figure 35. Inflation of Folding Scheme One.

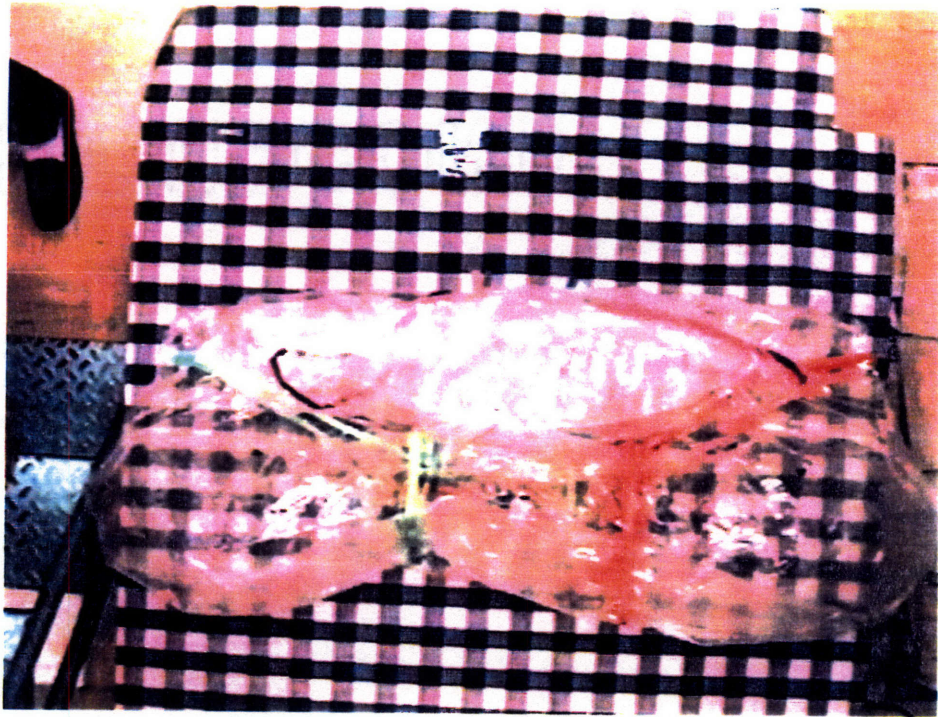
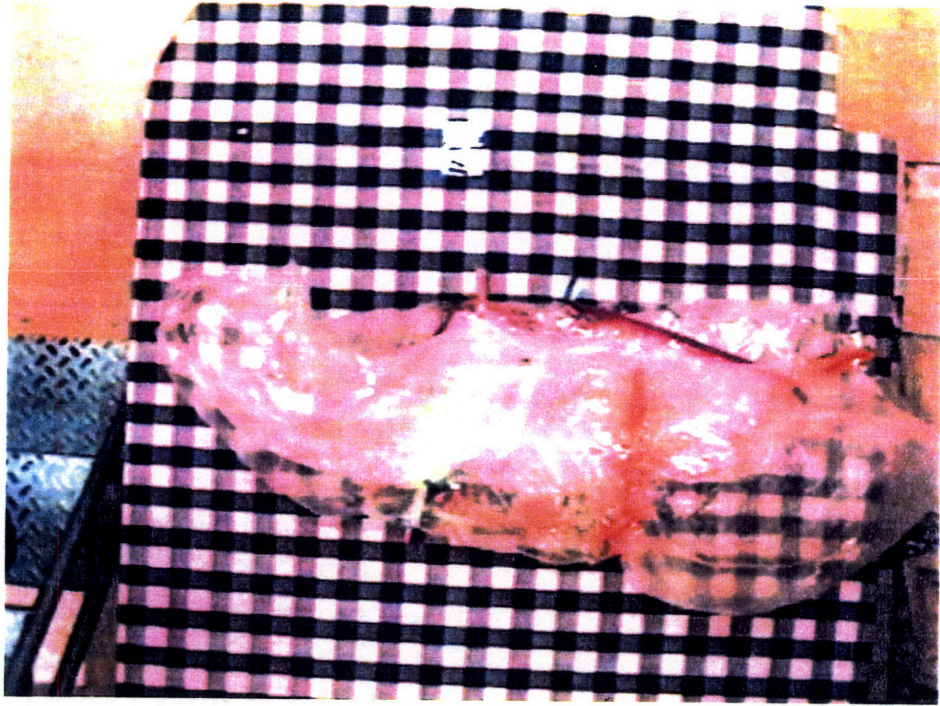


Figure 35. Inflation of Folding Scheme One.

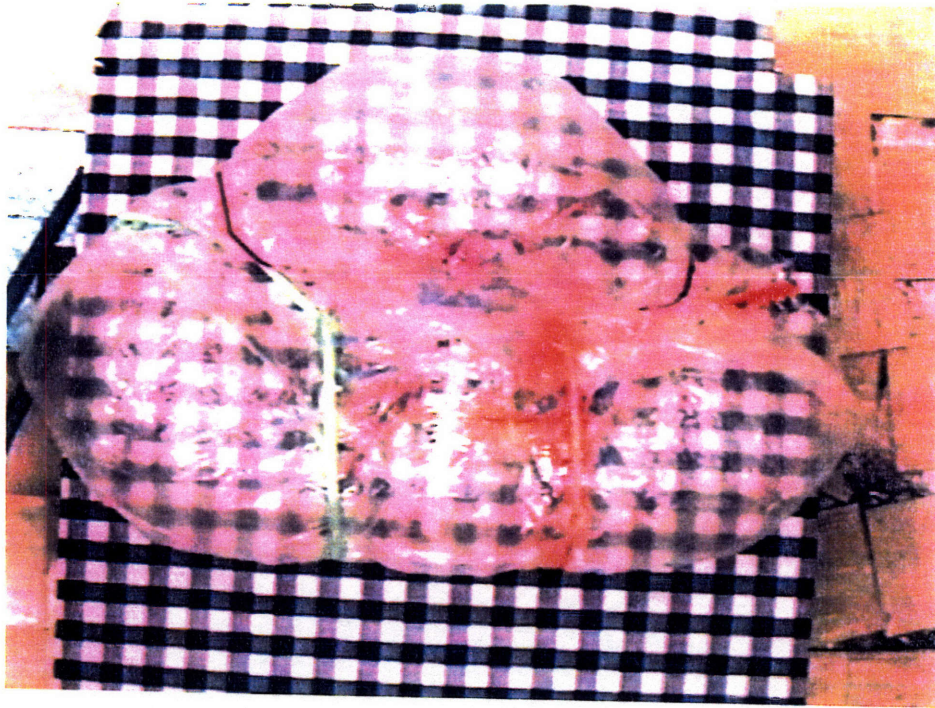


Figure 35. Inflation of Folding Scheme One.

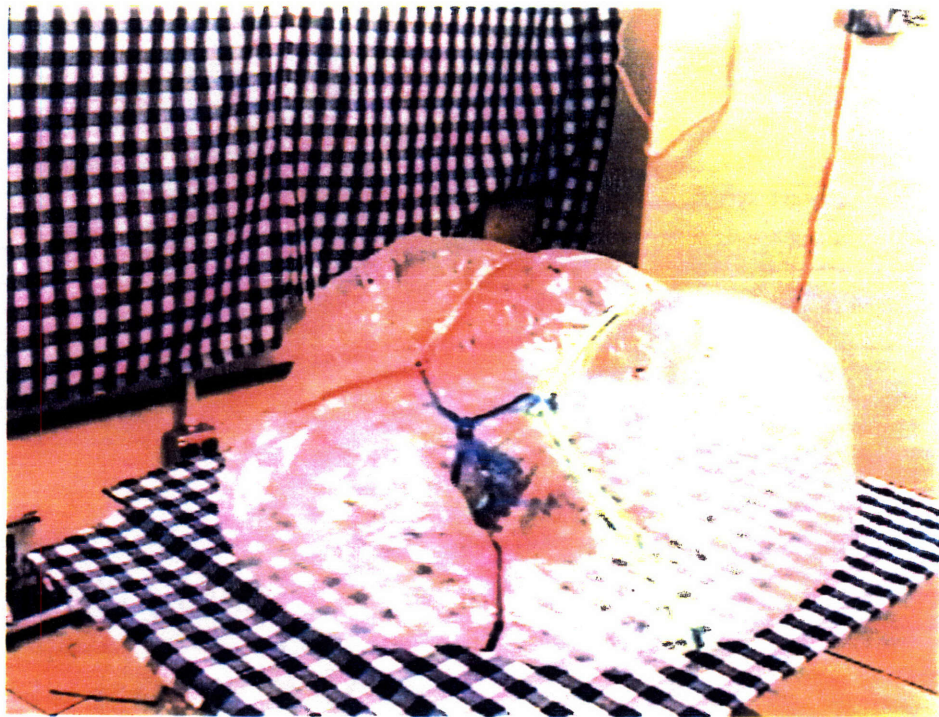


Figure 35. Inflation of Folding Scheme One.

fold (respectively) unfurling and inflating, and the last three show the same inflation from a different angle. In the first side view shot of the inflation, the right and left flaps of Folding Scheme One have already unfurled, and the bottom fold has come undone and begun to inflate. The next two pictures from the side show that the top fold (the first one to be made in the folding scheme) does not unfurl until after the whole bottom half of the airbag is fully inflated. Because a smooth, even increase in drag-area was the objective for optimal inflation of the airbag subsystem, it was concluded that Folding Scheme One was not a satisfactory airbag packaging option. Inflations of Folding Scheme One may be viewed in several trials on the video tape. Please refer to Appendix A: Video Tape Program Guide for more detailed time segments.

FOLDING SCHEME TWO

Folding Scheme Two produced much better results than Scheme One. The helical accordion was an idea drawn from nature, and ended up allowing the folds to unfurl in a smooth motion. With the exception of the last three flaps, which were left overhanging the otherwise compact packaging of the airbag in every scheme that was triangularly symmetric, Folding Scheme Two was the best of all four.

In contrast to Scheme One, which contained many straight folds that oppose each other and required large deployment forces, Scheme Two had many smaller folds that were not only easier to deploy due to their size, but also because of their orientation. Their size aided the inflation of the airbag because it was easier for the gas flow to move small amounts of mass in small increments, as opposed to Scheme One where larger forces were required to move the massive flaps of material. As each fold in the helical

pattern unfolded, it tugged on the corner of the fold to be undone next in the series. The seemingly small tug actually aided inflation a considerable amount, because it allowed the gas glow to ease into the next fold as it did its work to unfold and inflate it. The inflation of Scheme Two was smoother than Scheme One, in general, and the deployment loads on the material were considerably less, which will be of extreme importance in the full scale airbag subsystem. Another positive characteristic of Folding Scheme Two was the way it allowed the airbag to inflate smoothly and symmetrically from the center, whereas Scheme One sent large masses of material flying upward and outward from the center of the petal as it inflated.

A negative attribute of Scheme Two, as well as all other triangularly symmetric schemes attempted in these experiments, were the three flaps of material always left overhanging the perimeter of the lander petal. Scheme Two was successful in addressing the main problem encountered in Scheme One, namely the violent unfurling of large flaps of material in the beginning stages of the inflation, but was unsuccessful in tackling the problem of the three thin flaps left after the helical pattern was fully packaged. Though the three flaps of the second scheme unfolded and inflated much less violently than the final flaps of Scheme One, they presented a genuine problem in an otherwise optimal folding scheme, nonetheless.

Several inflations of Folding Scheme Two may be seen on the video tape. (Refer to Appendix A: Video Tape Program Guide for exact program segments.) Pictures of the inflations are included in Figure 36. Note the smooth, even nature of the unfolding, as compared to Folding Scheme One in Figure 35.

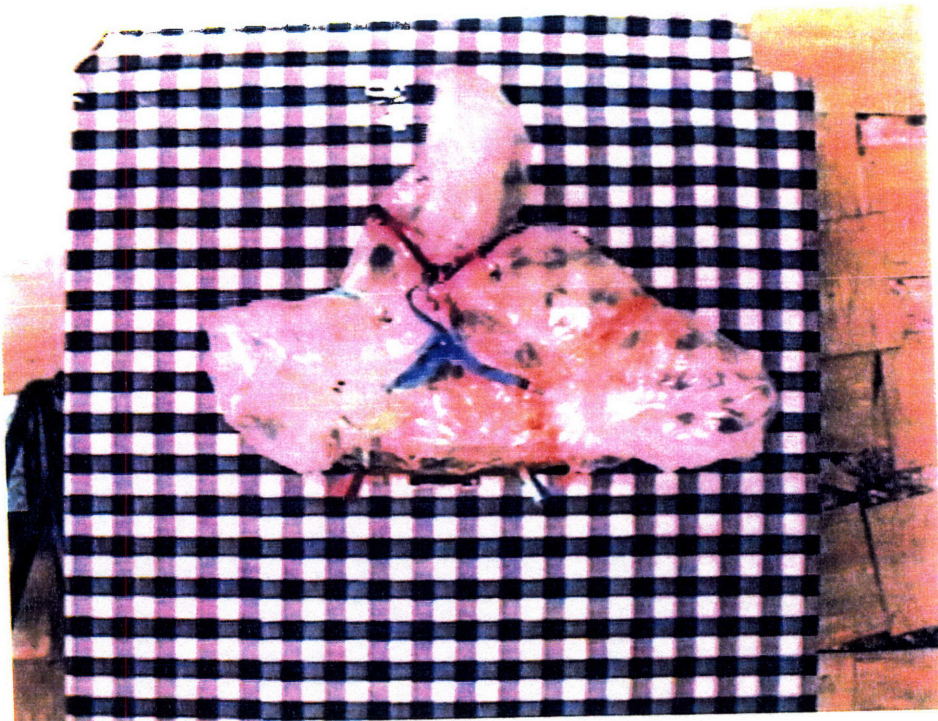


Figure 36. Inflation of Folding Scheme Two.

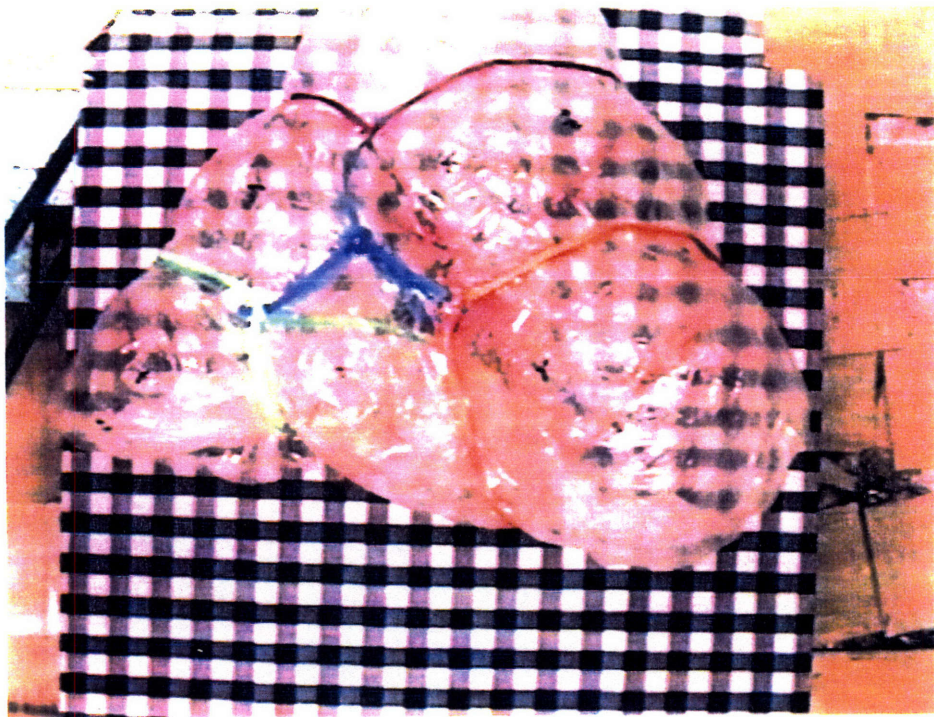
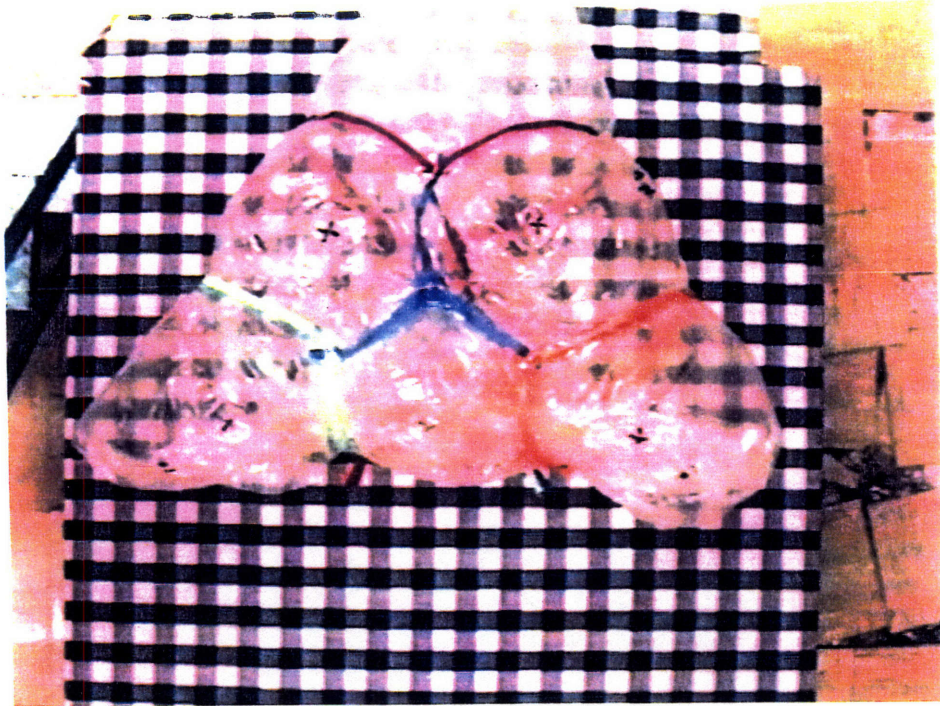


Figure 36. Inflation of Folding Scheme Two.

FOLDING SCHEME THREE

Folding Scheme Three was an attempt to get rid of the last three flaps of material left after what was an otherwise optimal folding scheme (Scheme Two) while maintaining the good characteristics -- small folds. The helix design was not carried over into the third scheme because whether done from the top of the airbag toward the bottom, or vice versa, three flaps always remained. Small folds oriented in a manner such that inflation was uninhibited by successive folds, however, were maintained.

The outermost corners of the triangular six-lobed airbag were folded in on themselves to give a nearly circular shape with which to work. Three small flaps were left after the vertical stacking of folds along each edge. They unfurled quickly and easily, but the vertically stacked "S" folds did not produce inflation dynamics as desirable as those produced with Scheme Two. The extraneous flaps were eliminated, but smooth unfurling of the folds was sacrificed. Scheme Three inflations are included in several trials on the video tape, and pictures of the inflation follow in Figure 37. The short flaps can be seen unfolding away from the lander petal in the first shot, and the next few show first the bottom, then the right, then the left stacks of "S" folds coming undone. Beyond the unfurling of the "S" folds, the inflation was relatively smooth, as seen in the last two shots.

FOLDING SCHEME FOUR

Folding Scheme Four was the product of Skip Wilson, among others, from ILC Dover, Incorporated. It was performed on JPL's quarter scale mock-up for comparison purposes so that the first three folding schemes could be ranked against ILC Dover's

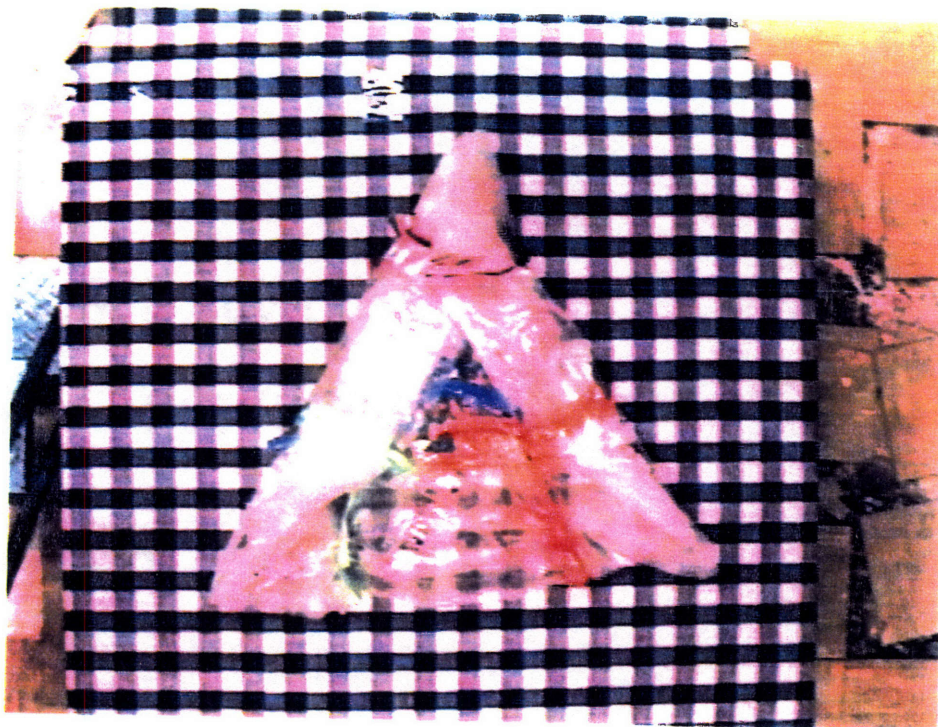
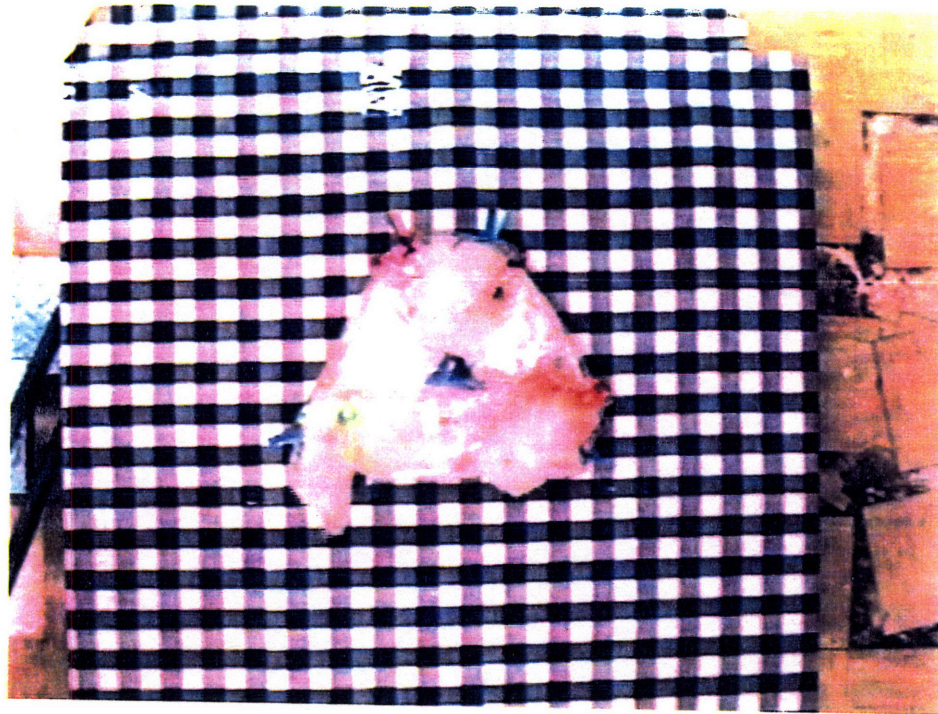


Figure 37. Inflation of Folding Scheme Three.

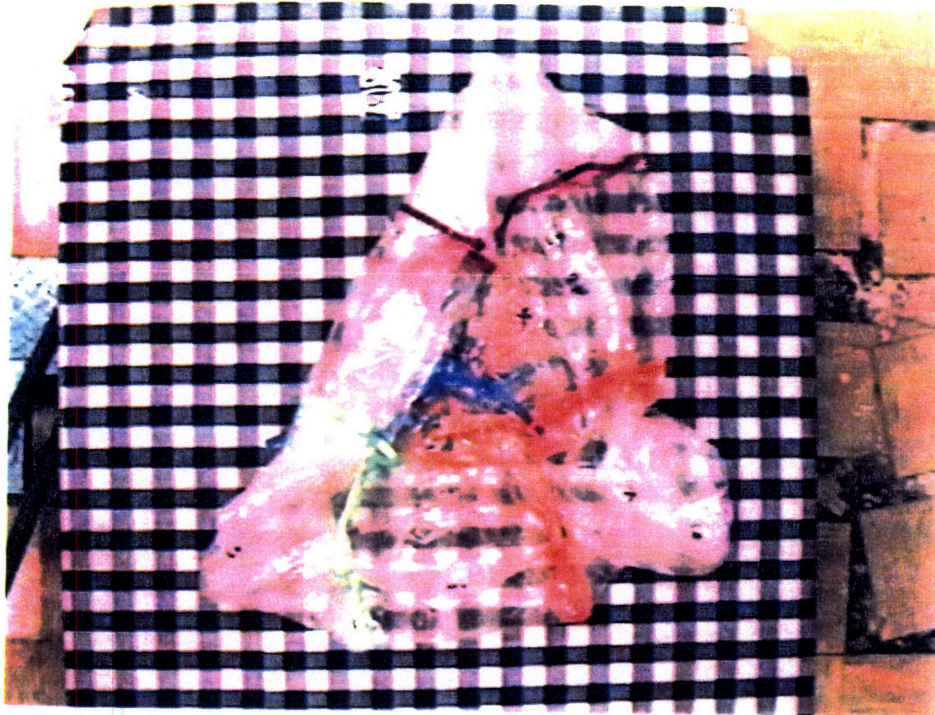
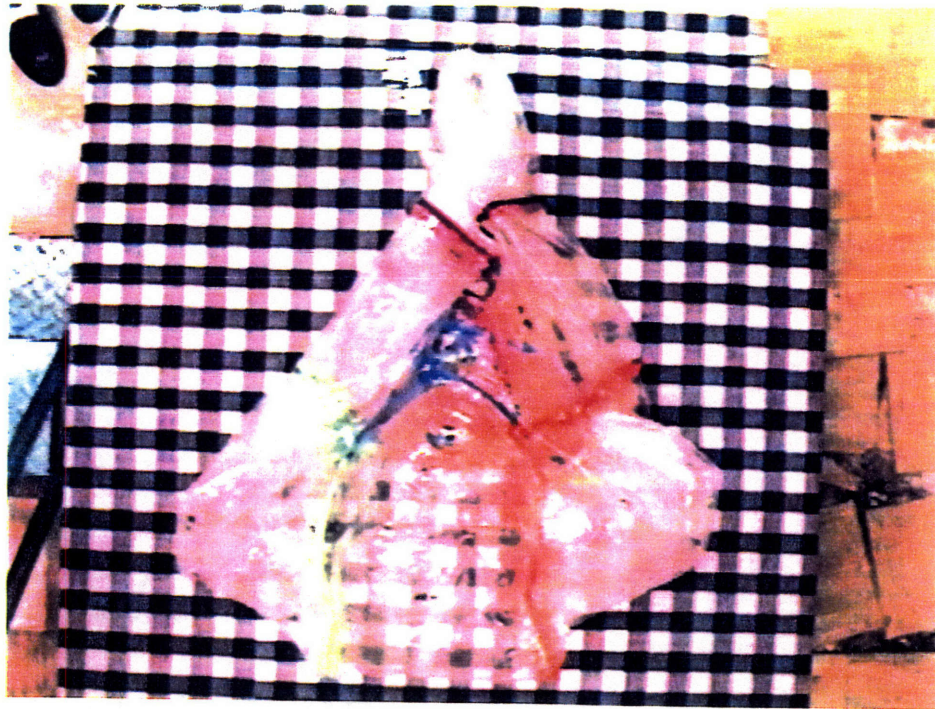


Figure 37. Inflation of Folding Scheme Three.



Figure 37. Inflation of Folding Scheme Three.

proposed airbag packaging design. It was similar to Folding Scheme Two in that it made “S” folds from the base of the airbag up toward the top and it had three flaps left at the end of the folding process. It was different from Scheme Two in that the “S” folds were done with all of the material along a petal edge before moving to the next edge. The material along the second edge was folded up in vertical stacks, as was the third, and then the three flaps remaining afterwards were folded into the triangular perimeter of the lander petal.

The vertical stacks of “S” folds behaved much like those in Scheme Three, but Scheme Four still had three long flaps of material to punch out before beginning to unfurl the smaller folds. Inflations of Scheme Four are also included on the video tape.

COMPARISONS BETWEEN THE FOLDING SCHEMES

Scheme One had considerably worse inflation dynamics than Schemes Two through Four. The helix design of Folding Scheme Two allowed for amazingly smooth inflations, but had the three flaps to unfurl in the beginning stages of its deployment. Scheme Three, which was an attempt to eliminate the three flaps of Scheme Two, succeeded in downsizing the flaps, but the inflation was not nearly as smooth as the helical pattern. Scheme Four had neither the shorter flaps nor the smooth unfurling of the folds, when compared to the best attributes of Schemes Two and Three. Therefore, further work on a hybrid design incorporating the helical folding steps of Folding Scheme Two and the shortened final flaps (due to the elimination of the corners of the original triangle) of Scheme Three should be pursued.

DIFFUSERS AND DEFLECTORS

In general, the choice of diffuser did not affect the way in which a given folding scheme deployed to any great extent; it only affected the inflation time. The choice of deflector did, however, affect the inflation dynamics.

DIFFUSERS

The low porosity diffuser used in Trials One through Six resulted in very long inflation times, which aided in noticing deployment dynamics such as the order in which folds unfurled. It did not, however, allow the airbag to inflate in a timeframe that was short enough to allow the results to be compared to what might actually happen with the full scale airbag. (It was originally proposed that perhaps the rapid inflation of the airbag did not behave in the same way as a slower inflation.) Therefore, the high porosity diffuser was used in Trials Seven through Ten to achieve more rapid inflations, and it was found that the folding schemes deployed in the same manner as before, but more rapidly. The results of the use of the two different diffusers indicate that aside from inflation time, there is essentially no difference in deployment dynamics. The validity of this conclusion is discussed in the following chapter.

DEFLECTORS

Because ILC Dover was unsuccessful in implementing a tri-chute deflector, it was felt that JPL should try, because the redirection of gas flow into the three corners of the triangular airbag seemed like a good option to both parties. The rapid mass flow rate and short time requirement on inflation were two reasons that the tri-chute deflector fabricated here on lab did not function properly. It was essentially destroyed with its first

inflation, which is the same result that ILC Dover experienced with this method of flow redirection. Because the deflector was destroyed before any data was able to be recorded, no folding schemes were inflated with the design. This issue is discussed in detail in the following chapter.

ILC Dover and JPL both also attempted flow redirection socks, and the results were similar again. Both parties found that the flow redirection socks routed the gas flow from the lower, center region of the lander petal toward the center, allowing for more even inflation of the schemes with vertical stacks of folds along the petal edges, namely Folding Schemes Three and Four. The redirection of the flow such that it effectively originates from the center of the lander petal as opposed to the edge did not affect the other two schemes. This result indicates that the choice of deflector depends on which folding scheme is ultimately decided upon, or vice versa.

Chapter Five: Discussion

GENERAL SCOPE OF THIS PROJECT

JPL's involvement in the design, testing, and fabrication of Mars Pathfinder Airbag Subsystem was limited, and the scope and intention of the work done warrants further discussion.

JPL'S INVOLVEMENT IN THE PATHFINDER EFFORTS

Because NASA contracted the Mars Pathfinder airbag subsystem design and fabrication out to ILC Dover, Incorporated and Thiokol Corporation, the extent of JPL's involvement in the project was limited. There were benefits and drawbacks to the nature of this project. Benefits of having the work done elsewhere include the use of fresh ideas coming from sources outside of NASA on spacecraft, as well as the expertise of a companies known for their prowess in the fields of space suit (ILC Dover, Incorporated) and gas generator (Thiokol) design and fabrication. Drawbacks of having the subsystem contracted out to other companies in the industry include the communication problems associated with iterations in designs and the lack of documentation pertaining to the history of a particular design.

It was often difficult to understand why things were done a certain way, what the constraints had been, and how solidified a design was when the companies that were responsible for a particular design were not within close proximity. For example, the design of the gas generator had not been solidified by the early stages of this project, so specific diffuser and deflector designs and mass flow rates, temperatures, and pressures were not available for the use of modeling and building the quarter scale mock-up.

Another design not solidified at the conception of these experiments was the number of lobes in the airbag. It was three lobes in June of 1994, and by July of 1994 the design had changed to six. Of course, the design change improved the coverage over the surfaces of the lander, but it also nullified all work done on packaging designs up to that point.

Having the majority of the Mars Pathfinder airbag subsystem engineers and resources many miles away was difficult, but was not all that troubling when the scope of this thesis was kept in mind.

THE SCOPE OF THIS THESIS

This was purely a conceptual exercise intended to produce creative folding schemes that might not be thought of by ILC Dover because they have a tried and true method of packaging inflatable devices. The same holds true for the diffuser and deflector designs. Exact metrics, numerical simulations of mass flow, structural calculations, and pursuits of that nature were not the objective of this work. JPL needed a core understanding of what comprised feasible folding schemes to have a baseline for understanding the issues surrounding packaging and inflating an airbag and in order to be able to converse intelligently with ILC Dover, Incorporated engineers. JPL had the same objectives in mind regarding the diffuser and deflector designs due to the anticipated future communications with Thiokol. Any knowledge gained about what enhances or detracts from a folding scheme or a flow diffusion or redirection device added to JPL's limited knowledge base in these two areas and gave JPL an idea which issues prove to be important ones in the deployment of the subsystem.

RESULTS

One problem with conveying the results of these experiments to anyone not familiar with how the Pathfinder Airbag Subsystem operates was that the results were entirely visual and difficult to quantify on paper and with normal empirical methods. No amount of modeling could have changed this, because the flow was very non-linear and the budget and time constraints did not allow for expansive models with nonlinear equations governing what would have been a two-phase flow into the airbag. It was decided upon by all parties involved in the design that back-of-the-envelope calculations and intuition would be enough to produce reasonable results.

Obviously this leaves considerable room for error, but it was felt that the objectives of these experiments would not be hampered by the lack of expensive, exact flow models and the like. The exact metrics will be dealt with by the companies responsible for the flight hardware. It was important to keep the scope -- the acquisition of baseline knowledge in the area of airbag packaging and deployment -- in mind throughout the project.

FOLDING SCHEMES

We questioned the validity of the inflation results from Trials One through Six because they deployed over such a long period of time. It was hypothesized that the airbag was unfurling mostly because of the spring rate of the material, as opposed to the gas flowing into the airbag. Trials Seven through Ten made sure that the inflation dynamics remained constant over varying inlet hole conditions.

DIFFUSERS AND DEFLECTORS

Having both tri-chute deflectors destroyed on or before their first inflations was not a good sign in the eyes of the engineers rooting for creative methods of flow redirection. Because of the slight difference in inflation when the flow redirection sock was used, it was decided that this area warrants further study. It is believed by both JPL and ILC Dover, Incorporated that the damage done to airbags during the beginning stages of an inflation and the ease of deployment of folding schemes both weigh heavily on the method of flow diffusion and redirection.

Also, the gas generator design will soon be finalized, which will pave the way for further modeling work to be done with the gas flow. Because the temperature and mass flow rate of the exhaust play an important role in diffusion and deflection options, the deployment of the airbags will ultimately be affected by whatever method of flow diffusion or redirection is chosen.

THREE FLAP PHENOMENON

One of the more important discoveries was the phenomenon of always ending up with three flaps overhanging the petal edge in triangularly symmetric packaging schemes. This was an unexpected finding that affects how ILC Dover, Incorporated plans to approach the rest of their folding scheme studies. These three flaps are what necessitated the tri-chute deflector. Because the deflector design requires a much more robust material and perhaps even an entirely different shape, the elimination of the three flaps would be ideal for both the packaging endeavors and the flow redirection endeavors.

If, however, the shape of the airbag changes, it could entirely change the possible folding schemes and the candidates for flow diffusion and redirection. At this point, a

change is highly unlikely, though, because the triangular six lobe design provides the most coverage over each petal of the lander, and a slight decrease in packing volume or slightly better inflation dynamics is not worth the risk of having less airbag coverage around the surfaces of the lander when it approaches the planet's surface. Work on possible folding schemes is being continued at ILC Dover, Incorporated as this document is being written.

Chapter Six: Conclusion

SUMMARY OF WORK DONE

For this thesis project done at the Jet Propulsion Laboratory, a series of experiments was performed using a quarter scale Mars Pathfinder Airbag Subsystem to achieve several goals. First, numerous folding methods were explored after taking cues from parachute rigging and the packaging of automotive airbags. Then the knowledge gained was incorporated into a coherent set of ‘good’ folding schemes, where ‘good’ schemes were defined as those that allowed for smooth deployment (no violent motions) and inflation without major damage to the airbag. After experimenting with different methods of recording the information being gathered with each folding scheme and it’s subsequent inflation, inflations were performed with many iterations of promising folding scheme candidates and varying inflation pressures, flow orifice sizes, diffusers, and deflectors in hopes of finding an optimal combination of variables.

The folding and inflation of four different folding schemes were recorded, as well as the inflation of each of the schemes with four varying gas inlet conditions to ensure that the schemes that were good candidates were good for a variety of inlet conditions, not just one. It was found that smaller folds built upon one another in succession resulted in smoother deployment of the airbag subsystem than large folds compounded on top of one another. It was also found that for any triangularly symmetric folding scheme, three flaps of material were always left overhanging the petal edge. This was a drawback to a few of the folding schemes, because they unfurled smoothly in every other way. It seemed that to get a nice pattern, one had to make a folding scheme triangularly

symmetric, but the ease of inflation within the first few milliseconds was always sacrificed in order to have the remainder of the deployment go smoothly. It was also found that flow diffusion and redirection devices were good or bad depending on the particular folding scheme they were utilized in. Different diffusers and deflectors changed deployment dynamics enough that their utility and benefits varied depending on the folding scheme they were paired with. The same could be said of the folding schemes, to a lesser extent. Their ease of deployment was affected by the choice of diffuser or deflector, but only marginally so.

RECOMMENDATIONS FOR FUTURE WORK

It is recommended that ILC Dover, Incorporated continue their studies of folding patterns and the effects of diffusers and deflectors on the deployment dynamics of each of the folding schemes under consideration. Their current proposal, as of the second week of December 1994, is Folding Scheme Four. It is hoped that they will seriously consider the drawbacks of Scheme Four (namely, the vertical stacks of "S" folds along each edge of the Mars Pathfinder lander petal) and perhaps opt for Scheme Two or Three, or some combination of the two. Further studies must be done in the area of flow diffusion and redirection once Thiokol Corporation finalizes the gas generator design, because their diffusion and deflection of the gas generator exhaust affects the deployment dynamics. The success of the two systems are not entirely separate; the use of devices to modify flow greatly affects the deployment dynamics of any given folding scheme used to package the airbag subsystem of Mars Pathfinder.

References

- Bickler, Don, Supervisor of Mechanical Systems and Technology Group, Mechanical Systems Development Section, Jet Propulsion Laboratory, meetings from June through December, 1994.
- Blackmon, Deborah, and Poynter, Dan, *Parachute Rigger Study Guide*, Para Publishing, Santa Barbara, California, 1994.
- Butler, P. Barry, Kang, Jian, and Krier, Herman, "Modelling and Numerical Simulation of the Internal Thermochemistry of Automotive Airbag Inflators," *Progress in Energy Combustion Science*, Volume 19, 1993.
- Carr, Michael H., *The Surface of Mars*, Yale University Press, New Haven, Connecticut, 1981.
- Gerhart, Philip M., Gross, Richard J., and Hochstein, John I., *Fundamentals of Fluid Mechanics, Second Edition*, Addison-Wesley Publishing Company, Reading, Massachusetts, 1992.
- Kirschner, T. J., and Gleeson, R. G., "Gas Generator" Section of ILC Dover, Incorporated's *Proposal for MESUR Pathfinder Flight Airbag Subsystem*, Volume 1 - Technical/Management, Part A - Technical Approach, May 2, 1994.
- Knacke, Theo W., *Parachute Recovery Systems Design Manual*, Aerosystems Department of the Recovery Systems Division, Naval Weapons Center, China Lake, California, 93555-6001, March 1991.

Lakshminarayan, V., and Lasry, David, *Finite Element Simulation of Driver Folded Air Bag Deployment*, Vehicle systems CAE, Ford Motor Company, and ESI International, Paris, France.

Lilienthal, Jerry, Supervisor of Mechanical Components Technology Group, Mechanical Systems Development Section, Jet Propulsion Laboratory, meeting on September 7, 1994.

McMahon, Thomas A., and Bonner, John Tyler, *On Size and Life*, Scientific American Books, Incorporated, New York, New York, 1983.

Poynter, Dan, and Schlatter, Mark, *Parachute Rigging Course: A Course of Study for the FAA Senior Rigging Certificate*, Para Publishing, Santa Barbara, California, 1994.

Rivellini, Tom, Member of Technical Staff, Mechanical Systems Development Section, Jet Propulsion Laboratory, meetings from June through December, 1994.

Spear, Anthony J., *Low Cost Approach to Mars Pathfinder and Small Landers*, Jet Propulsion Laboratory, April 14, 1994.

Spear, Anthony J., *Mars Pathfinder Fact Sheet*, Jet Propulsion Laboratory, May 10, 1994.

Wilson, Skip, Systems Engineer, ILC Dover, Incorporated, conversations from meetings at the Jet Propulsion Laboratory on September 28, 1994.

Appendix A: Video Tape Program Guide

- 00:00-08:30 Preliminary work on folding schemes and Trials One through Three.
- 08:30-13:30 Folding of Scheme One.
- 13:30-14:30 Three inflations of Scheme One with low porosity diffuser (Trial Four).
- 14:30-22:00 Folding of Scheme Two.
- 22:00-26:00 Three inflations of Scheme Two with low porosity diffuser (Trial Five).
- 26:00-36:00 Folding of Scheme Three.
- 36:00-38:00 Three Inflations of Scheme Three with low porosity diffuser (Trial Six).
- 38:00-39:00 Inflation of Folding Scheme One with high porosity diffuser (Trial Seven).
- 39:00-40:00 Inflation of Folding Scheme Two with high porosity diffuser (Trial Eight).
- 40:00-41:00 Inflation of Folding Scheme Three with high porosity diffuser (Trial Nine).
- 41:00-47:30 Folding of Scheme Four.
- 47:30-48:30 Two inflations of Scheme Four with high porosity diffuser (Trial Ten).
- 48:30-49:00 Inflation of Scheme One with flow redirection tube (Trial Eleven).
- 49:00-49:30 Inflation of Scheme Two with flow redirection tube (Trial Twelve).
- 49:30-50:00 Inflation of Scheme Three with flow redirection tube (Trial Thirteen).
- 50:00-51:00 Inflation of Scheme Four with flow redirection tube (Trial Fourteen).